High-contrast problems in linear elasticity for a coated half-space

Leyla Sultanova

School of Computing and Mathematics

Keele University

A thesis submitted for the degree of

Doctor of Philosophy

June, 2019

Declaration

I certify that this thesis submitted for the degree of Doctor of Philosophy is the result of my own research, except where otherwise acknowledged, and that this thesis (or any part of the same) has not been submitted for a higher degree to any other university or institution.

Signed: _____ Date: _____

(Leyla Sultanova)

Abstract

The thesis is concerned with asymptotic analysis of static as well as dynamic problems for a solid coated by a thin isotropic elastic layer with a high contrast in their material parameters. First, the static anti-plane shear deformation problem is considered with the layer being relatively soft or stiff in order to investigate the behaviour of the coating. The two-parametric asymptotic procedure is introduced motivated by the scaling obtained from the exact solution of a model problem. As a result, Winkler-type behaviour appears for a relatively soft coating, whereas for a relatively stiff one, the equations of plate shear are valid. Further, the formulation is extended to a 3D case with vertical force applied at the surface aiming at asymptotic investigation of the area of validity of the Winkler-Fuss hypothesis and the Kirchhoff plate theory. It is established that the aforementioned theories are valid only at a rather high contrast in stiffness of the layer and the half-space. However, a uniformly valid formula is deduced in case of a layer being soft, and for low contrast with the coating being stiff, several approximate formulations are suggested based on the reduced problems for the half-space. Then, the problem is considered in dynamic formulation yielding the higher order effective boundary conditions modelling the presence of the coating layer. The obtained results indicate again the inconsistency of the conditions earlier presented in [22]. The validity of the asymptotic results is demonstrated by comparison with

the long-wave expansion of the exact solutions of plane and anti-plane time-harmonic problems for the coating. Finally, the dynamic problem for a coated half-space with clamped surface is considered. The exact solutions are obtained in an anti-plane and plane strain formulations resulting in the range of material parameters for which the sought for localised wave exists. The effective boundary conditions are obtained and the model for Rayleigh wave field is applied for the layer being thin and soft, leading to an explicit correction to the classical Rayleigh wave speed.

Acknowledgements

First of all, I would like to express my sincere gratitude to both of my supervisors Dr Danila Prikazchikov and Prof Julius Kaplunov for their wise guidance and invaluable support during my PhD studies. None of this would have been possible without their constant encouragement and enthusiasm. I learnt a lot from Dr Prikazchikov and Prof Kaplunov during many hours of discussions, their work and fruitful ideas have always been very inspiring to me.

I am thankful for all the help that Dr Prikazchikov and his wife Dr Luda Prikazchikova provided to me, especially during my first year in the UK, their exceptional hospitality and friendly attitude made me feel like home.

I gratefully acknowledge the support of the ACORN Scholarship from Keele University, which gave me the opportunity to conduct this research project and to attend various conferences and workshops.

Finally, I would like to extend my thanks to Peter Wootton for being a good friend and officemate during my time at Keele. I owe special gratitude to my beloved husband Pavlos for his support and patience through the toughest moments of my research. Last, but certainly not least, I greatly appreciate the support of my mother Veronika who has always been there for me through my entire life.

Contents

List of Figures

List of Tables

Nomenclature

Indices

$i, j = 1, 2, 3,$	$m, n = 1, 2;$	$m \neq n,$	$s = 1, 3,$	$d = 1, ..., 4,$
$y = 1, 2, 3, ...,$	$q = 1, ..., 6,$	$z = 1, 3, 5, ...,$	$b = 2, 4, 6, ...$	

Variables

Dimensional		Dimensionless
x_i	coordinates	ξ_m, $\xi_3^{\pm}$
$\sigma_{ij}^{\pm}$	stresses	
$u_i^{\pm}$	displacements	
$\rho^{\pm}$	volume mass densities	
ω	frequency	$\Omega^{\pm}$
k	wave number	K
c	phase velocity	$\zeta^{\pm}$
$\epsilon_{ij}^{\pm}$	strains	
	Kronecker delta	δ_{ij}
$\lambda^{\pm}$, $\mu^{\pm}$	Lamé elastic constants	

Variables

Dimentional		Dimensionless
$E^{\pm}$	Young's modulus	
$\nu^{\pm}$	Poisson's ratio	
$c_1^{\pm}$	longitudinal wave speed	
$c_2^{\pm}$	transverse wave speed	
$\varphi^{\pm}$	longitudinal elastic potentials	
$\psi_i^{\pm}$	transverse elastic potentials	
t	time	τ_l, τ_h
	small geometrical parameter	ε
h	thickness of the layer	
l	typical length	
	material parameter	μ
	level of contrast	α
P	applied load	
r	foundation modulus	
w_0	deflection of a surface	
w_p	deflection of a plate	W_p
D	plate bending stiffness	
	shear of a plate	V
c_R	Rayleigh speed	ζ_R
w_h	vertical interfacial displacement	

Introduction

Coated structures find numerous applications in modern engineering and technology, including, in particular, biomedical sciences and structural mechanics, see e.g. [20, 29, 67, 110, 134, 138, 163].

The presence of a coating layer usually motivates an asymptotic approach relying on a geometric parameter namely the ratio between thickness of the coating and a typical length. If this parameter is considered to be of order one, the coating is referred to a "thick layer", while a small parameter is a characteristic of a "thin" one. In case of a dynamic problem, the typical length is in fact the wave length and the limits, therefore, correspond to the short- and long-wave approximations, respectively.

Originally, asymptotic methods started developing in the field of statics and low-frequency dynamics for plates and shells, see e.g. [4, 11, 12, 49, 57, 58, 59, 60, 65, 104, 148, 149]. Low-frequency approximations are characterised by polynomial variation across the thickness of the plate. Asymptotic methods, including, in particular, the method of direct asymptotic integration of the equations in elasticity [57, 58, 60], were also applied in more general dynamic problems with high-frequency approximations considered for both long- and short-wave limits. In contrast to low-frequency approximations, high-frequency ones involve sinusoidal thickness variation. High-frequency long-wave approximations of modes arising in the neighbourhood of the

cut-off frequencies or the so-called thickness resonance frequencies [14, 89, 109] were later found for various problem formulations, including pre-stressed and anisotropic structures, see e.g. [88, 92, 108, 131, 139, 140, 150, 151], high-frequency trapped modes [66, 94, 116, 143, 161], layers interacting with media [90], bodies with clamped faces [87, 91], and layered structures [35, 113, 153]. A high-frequency approximation for short-wave motion was studied in [89, 93]. A similar asymptotic approach has been recently implemented in [30, 31] for non-local elasticity, highlighting the importance of incorporation of near-surface boundary layers.

Approximate 2D models of thin structures have found a great variety of fresh applications in recent years, inspired by exciting modern developments in high-tech domains, for example, in the context of cloaking of waves, see e.g. [34] addressing an issue of cloaking transformations for flexural waves in thin plates, [23, 132, 133] dealing with cloaking of finite rigid inclusions in a thin elastic plate in the presence of incident flexural waves. Studies on propagation of bending waves in a perforated thin plate are presented in [125, 144]. We also mention considerations in [154, 155], aiming at investigation of the temperature distribution in a system of thin channels connected by thin conducting walls. In addition, we note [52] focusing on the buckling of a uni-axially compressed neo-Hookean thin film bonded to a neo-Hookean substrate.

The effect of a thin coating can be modelled by imposing the so-called effective boundary conditions along the surface of a substrate. These conditions first were derived in [160] using *adhoc* assumptions originating from the classical theory of plate extensions. Later on, it was suggested in [22] that the results of [160] are not consistent, and refined boundary conditions were proposed starting from rather heuristic arguments. The asymptotic procedure exposed in [36] justifies at leading order the

consistency of the effective boundary conditions in [160] and also reveals that the extra terms found in [22] are in fact of a higher order. Moreover, as it was briefly mentioned in [36], the treatement in [22] is not asymptotically consistent at the next order as well. It is remarkable that the boundary conditions in [22] were exploited not only before but also after the publication of the critical comments in [36], e.g. see [114, 127, 170] along with [56, 165, 168]. This is partly an inspiration for revisiting the original problem for a coated elastic half-space aiming at establishing higher order effective conditions. The idea of establishing effective boundary conditions representing the effect of a layer was also implemented in [166] for an isotropic elastic layer and in [164, 167] for an orthotropic one.

The effective boundary conditions can be then used to take into consideration the effect of the coating. Indeed, in [36], for a coated half-space subject to surface loading, the presence of a coating layer expressed through the effective boundary conditions is incorporated, leading to an explicit model for the surface wave.

This model was originally derived in [95] using the symbolic Lourier approach, see e.g. [89] and references therein, and then, was further developed in [86] using a multi-scale procedure utilizing a slow time perturbation scheme applied to the eigensolution for a homogeneous surface wave of arbitrary profile, see [26] and also earlier publications [48, 157], as well as more recent papers, including [2, 99, 100, 101, 135, 136, 145, 152]. In a general setup, the aforementioned multiscale procedure is presented in [81, 82] dealing with Rayleigh and Rayleigh-type waves induced by surface stresses. The fact that the eigensolution in [26] can be expressed in terms of a single harmonic function results in a hyperbolic-elliptic theory for Rayleigh waves induced by prescribed surface stresses, which involves a wave equation for one of the Lamé potentials that

governs propagation of surface disturbances along with pseudo-static elliptic equations for calculating the Lamé potentials over the interior. The 2D formulation in [86] is then extended to the 3D case, see [81, 82] employing the integral Radon transform. A similar theory is also established for surface Rayleigh-type waves for a coated half-space, for which a hyperbolic equation along the surface is regularly perturbed by a pseudo-differential operator. The formulation has been applied to various moving load problems, see [43, 76, 83]. The effects of anisotropy, pre-stress and mixed boundary conditions have also been addressed in [42, 97, 130]. Recently, composite wave models for elastic plates have been constructed, see [41], combining both equations of plate bending over the long wave low-frequency region and surface waves over the short-wave one.

It has been known though that the Rayleigh wave on a homogeneous elastic half-space does not exist if the surface is clamped. Recent rigorous analysis of a layered half-space with clamped surface in [33] demonstrates a possibility of a Rayleigh-type wave for certain setups. Therefore, a part of the thesis is dedicated to the consideration of a particular problem of a coated elastic half-space with clamped surface, in order to produce a qualitative physical analysis of its behaviour using a multiparametric treatment and investigate the existence of surface waves.

Often, in addition, there is a contrast in stiffness of the coating and the half-space, which implies a material parameter, leading to two types of asymptotic behaviour corresponding to a relatively soft and a relatively stiff coating.

Usually, if a layer is considered to be relatively soft compared to a substrate, the model of elastic foundation is implemented, for example, that based on the Winkler-Fuss assumption treating a continuum as a system of vertical springs. For further

historical remarks on the Winkler-Fuss model the reader is reffered to [50]. A detailed critical review of the Winkler-Fuss, as well as other elastic foundation models, can be found in [69]. Another useful review of foundation models is presented also in [96], taking into account viscoelastic behaviour. One of the focuses of the recent monograph [3] is on the asymptotic analysis of layered and inhomogeneous foundations. In addition, we mention [124] as an example of modelling thin interlayers using Winkler-Fuss assumption. The Winkler-Fuss approximation is widely used in civil engineering, e.g. see [39, 54, 111, 128, 171, 173] and also in contact mechanics, including, in particular, analysis and interpretation of the experimental results for a depth-sensing indentation, see [19] and references therein.

Depth-sensing indentation means that the relation between the load applied to an indenter and the displacement in a material sample is continuously monitored. We specially mention nanoindentation technique, see e.g. [47], which is currently of interest for estimation of mechanical properties of small specimens or very thin films for which conventional testing is not feasible. For the latter, there is a great potential for using asymptotic methods. Dynamic indentation tests have been also shown to be useful in application to biological tissues, such as articular cartilage. The study of the dynamic indentation stiffness of an articular cartilage tissue modelled as a viscoelastic material is reported in [8] aiming at formulation of a criteria for evaluation of its quality. We also mention a recently published book [10] that presents a unifying approach to analytical evaluation of properties of biological materials.

For a relatively stiff layer lying on a half-space, a variety of problems in structural mechanics are modelled by a thin Kirchhoff plate resting on an elastic substrate, e.g. see [61, 62, 63, 69, 70, 106]. In addition, we cite an influential paper [18] and also a useful

survey of mathematical techniques for treating plates on a linear elastic foundation in [142]. Among modern considerations on the subject, we also mention [16] inspired by modelling of advanced resonant devices, and [17, 24, 37, 51, 55, 158] tackling a variety of vibration and stability phenomena.

As a rule, the Winkler-Fuss model and the Kirchhoff plate theory may be implemented provided that there is a high contrast in the stiffness of a substrate and a coating, i.e. when the substrate is much stiffer or softer than the coating, respectively. At the same time, for a thin coating supported by an infinite substrate, a limited amount of effort has been made to provide a mathematical justification of both models, see e.g. [102, 115]. The effect of high contrast in stiffness was briefly addressed in [5], studying a contact problem for a coated half-space, without linking it to the relative thickness of the coating. In addition, we refer to [6], also accounting for the importance of high contrast limit. These contributions appreciate the general challenge, however, they do not take into consideration a two-parametric nature of the problem, involving geometric and material parameters expressing relative thickness and stiffness, respectively. For a stiff coating, only very few papers, e.g. [25], explicitly take into account the limitation associated with a specific asymptotic ratio of plate and substrate stiffness. The Winkler-Fuss assumption, in turn, was only fully validated for a layered foundation clamped at the bottom, although without a special emphasis on the contrast properties of the layers, see [3]. Thus, in order to investigate the area of validity of the Winkler-Fuss model and the Kirchhoff plate theory in application to coated solids, a multiparametric asymptotic treatment is required, and one of the aims of the thesis is to develop it, allowing a variety of scenarios depending on the relation between the dimensionless thickness and stiffness.

Similar multiparametric approach in plate dynamics has been recently reported in [84, 146], analysing elastic wave propagation in a three-layered plate with high-contrast mechanical and geometric properties of the layers for four specific types of contrast. In addition, we note [141] studying scattering of plane elastic waves by arrays of circular cylindrical inclusions connected to the surrounding medium via a thin soft elastic layer, and [53] considering propagation of non-linear travelling waves in a coated elastic half-space with both the coating and half-space composed of neo-Hookean materials of the same density but of different shear moduli. We also mention considerations focusing on strongly inhomogeneous multi-layered and multi-component structures, see, for instant, asymptotic developments on the subject in [15, 21, 77, 85, 105, 162, 169], along with [7, 126] using *adhoc* layerwise theories, and [28] developing finite-product approximations to the exact Rayleigh-Lamb dispersion relation for a three-layered plate. Related problems for homogenization of high-contrast periodic structures are reported in [32, 45, 75, 156]. Similarity of the asymptotic procedures underlying multi-layered plate theories and homogenization for periodic media has been recently addressed in [35].

The thesis consists of five chapters, concluding remarks and bibliography.

Chapter 1 contains basic equations and key problem parameters used throughout the thesis, formulations of the Winkler-Fuss hypothesis and the Kirchhoff plate theory, as well as description of main types of guided waves.

In Chapter 2, an anti-plane shear deformation of an elastic half-space coated by a soft or a stiff elastic layer is considered. Analysis of an anti-plane shear is of interest within linear and nonlinear solid mechanics, since it allows establishing a simpler mathematical setup without loss of essential physical features, see e.g. [72]. First, we derive

the exact expressions for anti-plane deformations caused by a sinusoidal shear load. Then, a multiparametric asymptotic scheme for an arbitrary shear load is adapted for a coated elastic half-space, considering two problem parameters. The first of them is a geometrical parameter ε, characteristic of thin plates and coatings [3, 36, 44, 60]. The second parameter, μ, stands for the contrast in stiffness of the layer and the half-space. The static behaviour of the coated structure is studied depending on the value of parameter α relating the quantities above by the formula $\mu = \varepsilon^\alpha$. The original scaling of displacements and stresses within the adapted asymptotic technique is motivated by the exact solution, see [3, 9, 60] for more detail. An asymptotic classification following from the relation between the two analysed parameters is established. The results for anti-plane displacement and stress components are obtained. In particular, we focus on the relation between the shear load and the displacement, which results in Winkler-type behaviour for a rather soft coating and involves the equations of plate shear in case of a soft layer. The derived asymptotic formulae are compared numerically with the exact solution for a shear sinusoidal load.

In Chapter 3, we extend the methodology presented in Chapter 2 to a 3D problem. Again, we operate with two small parameters, corresponding to the relative stiffness and thickness of the layer, adapting an asymptotic procedure. The limiting forms of the original equations for various ratios between these two parameters are derived. First, we establish the asymptotic behaviour of displacement and stress components for a model plane strain problem in case of a vertical sinusoidal load. Next, we adapt the initial settings coming from the model problem to the general 3D setup. As a result, a 3D problem in linear elasticity for a soft or stiff layer attached to a substrate is treated for a broad range of ratios between relative stiffness and wavelengths, resulting, in

particular, in the justification and refinement of the Winkler-Fuss hypothesis and the Kirchhoff plate theory for a soft and a stiff layer, respectively.

It is shown that the Winkler-Fuss model is justified only for a rather high contrast, when $\alpha > 1$, while for lower contrast ($0 \leq \alpha \leq 1$) it fails already at leading order. A robust alternative approach valid at $0 \leq \alpha \leq 1$ is proposed starting from the transmission of the prescribed load to the interface between the layer and the half-space. Asymptotic corrections to the Winkler-Fuss hypothesis are also presented over various intervals of parameter α, including that corresponding to the refined Pasternak model, see [74, 129, 137].

For a stiff layer, initially, the procedure was developed for Neumann boundary value problems for plates and shells assuming prescribed stresses along the faces. Later on, it was extended to Dirichlet and various mixed boundary value problems, characteristic of thin coatings and interlayers, see e.g. [3] and references therein. For both setups, the displacements and stresses are expanded into series in the thickness variable, resulting in the 3D to 2D dimension reduction. The peculiarity of the studied configuration is that the contact with the substrate results in asymptotic consideration of a rather sophisticated boundary value problem for the thin layer. In particular, we confirm the scaling in [25] corresponding to a coupled problem for a Kirchhoff plate resting on an elastic half-space, and for a softer substrate we arrive at leading order at an uncoupled problem for plate bending. At the same time, for a stiffer substrate, which is still much softer than the layer, any plate bending theory fails. In the latter case, however, we formulate a set of boundary value problems for a homogeneous half-space. Among them, in particular, there are effective boundary conditions originally derived in [160] and later justified in [36]. The validity of all the shortened approximate formulations

is justified by comparison with the exact solution of the aforementioned plane strain problem.

In Chapter 4, as in [36], using asymptotic methodology, we validate again the results in [160] at leading order. At next order, we arrive at refined effective conditions. They are tested by comparison with the exact solution of a plane strain time-harmonic problem. As it might be expected, the comparison demonstrates that the boundary conditions in [22] are not consistent at higher order.

Chapter 5 is concerned with dynamics of a coated elastic half-space with clamped surface. First, an anti-plane and plane strain problems are considered leading to the exact dispersion relations. Analysis of the obtained dispersion relations makes it possible to evaluate the range of parameters, for which the sought for surface wave exists. Then, for a relatively small thickness of the coating, similarly to [36], we perform an asymptotic analysis resulting in effective boundary conditions on the surface of a homogeneous half-space. Then, assuming the layer to be much softer than the substrate, the problem is reduced to a regularly perturbed hyperbolic equation for Rayleigh-type waves using earlier established asymptotic technique, e.g. see [36, 82]. Finally, an explicit correction to the classical Rayleigh wave speed is derived. The produced asymptotic results are compared numerically with the exact solution.

Chapter 1

Preliminaries

Basic equations of elasticity theory are summarized in this chapter, along with parameters used throughout the thesis. Brief descriptions of Winkler-Fuss hypothesis and Kirchhoff plate theory are also given together with derivations of Rayleigh, Rayleigh-Lamb and Love waves.

1.1 Equations of elasticity theory and main parameters

In the present study, we consider a composite solid consisting of a layer of thickness h and a substrate, see Figure 1.1. Both media are considered to be linearly elastic and isotropic. In what follows, the parameters of the coating are denoted with superscript "$-$", and that of the half-space with "$+$".

We contemplate the absence of body forces, therefore the conventional stress equations of motion can be taken as, see e.g. [1],

$$\sigma^{\pm}_{i1,1} + \sigma^{\pm}_{i2,2} + \sigma^{\pm}_{i3,3} = \rho^{\pm} u^{\pm}_{i,tt}, \tag{1.1}$$

where $\sigma^{\pm}_{ij}$ are Cauchy stresses, $u^{\pm}_{i}$ are displacements and $\rho^{\pm}$ denote volume mass densi-

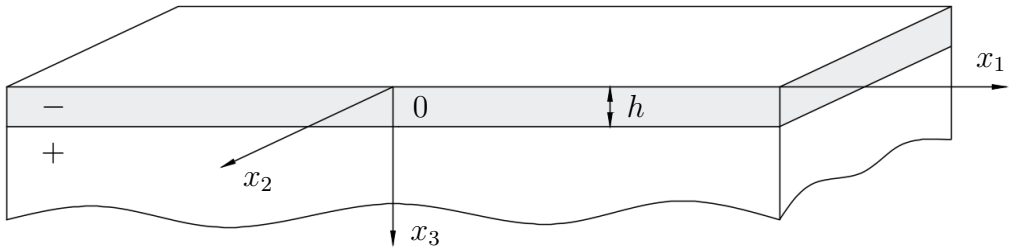

Figure 1.1: Layer on a substrate

ties of the layer and the half-space. Here and below, $i, j = 1, 2, 3$ and comma indicates differentiation along the associated spatial coordinate or time.

If the motion is considered to be time-harmonic, i.e. $u_i^{\pm} \sim \mathrm{e}^{ik(x_1 - ct)}$, then equations (1.1) become

$$\sigma_{i1,1}^{\pm} + \sigma_{i2,2}^{\pm} + \sigma_{i3,3}^{\pm} = -\rho^{\pm}\omega^2 u_i^{\pm}, \tag{1.2}$$

where

$$\omega = kc \tag{1.3}$$

is a radian frequency, k and c represent a wave number and a phase velocity, respectively.

The Hook's law for an isotropic material is given by

$$\sigma_{ij}^{\pm} = \lambda^{\pm}\delta_{ij}(\epsilon_{11}^{\pm} + \epsilon_{22}^{\pm} + \epsilon_{33}^{\pm}) + 2\mu^{\pm}\epsilon_{ij}^{\pm}, \tag{1.4}$$

where $\epsilon_{ij}^{\pm}$ are strain tensors, δ_{ij} is the Kronecker delta defined as

$$\delta_{ij} = \begin{cases} 0, & i \neq j, \\ 1, & i = j, \end{cases} \tag{1.5}$$

$\lambda^{\pm}$ and $\mu^{\pm}$ are the Lamé elastic constants, which can be represented as

$$\lambda^{\pm} = \frac{E^{\pm}\nu^{\pm}}{(1+\nu^{\pm})(1-2\nu^{\pm})}, \qquad \mu^{\pm} = \frac{E^{\pm}}{2(1+\nu^{\pm})}, \tag{1.6}$$

with $E^{\pm}$ and $\nu^{\pm}$ denoting the Young's modulus and the Poisson's ratios, respectively, of the layer and the substrate.

Strain tensors are expressed as

$$\epsilon_{ij}^{\pm} = \frac{1}{2}(u_{i,j}^{\pm} + u_{j,i}^{\pm}), \tag{1.7}$$

therefore, the Hook's law (1.4) together with the strain-displacement relations (1.7) lead to the constitutive relations adopted in the form

$$\sigma_{ij}^{\pm} = \lambda^{\pm}\delta_{ij}(u_{1,1}^{\pm} + u_{2,2}^{\pm} + u_{3,3}^{\pm}) + \mu^{\pm}(u_{i,j}^{\pm} + u_{j,i}^{\pm}). \tag{1.8}$$

Substituting the latter into (1.1), we obtain equations of motion in terms of displacements

$$(\lambda^{\pm} + \mu^{\pm})\,\mathrm{grad}\,(\mathrm{div}\,\mathbf{u}^{\pm}) + \mu^{\pm}\Delta\mathbf{u}^{\pm} = \rho^{\pm}\mathbf{u}_{,tt}^{\pm}, \tag{1.9}$$

where Δ is the 3D Laplace operator in x_1, x_2 and x_3 and $\mathbf{u}^{\pm} = (u_i^{\pm})$. The latter can be also rewritten as

$$(c_1^{\pm})^2\mathrm{grad}\,(\mathrm{div}\,\mathbf{u}^{\pm}) - (c_2^{\pm})^2\mathrm{curl}\,(\mathrm{curl}\,\mathbf{u}^{\pm}) = \mathbf{u}_{,tt}^{\pm}. \tag{1.10}$$

where

$$c_1^{\pm} = \sqrt{\frac{\lambda^{\pm} + 2\mu^{\pm}}{\rho^{\pm}}}, \qquad c_2^{\pm} = \sqrt{\frac{\mu^{\pm}}{\rho^{\pm}}} \tag{1.11}$$

are longitudinal and transverse wave speeds, respectively. We also introduce

$$\gamma^{\pm} = (\kappa^{\pm})^2, \tag{1.12}$$

with $\kappa^{\pm}$ being a ratio of aforementioned speeds, i.e.

$$\kappa^{\pm} = \frac{c_1^{\pm}}{c_2^{\pm}} = \sqrt{\frac{2 - 2\nu^{\pm}}{1 - 2\nu^{\pm}}}. \tag{1.13}$$

The displacement field can be decomposed according to the Helmholtz theorem as

$$\mathbf{u}^{\pm} = \mathrm{grad}\varphi^{\pm} + \mathrm{curl}\boldsymbol{\psi}^{\pm}, \tag{1.14}$$

where $\varphi^{\pm}$ and $\boldsymbol{\psi}^{\pm} = (\psi_i^{\pm})$ are scalar longitudinal and vector transverse elastic potentials, respectively. Substituting the latter into equations of motion (1.9) and taking into account that $\mathrm{div}\,\mathrm{grad} \equiv \Delta$ and $\mathrm{div}\,\mathrm{curl} \equiv 0$, we have

$$\mathrm{grad}\left[(\lambda^{\pm} + 2\mu^{\pm})\Delta\varphi^{\pm} - \rho^{\pm}\varphi^{\pm}_{,tt}\right] + \mathrm{curl}\left[\mu^{\pm}\Delta\boldsymbol{\psi}^{\pm} - \rho^{\pm}\boldsymbol{\psi}^{\pm}_{,tt}\right] = 0. \tag{1.15}$$

If we apply the divergence operator to (1.15), we derive the wave equation

$$(c_1^{\pm})^2\Delta\varphi^{\pm} - \varphi^{\pm}_{,tt} = 0, \tag{1.16}$$

whereas utilization of the curl leads to

$$(c_2^{\pm})^2\Delta\boldsymbol{\psi}^{\pm} - \boldsymbol{\psi}^{\pm}_{,tt} = 0. \tag{1.17}$$

The dimensionless coordinates can be written as

$$\xi_m = \frac{x_m}{l}, \qquad \xi_3^- = \frac{x_3}{h}, \qquad \xi_3^+ = \frac{x_3 - h}{l}, \tag{1.18}$$

where ξ_3^- is applicable for the layer and ξ_3^+ for the half-space. In the above, l is a typical length (e.g. wave length in case of a dynamic problem or a length scale related to the load variation along the coordinates x_1, x_2 in case of a static problem) and $m = 1, 2$. In view of (1.18), constitutive relations (1.8) can be rearranged as

$$\begin{aligned}
\sigma^-_{mm} &= \frac{\lambda^- + 2\mu^-}{l}u^-_{m,m} + \frac{\lambda^-}{l}u^-_{n,n} + \frac{\lambda^-}{h}u^-_{3,3},\\
\sigma^-_{33} &= \frac{\lambda^-}{l}u^-_{1,1} + \frac{\lambda^-}{l}u^-_{2,2} + \frac{\lambda^- + 2\mu^-}{h}u^-_{3,3},\\
\sigma^-_{12} &= \frac{\mu^-}{l}(u^-_{1,2} + u^-_{2,1}),\\
\sigma^-_{m3} &= \frac{\mu^-}{h}(u^-_{m,3} + \frac{h}{l}u^-_{3,m}),
\end{aligned} \tag{1.19}$$

for the layer, and

$$\begin{aligned}
\sigma^+_{mm} &= \frac{1}{l}((\lambda^+ + 2\mu^+)u^+_{m,m} + \lambda^+ u^+_{n,n} + \lambda^+ u^+_{3,3}),\\
\sigma^+_{33} &= \frac{1}{l}(\lambda^+ u^+_{1,1} + \lambda^+ u^+_{2,2} + (\lambda^+ + 2\mu^+)u^+_{3,3}),\\
\sigma^+_{12} &= \frac{\mu^+}{l}(u^+_{1,2} + u^+_{2,1}),\\
\sigma^+_{m3} &= \frac{\mu^+}{l}(u^+_{m,3} + u^+_{3,m}),
\end{aligned} \tag{1.20}$$

for the half-space, with $n = 1, 2$; $n \neq m$.

Introducing the dimensionless time as

$$\tau_l = \frac{tc_2^-}{l}, \tag{1.21}$$

basic relations (1.1), then, can be written in dimensionless form as

$$\sigma^-_{i1,1} + \sigma^-_{i2,2} + \frac{l}{h}\sigma^-_{i3,3} = \frac{\mu^-}{l}u^-_{i,\tau_l\tau_l}, \qquad \sigma^+_{i1,1} + \sigma^+_{i2,2} + \sigma^+_{i3,3} = \frac{\mu^-}{l\rho}u^+_{i,\tau_l\tau_l}, \tag{1.22}$$

where

$$\rho = \frac{\rho^-}{\rho^+}. \tag{1.23}$$

In case of a static problem, equations (1.22) yield

$$\sigma^-_{i1,1} + \sigma^-_{i2,2} + \frac{l}{h}\sigma^-_{i3,3} = 0, \qquad \sigma^+_{i1,1} + \sigma^+_{i2,2} + \sigma^+_{i3,3} = 0. \tag{1.24}$$

For time-harmonic type of motion, the dimensionless variables can be expressed as

$$\Omega^\pm = \frac{\omega h}{c_2^\pm}, \qquad K = kh, \qquad \zeta^\pm = \frac{c}{c_2^\pm}. \tag{1.25}$$

In this case, accounting for (1.18), equations of motion (1.2) become

$$\sigma^-_{i1,1} + \sigma^-_{i2,2} + \frac{l}{h}\sigma^-_{i3,3} = -\frac{\mu^- l}{h^2}(\Omega^-)^2 u^-_i, \quad \sigma^+_{i1,1} + \sigma^+_{i2,2} + \sigma^+_{i3,3} = -\frac{\mu^+ l}{h^2}(\Omega^+)^2 u^-_i. \tag{1.26}$$

Note, that taking the dimensionless variables as (1.25) results in having the dimensionless time in the following form

$$\tau_h = \frac{tc_2^-}{h} \tag{1.27}$$

instead of (1.21) introduced earlier.

Let us also specify here that if the problem is considered in an anti-plane formulation then $u_1^{\pm} = u_3^{\pm} = 0$ and $u_2^{\pm} = u_2^{\pm}(x_1, x_3, t)$, where $u_2^{\pm}$ are known as anti-plane shear deformations. In case of a a plane strain assumption, $u_2^{\pm} = 0$ and $u_s^{\pm} = u_s^{\pm}(x_1, x_3, t)$, $s = 1, 3$.

If the thickness of the layer is assumed to be small compared to a typical length l, a small geometrical parameter can be introduced

$$\varepsilon = \frac{h}{l} \ll 1. \tag{1.28}$$

The presence of a contrast in stiffness of the coating and the half-space, in turn, implies a material parameter μ, which can be expressed as

$$\mu = \begin{cases} \dfrac{\mu^-}{\mu^+}, & \mu^- \leq \mu^+, \\ \dfrac{\mu^+}{\mu^-}, & \mu^+ \leq \mu^-, \end{cases} \lesssim 1, \tag{1.29}$$

where the first line corresponds to the case of the layer being softer than the half-space, and the second line is for a relatively stiff coating.

These geometrical and material parameters above can be related to each other as

$$\mu = \varepsilon^{\alpha}, \qquad \alpha \geq 0, \tag{1.30}$$

where for a fixed ε, α represents the level of the contrast, i.e. with an increase of α, the contrast in stiffness of the layer and the half-space becomes more pronounced. Note, that the limiting case $\alpha = 0$, associated with a non-contrast setup $\mu = 1$, is also included.

1.2 Models of elastic foundation

If a high contrast in stiffness of the layer and the half-space is assumed with the substrate being much stiffer, the model of elastic foundation is often implemented.

The simplest and apparently the most popular structural model of an elastic foundation is based on the Winkler-Fuss assumption treating a continuum as a system of vertical springs. Such a foundation is equivalent to a liquid base. In fact, as mentioned in [106], N. Fuss came to this hypothesis studying a beam floating along the surface of an incompressible fluid, whereas E. Winkler [172] considered a foundation as a mattress consisting of non-connected elastic springs, see also [40] for more detail. According to the hypothesis, the relation between the applied load P and the deflection of the surface w_0 is governed by the equation

$$P = rw_0, \tag{1.31}$$

where r is the foundation modulus or specific weight of the liquid base, and the deflection w_0 corresponds to the vertical displacement of the surface of the foundation, i.e. $w_0 = u_3^-\big|_{x_3=0}$, see Figure 1.2.

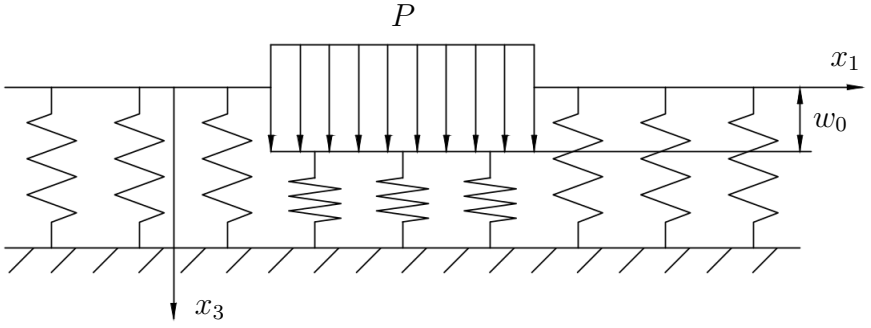

Figure 1.2: Winkler-Fuss foundation

It is also crucial that, according to the Winkler-Fuss hypothesis, the resulting dis-

placements occur only under the applied force, with the neighbouring area not affected. Therefore, in order to find a physically closer representation, some more advanced foundation models have been developed assuming some kind of interaction between the spring elements for the Winkler model. For example, the Filonenko-Borodich foundation [46] suggests a connection of the top ends of the independent springs with a stretched elastic membrane subjected to a constant-tension field. The Hetenyi model [68] is concerned with accomplishing the interaction by embedding an elastic beam or plate, which deform in bending only. The Pasternak foundation [137] proposes the existence of shear interactions between the spring elements, which may be achieved by connecting the ends of the springs to a beam or plate consisting of incompressible vertical elements deforming only by transverse shear. Thus, the relation between load P and the deflection of the surface w_0 is given by

$$P = rw_0 - T\Delta_{12}w_0, \tag{1.32}$$

where

$$\Delta_{12} = \frac{\partial^2}{\partial x_1^2} + \frac{\partial^2}{\partial x_2^2} \tag{1.33}$$

is the Laplace operator in x_1 and x_2. The second term on the right-hand side of (1.32) is due to the effect of shear interactions of the vertical elements.

1.3 Kirchhoff plate theory

In the opposite scenario, if the coating is considered to be much stiffer than the substrate, the model of a thin elastic plate is suggested by physical intuition as a natural approximation.

Let the mid-plane of the plate lie along the two in-plane dimensions with the normal extending along the vertical dimension, see Figure 1.3.

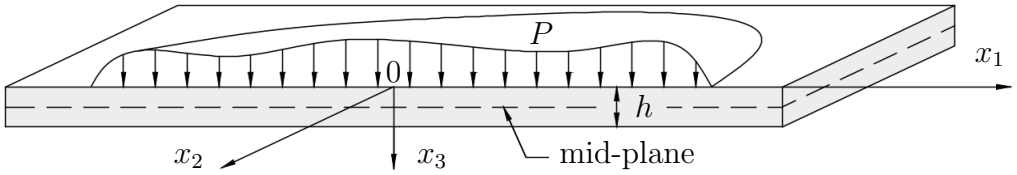

Figure 1.3: Kirchhoff plate

One of the most widely used theories for thin plates is the Kirchhoff plate theory [98], see e.g. [13] for a detailed review. It is based on assumptions dealing with the kinematics of a normal material line, i.e., a set of particles initially positioned in the direction normal to the mid-plane of the plate. A fundamental assumption of Kirchhoff plate theory is that the normal material line is infinitely rigid along its length, i.e., no deformations occur in the direction normal to the mid-plane. Also, during the deformation, the normal material line is assumed to remain straight and normal to the deformed mid-plane of the plate.

An investigation of the governing equations of Kirchhoff plate theory indicates that the initial problem can be separated into two simpler ones: in-plane and bending. The bending problem, in turn, can be reduced to a bi-harmonic partial differential equation for the deflection of the plate w_p as

$$D\Delta_{12}^2 w_p = P, \tag{1.34}$$

where

$$D = \frac{E^- h^3}{12[1-(\nu^-)^2]} \tag{1.35}$$

is the bending stiffness of the plate, P is the applied load, and the deflection is related to the transverse displacement, i.e. $w_p = u_3^-$.

Analysis of 3D equations of elasticity for bending of a thin layer also shows that the Kirchhoff theory is revealed as the leading order approximation of asymptotic expansion of the exact solution in the long-wave low-frequency limit, see [89].

1.4 Guided elastic waves

Considering dynamic problems for an elastic solid, we may distinguish three fundamental types of guided waves: Rayleigh [147], Rayleigh-Lamb [107] and Love waves. Brief derivations of these are given in this section, for detailed reviews see e.g. [1] and [89]. Rayleigh waves of arbitrary profile and hyperbolic-elliptic model for Rayleigh waves induced by surface stresses are also discussed in what follows.

1.4.1 Rayleigh surface waves

Let us start with a plane strain problem for an elastic isotropic half-space, see Figure 1.4.

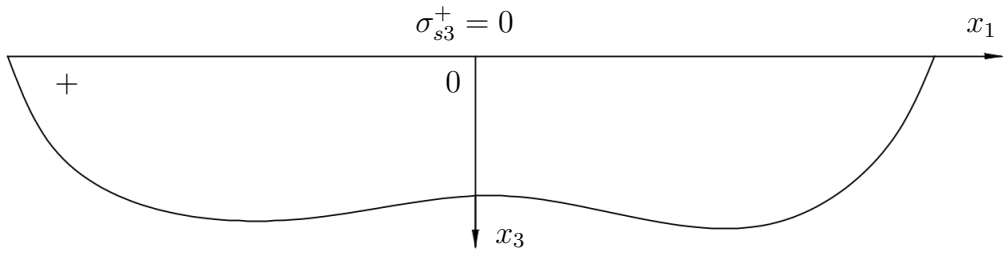

Figure 1.4: Plane strain problem for an elastic half-space

The surface is supposed to be traction free, therefore, the boundary conditions at $x_3 = 0$ are written as

$$\sigma_{s3}^{+} = 0. \tag{1.36}$$

The wave potentials are sought for in the form of travelling time-harmonic wave

solutions, namely

$$\varphi^+ = A\mathrm{e}^{ik(x_1-ct)-k\alpha^+x_3}, \qquad \psi_m^+ = 0, \quad m = 1,2, \qquad \psi_3^+ = B\mathrm{e}^{ik(x_1-ct)-k\beta^+x_3}, \quad (1.37)$$

decaying as $x_3 \to +\infty$. Substituting (1.37) into wave equations (1.16) and (1.17), we derive

$$\alpha^+ = \sqrt{1-\frac{c^2}{(c_1^+)^2}}, \qquad \beta^+ = \sqrt{1-\frac{c^2}{(c_2^+)^2}}. \quad (1.38)$$

Using (1.8) with (1.14) and (1.37), and substituting the result into (1.36), we have

$$\begin{aligned} 2i\alpha^+A + (1+(\beta^+)^2)B = 0, \\ (1+(\beta^+)^2)A - 2i\beta^+B = 0, \end{aligned} \quad (1.39)$$

which possesses a non-trivial solution provided that the related determinant equals zero, i.e.

$$4\alpha^+\beta^+ - (1+(\beta^+)^2)^2 = 0. \quad (1.40)$$

It is known that (1.40) has a unique solution $c = c_R$ called the Rayleigh wave speed, see e.g. [82], hence,

$$\alpha^+ = \alpha_R = \sqrt{1-\frac{c_R^2}{(c_1^+)^2}}, \qquad \beta^+ = \beta_R = \sqrt{1-\frac{c_R^2}{(c_2^+)^2}}. \quad (1.41)$$

Since the phase velocity is constant, the Rayleigh wave is non-dispersive.

1.4.2 Rayleigh waves of arbitrary profile

In the previous subsection the wave was considered to be time-harmonic (sinusoidal shape). Now, let us present the generalized version for an arbitrary profile, see [82].

Let us study the elastic potentials of the form

$$\varphi^+ = \varphi^+(x_1-ct, x_3), \qquad \psi_m^+ = 0, \qquad \psi_3^+ = \psi_3^+(x_1-ct, x_3), \quad (1.42)$$

corresponding to a wave of arbitrary shape propagating at a phase velocity c.

The boundary conditions (1.36) then can be rewritten as

$$2\varphi^+_{,13} + \psi^+_{3,11} - \psi^+_{3,33} = 0, \qquad (\gamma^- - 2)\varphi^+_{,11} + \gamma^-\varphi^+_{,33} + 2\psi^+_{3,13} = 0, \tag{1.43}$$

where γ^- is introduced in (1.12).

The wave equations (1.16) and (1.17) can be reduced to the elliptic equations

$$\varphi^+_{,33} + (\alpha^+)^2\varphi^+_{,11} = 0, \qquad \psi^+_{3,33} + (\beta^+)^2\psi^+_{3,11} = 0. \tag{1.44}$$

Thus, the eigensolutions for the elastic potentials are

$$\varphi^+ = \varphi^+(x_1 - ct, \alpha^+ x_3), \qquad \psi^+_3 = \psi^+_3(x_1 - ct, \beta^+ x_3), \tag{1.45}$$

which are harmonic functions.

Let us now employ the Cauchy-Riemann identities

$$f_{,3} = -\gamma H(f_{,1}), \qquad f_{,1} = \frac{1}{\gamma}H(f_{,3}), \qquad H(H(f)) = -f \tag{1.46}$$

for a harmonic function $f(x_1, \gamma x_3)$ being a solution of the equation

$$f_{,33} + \gamma^2 f_{,11} = 0, \tag{1.47}$$

where $H(f)$ is a Hilbert transform of function f, which is in fact its harmonic conjugate.

Applying aforementioned identities to the boundary conditions (1.45), we get

$$\begin{aligned} &-2\alpha^+ H(\varphi^+_{,11}) + (1 + (\beta^+)^2)\psi^+_{3,11} = 0, \\ &(1 + (\beta^+)^2)\varphi^+_{,11} + 2\beta^+ H(\psi^+_{3,11}) = 0. \end{aligned} \tag{1.48}$$

Then, after taking the Hilbert transform of the first equation, the solvability of (1.48) leads to Rayleigh equation (1.40). Hence, the sought for harmonic eigenfunctions are

$$\varphi^+ = \varphi^+(x_1 - c_R t, \alpha_R x_3), \qquad \psi^+_3 = \psi^+_3(x_1 - c_R t, \beta_R x_3), \tag{1.49}$$

where α_R and β_R are given in (1.41).

From boundary conditions (1.43) we obtain the relations between the potentials along the surface $x_3 = 0$

$$\psi^+_{3,1} = -\frac{2}{1+\beta_R^2}\varphi^+_{,3}, \qquad \psi^+_{3,3} = \frac{1+\beta_R^2}{2}\varphi^+_{,1}, \tag{1.50}$$

which after applying Cauchy-Riemann identities become

$$\psi^+_3 = \frac{2\alpha_R}{1+\beta_R^2}H(\varphi^+), \qquad \varphi^+ = -\frac{2\beta_R}{1+\beta_R^2}H(\psi^+_3). \tag{1.51}$$

Hence, the displacements along the surface $x_3 = 0$ can be expressed in terms of a single plane harmonic function, for example, in terms of the potential φ^+, as

$$u^+_1 = \left(1 - \frac{1+\beta_R^2}{2}\right)\varphi_{,1}, \qquad u^+_3 = \left(1 - \frac{2}{1+\beta_R^2}\right)\varphi_{,3}. \tag{1.52}$$

1.4.3 Hyperbolic-elliptic model for the Rayleigh waves induced by surface stresses

In this section we discuss the hyperbolic-elliptic model for Rayleigh wave field induced by surface stresses in a plane strain formulation, for more detail see [82] and [86].

We consider a plane strain problem for a half-space with prescribed stresses at the surface $x_3 = 0$ given by

$$\sigma^+_{33} = Q_1(x_1, t), \qquad \sigma^+_{13} = Q_2(x_1, t). \tag{1.53}$$

The problem is separated into vertical and horizontal considerations, i.e. with $Q_2 = 0$ and $Q_1 = 0$, respectively, and a slow-time perturbation procedure is applied.

As a result, using boundary conditions (1.53) for a vertical load Q_1 with $Q_2 = 0$, we obtain a 1D wave equation

$$\Box_R \varphi^+_N = \mathfrak{A} Q_1, \tag{1.54}$$

where

$$\Box_R = \frac{\partial^2}{\partial x_1^2} - \frac{1}{c_R^2}\frac{\partial^2}{\partial t^2} \tag{1.55}$$

is d'Alembert operator, φ_N^+ is a normal component of the potential φ^+ and

$$\mathfrak{A} = \frac{1+\beta_R^2}{2\mu^+ B}, \qquad \mathfrak{B} = \frac{\alpha_R}{\beta_R}(1-\beta_R^2) + \frac{\beta_R}{\alpha_R}(1-\alpha_R^2) - 1 + \beta_R^4. \tag{1.56}$$

The solution of the equation above provides a Dirichlet boundary condition at $x_3 = 0$ for the elliptic equation given by $(1.44)_1$ with $\alpha^+ = \alpha_R$.

Similarly, focusing on boundary conditions (1.53) for a horizontal load Q_2 with $Q_1 = 0$, we arrive at a problem for equation $(1.44)_2$ with $\beta^+ = \beta_R$ subject to the Dirichlet boundary condition in the form of the following wave equation

$$\Box_R \psi_{3T}^+ = -\mathfrak{A} Q_2, \tag{1.57}$$

where ψ_{3T}^+ is a transverse component of the potential ψ_3^+.

Taking into account relation between potentials $(1.51)_1$, equation (1.57) for a horizontal component can be rewritten as

$$\Box_R H(\varphi_T^+) = -\frac{\mathfrak{A}}{\Theta} Q_2, \tag{1.58}$$

which after applying Hilbert transform becomes

$$\Box_R \varphi_T^+ = \frac{\mathfrak{A}}{\Theta} H(Q_2). \tag{1.59}$$

In the above,

$$\Theta = \frac{2\alpha_R}{1+\beta_R^2}. \tag{1.60}$$

Combining equations (1.54) and (1.59) for vertical and horizontal components of the potential φ^+, respectively, and taking into account that $\varphi_T^+ + \varphi_N^+ = \varphi^+$, we arrive at

$$\Box_R \varphi^+ = \mathfrak{A}\left[Q_1 + \frac{H(Q_2)}{\Theta}\right]. \tag{1.61}$$

1.4.4 Rayleigh-Lamb waves

Now, let us consider a plane strain problem for an infinite layer of thickness $2h$, see Figure 1.5.

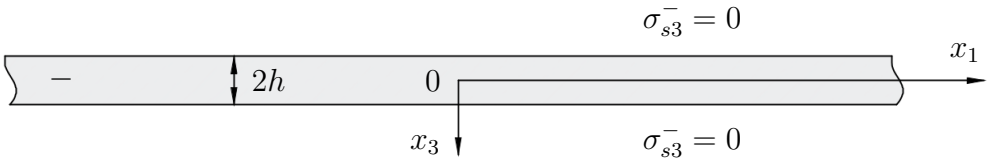

Figure 1.5: Plane strain problem for an infinite layer

We suppose the faces to be traction free, therefore, the boundary conditions at $x_3 = \pm h$ become

$$\sigma_{s3}^- = 0. \tag{1.62}$$

The wave potentials can be found as

$$\varphi^- = f(x_3)\mathrm{e}^{ik(x_1 - ct)}, \qquad \psi_m^- = 0, \qquad \psi_3^- = g(x_3)\mathrm{e}^{ik(x_1 - ct)}, \tag{1.63}$$

substitution of which into wave equations (1.16) and (1.17) leads to

$$\begin{aligned} f(x_3) &= A_1 \sin(\alpha^- k x_3) + A_2 \cos(\alpha^- k x_3), \\ g(x_3) &= B_1 \sin(\beta^- k x_3) + B_2 \cos(\beta^- k x_3), \end{aligned} \tag{1.64}$$

where

$$\alpha^- = \sqrt{\frac{c}{(c_1^-)^2} - 1}, \qquad \beta^- = \sqrt{\frac{c}{(c_2^-)^2} - 1}, \tag{1.65}$$

and A_m and B_m are arbitrary constants.

The modes of wave propagation corresponding to the above equations can be split up into two groups: symmetric and antisymmetric with respect to the mid-plane of the layer ($x_3 = 0$). Therefore, the displacement components can be written in terms

of elementary functions as

$$f = A_2 \cos(\alpha^- k x_3), \qquad g = B_1 \sin(\beta^- k x_3), \tag{1.66}$$

for the symmetric modes and

$$f = A_1 \sin(\alpha^- k x_3), \qquad g = B_2 \cos(\beta^- k x_3), \tag{1.67}$$

for the antisymmetric ones. Thus, for the symmetric modes the displacement u_1^- and the stresses σ_{ii}^- are even with respect to the thickness variable x_3 and the displacement u_3^- and the stress σ_{13}^- are odd and vice versa for the antisymmetric.

Substituting functions (1.66) into (1.63), (1.14) and (1.8), the boundary conditions (1.62) yield a system of two homogeneous equations for the constants A_2 and B_1 for symmetric modes. Similarly, for the antisymmetric modes two homogeneous equations for the constants A_1 and B_2 are obtained. Equating the determinants to zero we derive the Rayleigh-Lamb dispersion equations

$$\frac{\tan(\beta^- kh)}{\tan(\alpha^- kh)} = -\frac{4k^2\alpha^-\beta^-}{[(\beta^-)^2 - 1]^2} \tag{1.68}$$

and

$$\frac{\tan(\beta^- kh)}{\tan(\alpha^- kh)} = -\frac{[(\beta^-)^2 - 1]^2}{4k^2\alpha^-\beta^-} \tag{1.69}$$

for the symmetric and antisymmetric modes, respectively.

Employing the dimensionless variables Ω^- and K introduced in (1.25), dispersion relations (1.68) and (1.69) can be rewritten as

$$\frac{\tan\sqrt{(\Omega^-)^2 - K^2}}{\tan\sqrt{(\Omega^-/\kappa^-)^2 - K^2}} = -\frac{4K^2\sqrt{\left[(\Omega^-/\kappa^-)^2 - K^2\right]\left[(\Omega^-)^2 - K^2\right]}}{\left[(\Omega^-)^2 - 2K^2\right]^2} \tag{1.70}$$

and

$$\frac{\tan\sqrt{(\Omega^-)^2 - K^2}}{\tan\sqrt{(\Omega^-/\kappa^-)^2 - K^2}} = -\frac{\left[(\Omega^-)^2 - 2K^2\right]^2}{4K^2\sqrt{\left[(\Omega^-/\kappa^-)^2 - K^2\right]\left[(\Omega^-)^2 - K^2\right]}}, \tag{1.71}$$

where κ^- is defined in (1.13).

Let us now consider long-wave high-frequency approximation, i.e. $K \ll 1, \Omega \sim 1$. For small values of K, the dispersion relation for symmetric motions (1.70) is satisfied if

$$\sin(\Omega^-) = 0 \qquad \text{or} \qquad \cos\left(\frac{\Omega^-}{\kappa^-}\right) = 0, \tag{1.72}$$

and for antisymmetric motions (1.71) if

$$\sin\left(\frac{\Omega^-}{\kappa^-}\right) = 0 \qquad \text{or} \qquad \cos(\Omega^-) = 0, \tag{1.73}$$

resulting in

$$\begin{aligned} &\Omega^- = \Lambda_{st}^{sym} = \kappa^- \frac{\pi}{2} z, && \Omega^- = \Lambda_{st}^{anti} = \kappa^- \frac{\pi}{2} b, \\ &\Omega^- = \Lambda_{sh}^{sym} = \frac{\pi}{2} b, && \Omega^- = \Lambda_{sh}^{anti} = \frac{\pi}{2} z, \\ &z = 1, 3, 5, ..., && b = 2, 4, 6, ..., \end{aligned} \tag{1.74}$$

which are the so-called symmetric and antisymmetric thickness stretch and thickness shear resonance frequencies, respectively. They represent the natural frequencies of an infinitely thin transverse fibre of the layer and are eigenvalues of the problems

$$u_{1,33}^- + (\Omega^-)^2 u_1^- = 0, \qquad u_{3,33}^- + \left(\frac{\Omega^-}{\kappa^-}\right)^2 u_3^- = 0 \tag{1.75}$$

with $u_{s,3}^- = 0$, see Figure 1.6.

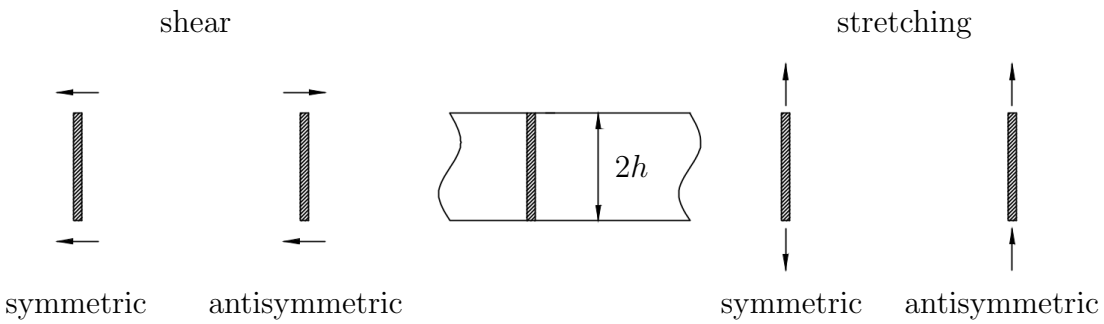

Figure 1.6: Infinitely thin transverse fibre of the layer

Note, that the Rayleigh wave equation can be obtained from the Rayleigh-Lamb dispersion relation in the short-wave limit.

1.4.5 Love waves

In this subsection we consider an anti-plane problem for a half-space coated by a layer of a different material, see Figure 1.1. Hence, equations of motion (1.10) take the form

$$u^{\pm}_{2,11} + u^{\pm}_{2,33} = \frac{1}{(c_2^{\pm})^2} u^{\pm}_{2,tt}. \tag{1.76}$$

We assume that the surface is free, therefore, the boundary condition is given by

$$\sigma^{-}_{23} = 0 \tag{1.77}$$

at $x_3 = 0$. We also impose continuity conditions at the interface $x_3 = h$

$$u^{-}_2 = u^{+}_2, \qquad \sigma^{-}_{23} = \sigma^{+}_{23}. \tag{1.78}$$

The displacements are sought for in the form

$$u^{\pm}_2 = f^{\pm}(x_3)\mathrm{e}^{ik(x_1 - ct)}. \tag{1.79}$$

In view of (1.79), equations of motion (1.76) become

$$f^{\pm\prime\prime} \pm k^2(\beta^{\pm})^2 f^{\pm} = 0, \tag{1.80}$$

where β^- and β^+ are defined in (1.65) and (1.38), respectively. The solution of (1.80) decaying at infinity can be found as

$$f^- = A\sin(\beta^- k x_3) + B\cos(\beta^- k x_3), \qquad f^+ = C\mathrm{e}^{-\beta^+ k x_3}, \tag{1.81}$$

where A, B and C are arbitrary constants. Using constitutive relation (1.8) together with (1.79) and (1.81) and substituting it into boundary and continuity conditions

(1.77) and (1.78), respectively, we obtain the dispersion relation

$$\tan(\beta^- kh) = \frac{\mu^- \beta^+}{\mu^+ \beta^-}. \tag{1.82}$$

Chapter 2

Anti-plane shear deformation

The anti-plane shear deformation problem of a half-space coated by a soft or a stiff thin layer is considered in the present chapter. The two-parametric asymptotic analysis is developed motivated by the scaling for the displacement and stress components obtained from the exact solution of a model problem for a shear sinusoidal load. It is shown that for a rather high contrast in stiffness of the layer and the half-space Winkler-type behaviour appears for a relatively soft coating, while for a relatively stiff one, the equations of plate shear are valid. For low contrast, an alternative approximation is suggested based on the reduced continuity conditions and the fact that the applied load may be transmitted to the interface. In case of a stiff layer, a simpler problem for a homogeneous half-space with effective boundary condition is also formulated, modelling the effect of the coating, whereas for a relatively soft layer a uniformly valid approximate formula is introduced. The results presented in this chapter were published in [159].

2.1 Statement of the problem

Consider an anti-plane problem of equilibrium for a homogeneous linearly elastic isotropic half-space coated by a thin isotropic layer of thickness h, subject to action of a smooth shear static force $P = P(x_1)$ at the surface of the coating ($x_3 = 0$), see Figure 2.1.

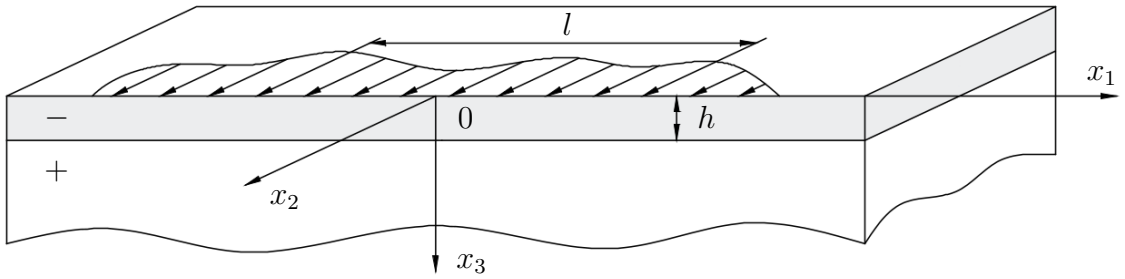

Figure 2.1: Anti-plane problem statement

We employ the dimensionless coordinates introduced in (1.18), and use, therefore, governing equations (1.19), (1.20) and (1.24), which, in anti-plane formulation, take the form

$$\frac{h}{l}\sigma^-_{12,1} + \sigma^-_{23,3} = 0, \qquad \sigma^-_{12} = \frac{\mu^-}{l}u^-_{2,1}, \qquad \sigma^-_{23} = \frac{\mu^-}{h}u^-_{2,3}, \tag{2.1}$$

for the layer, and

$$\sigma^+_{12,1} + \sigma^+_{23,3} = 0, \qquad \sigma^+_{12} = \frac{\mu^+}{l}u^+_{2,1}, \qquad \sigma^+_{m3} = \frac{\mu^+}{l}u^+_{2,3}, \tag{2.2}$$

for the half-space.

The boundary condition, modelling shear load at the surface of the layer, and continuity conditions at the interface take the form

$$\begin{aligned} &\sigma^-_{23} = -P, \qquad \xi^-_3 = 0, \\ &u^-_2 = u^+_2, \qquad \sigma^-_{23} = \sigma^+_{23}, \qquad \xi^-_3 = 1. \end{aligned} \tag{2.3}$$

We also impose the decay condition for the displacement, i.e. $u^+_2 \to 0$ as $\xi^+_3 \to +\infty$.

The layer is considered to be thin, leading to small geometrical parameter (1.28). A contrast in stiffness of the layer and the half-space is also assumed, represented by material parameter (1.29), see Section 1.1 for more detail. In what follows, we use relation (1.30) connecting these two parameters.

2.2 Model problem for a sinusoidal shear load

We begin the analysis with investigation of a model problem for a shear sinusoidal force

$$P = A\mu^{-} \sin \xi_1, \tag{2.4}$$

where A is a constant amplitude, see Figure 2.2.

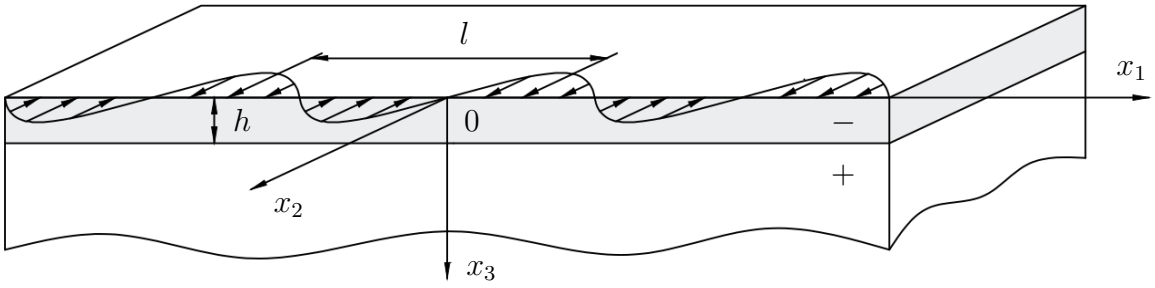

Figure 2.2: Model problem for a sinusoidal surface load

In this case, the displacements may be sought as

$$u_2^{\pm} = f^{\pm}(\xi_3^{\pm}) \sin \xi_1. \tag{2.5}$$

Substituting (2.5) into governing equations (2.1) and (2.2), we have

$$f^{-\prime\prime}(\xi_3^{-}) - \varepsilon^2 f^{-}(\xi_3^{-}) = 0, \qquad f^{+\prime\prime}(\xi_3^{+}) - f^{+}(\xi_3^{+}) = 0. \tag{2.6}$$

Taking into account boundary and continuity conditions (2.3), the solution of (2.6) decaying at infinity is written as

$$f^{-}(\xi_3^{-}) = C_1 e^{\varepsilon \xi_3^{-}} + C_2 e^{-\varepsilon \xi_3^{-}}, \qquad f^{+}(\xi_3^{+}) = C_3 e^{-\xi_3^{+}}, \tag{2.7}$$

where

$$C_i = \frac{N_i}{D}, \qquad i = 1, 2, 3,$$

with

$$N_1 = Ah(\mu^- - \mu^+), \qquad N_3 = 2Ah\mathrm{e}^{\varepsilon}\mu^-,$$

$$N_2 = Ah\mathrm{e}^{2\varepsilon}(\mu^- + \mu^+), \qquad D = \varepsilon\left[\mu^-(\mathrm{e}^{2\varepsilon} - 1) + \mu^+(\mathrm{e}^{2\varepsilon} + 1)\right].$$

Substituting the latter into relations (2.1) and (2.2), the stress components are found in the form

$$\begin{aligned} \sigma_{12}^{\pm} &= \frac{\mu^{\pm}}{l} f^{\pm}(\xi_3^{\pm}) \cos\xi_1, \qquad \sigma_{23}^{+} = -\frac{\mu^{+}}{l} f^{+}(\xi_3^{+}) \sin\xi_1, \\ \sigma_{23}^{-} &= \frac{\mu^{-}}{h} \varepsilon \left(C_1 e^{\varepsilon\xi_3^-} - C_2 e^{-\varepsilon\xi_3^-} \right) \sin\xi_1. \end{aligned} \tag{2.8}$$

Then, using (1.28) and (1.29) together with (1.30), we deduce the leading order asymptotic behaviour of the displacements and stresses obtained above, in terms of a small parameter ε, for a relatively soft and a stiff layer, see Table 2.1.

		u_2^-	σ_{12}^-	σ_{23}^-	u_2^+	σ_{12}^+	σ_{23}^+
Soft layer	$\alpha \geq 1$	1	ε	1	$\varepsilon^{\alpha-1}$	1	1
	$0 \leq \alpha \leq 1$	$\varepsilon^{\alpha-1}$	ε^{α}	1	$\varepsilon^{\alpha-1}$	1	1
Stiff layer	$\alpha \geq 1$	ε^{-2}	ε^{-1}	1	ε^{-2}	$\varepsilon^{\alpha-1}$	$\varepsilon^{\alpha-1}$
	$0 \leq \alpha \leq 1$	$\varepsilon^{-\alpha-1}$	$\varepsilon^{-\alpha}$	1	$\varepsilon^{-\alpha-1}$	1	1

Table 2.1: Asymptotic behaviour of displacements and stresses

Now, we study in more detail the relation between displacement u_2^- at the surface of the coating ($\xi_3^- = 0$) and prescribed load P by introducing the coefficient

$$r = \frac{P}{u_2^-\big|_{\xi_3^-=0}}. \tag{2.9}$$

Note, that this coefficient is constant only for the considered sinusoidal load. In general, the relation between displacement $u_2^-\big|_{\xi_3^-=0}$ and load P is a function of ξ_1. In case of a

shear sinusoidal load (2.4), it is given by

$$r = \frac{A\mu^- D}{N_1 + N_2}, \tag{2.10}$$

following from (2.5) and $(2.7)_1$. The leading order estimates of the coefficient r depending on the parameter α are presented in Table 2.2.

		$\alpha > 1$	$\alpha = 1$	$0 \leq \alpha < 1$
r	Soft layer	$\dfrac{\mu^-}{h}$	$\dfrac{\mu^-\mu^+}{h\mu^+ + l\mu^-}$	$\dfrac{\mu^+}{l}$
	Stiff layer	$\dfrac{\mu^- h}{l^2}$	$\dfrac{2\mu^- h}{l^2}$	$\dfrac{\mu^+}{l}$

Table 2.2: Leading order of the coefficient r for a sinusoidal shear force

Therefore, at $\alpha > 1$, the coefficient r does not depend on the stiffness of the half-space μ^+, meaning that the deformation of the substrate is neglected. In general, in case of a rather soft layer, it may be described as a Winkler-type behaviour, see Section 1.2 for more detail, while for a stiff layer, taking into account the term l^2, it indicates that the plate shear equation may be expected as a relation between $u_2^-\big|_{\xi_3^-=0}$ and P, see Section 1.3. In the range $0 \leq \alpha < 1$, the relation is entirely affected by the presence of the half-space, i.e. the layer may no longer be separated, and the original problem for a coated solid should be considered. The case $\alpha = 1$ seems to be a transition point, since, for instance, for a soft layer, r depends on both μ^- and μ^+, but, at the same time, according to assumptions (1.28), $(1.29)_1$ and relation (1.30), $\dfrac{h}{l} = \dfrac{\mu^-}{\mu^+} = \varepsilon$, thus, it may also be written as $r = \dfrac{\mu^-}{2h}$.

2.3 Asymptotic analysis

In this section we proceed with a more general insight for an arbitrary load acting on the surface of the layer, adopting asymptotic procedure widely used in mechanics of thin elastic structures, see e.g. [3, 36, 44]. Note that the scaling is motivated by the asymptotic orders in Table 2.1, obtained for a sinusoidal shear force.

2.3.1 Soft layer, $\alpha \geq 1$ ($\mu \lesssim \varepsilon$)

First, we scale the displacement and stress components according to the first row of the Table 2.1, having for a relatively soft layer

$$u_2^- = h u_2^{-*}, \qquad \sigma_{12}^- = \mu^- \varepsilon \sigma_{12}^{-*}, \qquad \sigma_{23}^- = \mu^- \sigma_{23}^{-*}, \tag{2.11}$$

where the quantities with the asterisk in superscript are assumed to be of the same asymptotic order. Hence, governing equations (2.1) become

$$\varepsilon^2 \sigma_{12,1}^{-*} + \sigma_{23,3}^{-*} = 0, \qquad \sigma_{12}^{-*} = u_{2,1}^{-*}, \qquad \sigma_{23}^{-*} = u_{2,3}^{-*}. \tag{2.12}$$

Similarly, substituting the scaling for the half-space given by

$$u_2^+ = h\varepsilon^{\alpha-1} u_2^{+*}, \qquad \sigma_{12}^+ = \mu^- \sigma_{12}^{+*}, \qquad \sigma_{23}^+ = \mu^- \sigma_{23}^{+*}, \tag{2.13}$$

into equations (2.2), we get

$$\sigma_{12,1}^{+*} + \sigma_{23,3}^{+*} = 0, \qquad \sigma_{12}^{+*} = u_{2,1}^{+*}, \qquad \sigma_{23}^{+*} = u_{2,3}^{+*}. \tag{2.14}$$

Here and below, the applied load is scaled as

$$P = \mu^- p^*. \tag{2.15}$$

In what follows, boundary and continuity conditions (2.3), may be rewritten as

$$\begin{aligned} &\sigma_{23}^{-*} = -p^*, \qquad \xi_3^- = 0, \\ &u_2^{-*} = \varepsilon^{\alpha-1} u_2^{+*}, \qquad \sigma_{23}^{-*} = \sigma_{23}^{+*}, \qquad \xi_3^- = 1. \end{aligned} \tag{2.16}$$

Next, we expand the displacements and stresses of the layer in asymptotic series

$$\begin{pmatrix} u_2^{-*} \\ \sigma_{12}^{-*} \\ \sigma_{23}^{-*} \end{pmatrix} = \begin{pmatrix} u_2^{-(0)} \\ \sigma_{12}^{-(0)} \\ \sigma_{23}^{-(0)} \end{pmatrix} + \dots . \tag{2.17}$$

Thus, at leading order we have from (2.12)

$$\sigma_{23,3}^{-(0)} = 0, \qquad \sigma_{12}^{-(0)} = u_{2,1}^{-(0)}, \qquad \sigma_{23}^{-(0)} = u_{2,3}^{-(0)}, \tag{2.18}$$

subject to boundary conditions at $\xi_3^- = 0$

$$\sigma_{23}^{-(0)} = -p^*. \tag{2.19}$$

In view of (2.16), $u_2^{-*} \gg u_2^{+*}$ at $\alpha > 1$ while $u_2^{-*} \sim u_2^{+*}$ at $\alpha = 1$, therefore, the leading order continuity conditions at $\xi_3^- = 1$ become

$$\sigma_{23}^{-(0)} = \sigma_{23}^{+(0)}, \qquad u_2^{-(0)} = 0, \quad \alpha > 1, \qquad u_2^{-(0)} = u_2^{+(0)}, \quad \alpha = 1. \tag{2.20}$$

From $(2.18)_1$ and satisfying (2.19), we obtain

$$\sigma_{23}^{-(0)} = -p^*, \tag{2.21}$$

Then, using $(2.18)_3$ together with (2.20), we deduce

$$\begin{aligned} &u_2^{-(0)} = p^*(1 - \xi_3^-), \quad \alpha > 1, \\ &u_2^{-(0)} = p^*(1 - \xi_3^-) + u_2^{+(0)}\Big|_{\xi_3^- = 1}, \quad \alpha = 1. \end{aligned} \tag{2.22}$$

Therefore, as it was discussed above, at $\xi_3^- = 0$, the relation between displacement and applied load at $\alpha > 1$ is not affected by the presence of the substrate, which may be

described as Winkler-type behaviour, while for $\alpha = 1$ the reaction of the half-space is involved. The same happens for shear stress $\sigma_{12}^{-(0)}$, for which we have from $(2.18)_2$ and (2.22)

$$\begin{aligned} \sigma_{12}^{-(0)} &= \frac{\partial p^*}{\partial \xi_1}(1-\xi_3^-), \quad \alpha > 1, \\ \sigma_{12}^{-(0)} &= \frac{\partial p^*}{\partial \xi_1}(1-\xi_3^-) + \left.\frac{\partial u_2^{+(0)}}{\partial \xi_1}\right|_{\xi_3^-=1}, \quad \alpha = 1. \end{aligned} \tag{2.23}$$

2.3.2 Soft layer, $0 \leq \alpha < 1$ ($\varepsilon \lesssim \mu \ll 1$)

The scaling for the layer now takes the form

$$u_2^- = h\varepsilon^{\alpha-1}u_2^{-*}, \qquad \sigma_{12}^- = \mu^-\varepsilon^\alpha\sigma_{12}^{-*}, \qquad \sigma_{23}^- = \mu^-\sigma_{23}^{-*}, \tag{2.24}$$

leading to

$$\varepsilon^{\alpha+1}\sigma_{12,1}^{-*} + \sigma_{23,3}^{-*} = 0, \qquad \sigma_{12}^{-*} = u_{2,1}^{-*}, \qquad \varepsilon^{1-\alpha}\sigma_{23}^{-*} = u_{2,3}^{-*}. \tag{2.25}$$

The scaling and the equations for the half-space are taken as (2.13) and (2.14), respectively, with boundary condition $(2.16)_1$, whereas the continuity conditions at $\xi_3^- = 1$ become

$$\sigma_{23}^{-*} = \sigma_{23}^{+*}, \qquad u_2^{-*} = u_2^{+*}. \tag{2.26}$$

At leading order, the equations for the layer are

$$\sigma_{23,3}^{-(0)} = 0, \qquad \sigma_{12}^{-(0)} = u_{2,1}^{-(0)}, \qquad u_{2,3}^{-(0)} = 0, \tag{2.27}$$

subject to boundary condition (2.19) and the following continuity conditions at $\xi_3^- = 1$

$$\sigma_{23}^{-(0)} = \sigma_{23}^{+(0)}, \qquad u_2^{-(0)} = u_2^{+(0)}. \tag{2.28}$$

As above, quantity $\sigma_{23}^{-(0)}$ is expressed as (2.21). Then, $(2.27)_3$ and $(2.28)_2$ imply

$$u_2^{-(0)} = \left.u_2^{+(0)}\right|_{\xi_3^-=1}. \tag{2.29}$$

Finally, $(2.27)_2$ yields

$$\sigma_{12}^{-(0)} = \left.\frac{\partial u_2^{+(0)}}{\partial \xi_1}\right|_{\xi_3^-=1}. \tag{2.30}$$

Hence, shear displacement and stress depend only on the deformation of the substrate.

2.3.3 Stiff layer, $\alpha \geq 1$ ($\mu \lesssim \varepsilon$)

For a stiff layer, we scale the displacements and stresses according to the third row in Table 2.1

$$u_2^- = h\varepsilon^{-2} u_2^{-*}, \qquad \sigma_{12}^- = \mu^- \varepsilon^{-1} \sigma_{12}^{-*}, \qquad \sigma_{23}^- = \mu^- \sigma_{23}^{-*}, \tag{2.31}$$

which implies

$$\sigma_{12,1}^{-*} + \sigma_{23,3}^{-*} = 0, \qquad \sigma_{12}^{-*} = u_{2,1}^{-*}, \qquad \varepsilon^2 \sigma_{23}^{-*} = u_{2,3}^{-*}. \tag{2.32}$$

The scaling for the half-space is taken as

$$u_2^+ = h\varepsilon^{-2} u_2^{+*}, \qquad \sigma_{12}^+ = \mu^- \varepsilon^{\alpha-1} \sigma_{12}^{+*}, \qquad \sigma_{23}^+ = \mu^- \varepsilon^{\alpha-1} \sigma_{23}^{+*}, \tag{2.33}$$

which, substituted into (2.2), gives (2.14). Boundary condition, again, is expressed as (2.19), while the continuity conditions at $\xi_3^- = 1$ are

$$u_2^{-*} = u_2^{+*}, \qquad \sigma_{23}^{-*} = \varepsilon^{\alpha-1} \sigma_{23}^{+*}. \tag{2.34}$$

At leading order for the layer we have

$$\sigma_{12,1}^{-(0)} + \sigma_{23,3}^{-(0)} = 0, \qquad \sigma_{12}^{-(0)} = u_{2,1}^{-(0)}, \qquad u_{2,3}^{-(0)} = 0, \tag{2.35}$$

with boundary condition (2.19). Taking into account $(2.34)_2$, i.e. $\sigma_{23}^{-*} \gg \sigma_{23}^{+*}$ at $\alpha > 1$, and $\sigma_{23}^{-*} \sim \sigma_{23}^{+*}$ at $\alpha = 1$, the continuity conditions at $\xi_3^- = 1$ are

$$u_2^{-(0)} = u_2^{+(0)}, \qquad \sigma_{23}^{-(0)} = 0, \quad \alpha > 1, \qquad \sigma_{23}^{-(0)} = \sigma_{23}^{+(0)}, \quad \alpha = 1. \tag{2.36}$$

From $(2.35)_3$ we have

$$u_2^{-(0)} = V, \tag{2.37}$$

where $V = V(\xi_1)$ which may be denoted as a dimensionless shear of the coating, thus, displacement $u_2^{-(0)}$ is constant across the thickness of the layer. Next, we deduce from $(2.35)_2$

$$\sigma_{12}^{-(0)} = \frac{\partial V}{\partial \xi_1}. \tag{2.38}$$

Using $(2.35)_1$ and satisfying boundary condition (2.19), we obtain

$$\sigma_{23}^{-(0)} = -\frac{\partial^2 V}{\partial \xi_1^2}\xi_3^- - p^*. \tag{2.39}$$

Finally, from continuity conditions (2.36), we have

$$\begin{aligned} &\frac{\partial^2 V}{\partial \xi_1^2} = -p^*, \quad \alpha > 1, \\ &\frac{\partial^2 V}{\partial \xi_1^2} = -p^* - \sigma_{23}^{+(0)}\Big|_{\xi_3^- = 1}, \quad \alpha = 1, \end{aligned} \tag{2.40}$$

which are in fact the equations of plate shear, with the substrate reaction equal to 0 at $\alpha > 1$.

2.3.4 Stiff layer, $0 \leq \alpha < 1$ $(\varepsilon \lesssim \mu \ll 1)$

In this case, the scaling for the layer is given by

$$u_2^- = h\varepsilon^{-\alpha-1}u_2^{-*}, \qquad \sigma_{12}^- = \mu^-\varepsilon^{-\alpha}\sigma_{12}^{-*}, \qquad \sigma_{23}^- = \mu^-\sigma_{23}^{-*}, \tag{2.41}$$

with the governing equations

$$\varepsilon^{1-\alpha}\sigma_{12,1}^{-*} + \sigma_{23,3}^{-*} = 0, \qquad \sigma_{12}^{-*} = u_{2,1}^{-*}, \qquad \varepsilon^{\alpha+1}\sigma_{23}^{-*} = u_{2,3}^{-*}. \tag{2.42}$$

The scaling for the half-space is

$$u_2^+ = h\varepsilon^{-\alpha-1}u_2^{+*}, \qquad \sigma_{12}^+ = \mu^-\sigma_{12}^{+*}, \qquad \sigma_{23}^+ = \mu^-\sigma_{23}^{+*}, \tag{2.43}$$

with equations (2.14). Boundary and continuity conditions are taken as (2.19) and (2.28).

The leading order equations and results are the same as in Subsection 2.3.2.

2.3.5 Reduced problem formulations for a half-space

As it follows from the analysis above, for some cases the expressions for stresses and displacements involve the interfacial displacement $u_2^{+(0)}\Big|_{\xi_3^-=1}$ and stress $\sigma_{23}^{+(0)}\Big|_{\xi_3^-=1}$, see $(2.22)_2$, $(2.23)_2$, (2.29) and $(2.40)_2$. The asymptotic treatment allows us to formulate reduced problems for the half-space separately from the layer, from the solutions of which these interfacial values can be derived.

For a soft layer, shear stress $\sigma_{23}^{-(0)}$ is uniform across the thickness of the layer, see (2.21), and may be transmitted to the interface. Therefore, taking into account continuity conditions $(2.20)_1$ and $(2.28)_1$, the problem for a homogeneous half-space may be formulated with the following boundary conditions at the interface $\xi_3^+ = 0$

$$\sigma_{23}^{+} = P. \tag{2.44}$$

Hence, the value of interfacial displacement $u_2^{+(0)}\Big|_{\xi_3^-=1}$ in formulae $(2.22)_2$, $(2.23)_2$ and (2.29) follow from the solution of the stated problem.

In case of a stiff layer, for $\alpha = 1$, taking into account continuity conditions $(2.36)_1$ and $(2.36)_3$, the expression for the shear of the layer (2.37) and the equation of plate shear $(2.40)_2$, we arrive at the following effective boundary condition for a half-space

$$\sigma_{23}^{+} = -P - \frac{\mu^+}{l}\frac{\partial^2 u_2^+}{\partial \xi_1^2}\bigg|_{\xi_3^+=0}. \tag{2.45}$$

Thus, the value of the shear V for $\alpha = 1$ can be obtained by solving this reduced problem.

Let us now present solutions of the problems discussed above for sinusoidal P. In what follows, we consider a homogeneous elastic half-space ($\xi_3^+ \geq 0$) subject to boundary conditions (2.44) and (2.45) for load (2.4) denoted as Case 1 and Case 2 in Table 2.3, respectively.

The equations of the formulated problems and the solutions are given by (2.2) and (2.5) with functions $(2.7)_2$, where the values of the coefficient C_3, corresponding to the related case of the applied boundary conditions, are presented in Table 2.3, together with the displacement and stress components at the surface $\xi_3^+ = 0$.

	Case 1	Case 2
Boundary conditions		
σ_{23}^+	$-A\mu^- \sin\xi_1$	$-A\mu^- \sin\xi_1 - \dfrac{\mu^+}{l}\dfrac{\partial^2 u_2^+}{\partial \xi_1^2}\Big\vert_{\xi_3^+=0}$
Coefficient in $(2.7)_2$		
C_3	$\dfrac{Aa\mu^-}{\mu^+}$	$\dfrac{Aa\mu^-}{2\mu^+}$
Displacements and stresses at the surface		
u_2^+	$\dfrac{Aa\mu^- \sin\xi_1}{\mu^+}$	$\dfrac{Aa\mu^- \sin\xi_1}{2\mu^+}$
σ_{12}^+	$A\mu^- \cos\xi_1$	$\dfrac{A\mu^- \cos\xi_1}{2}$
σ_{23}^+	$-A\mu^- \sin\xi_1$	$-\dfrac{A\mu^- \sin\xi_1}{2}$

Table 2.3: Anti-plane BVPs for a homogeneous half-space

2.4 Numerical comparison of the asymptotic results with the exact solution

In this section the derived asymptotic results are tested by comparison with the exact solution of a problem for sinusoidal load (2.4) applied at the surface of the layer $x_3 = 0$. In doing so, we study the coefficient r introduced in (2.9).

For the exact solution, coefficient r follows from (2.10).

For the asymptotic results, in case of a soft layer, we use relations (2.22) for $\alpha > 1$ and $\alpha = 1$, and (2.29) for $0 \leq \alpha < 1$. The value of the interfacial displacement $u_2^{+(0)}\Big|_{\xi_3^- = 1}$, due to continuity conditions $(2.20)_3$ and $(2.28)_2$, may be found from a simpler problem for a homogeneous half-space discussed in Subsection 2.3.5. Its solution for sinusoidal load (2.4) is presented as Case 1 in Table 2.3.

In order to derive r for a stiff layer, we solve plate shear equations (2.40) for $\alpha > 1$ and $\alpha = 1$. For the latter case, taking into account continuity condition $(2.36)_1$, the shear of the layer, see (2.37), may be again derived from a problem for a half-space, see Subsection 2.3.5 (Case 2 in Table 2.3 for a solution for a sinusoidal load). The case $0 \leq \alpha < 1$ is identical to one for a soft layer.

As a result, asymptotic formulae for coefficient r coincide with leading order exact solution presented in Table 2.2.

As an illustration, we plot the dimensionless coefficient

$$r_* = \frac{h}{\mu^-} r, \tag{2.46}$$

in Figure 2.3 for a soft and a stiff layer, with $\alpha = \log_\varepsilon \mu$, Poisson's ratios $\nu^- = 0.25$ and $\nu^+ = 0.3$, and $\varepsilon = 0.1$.

(a) soft coating

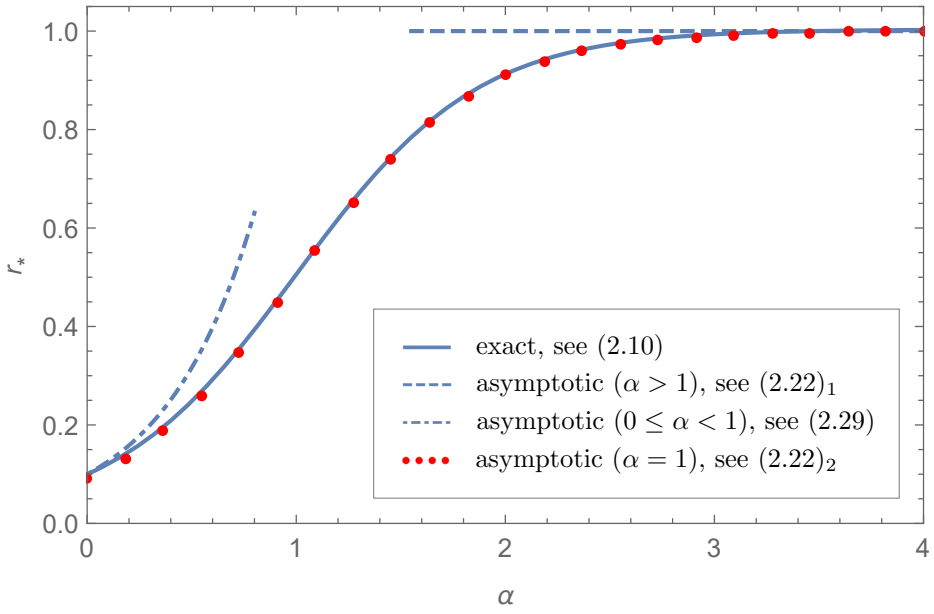

(b) stiff coating

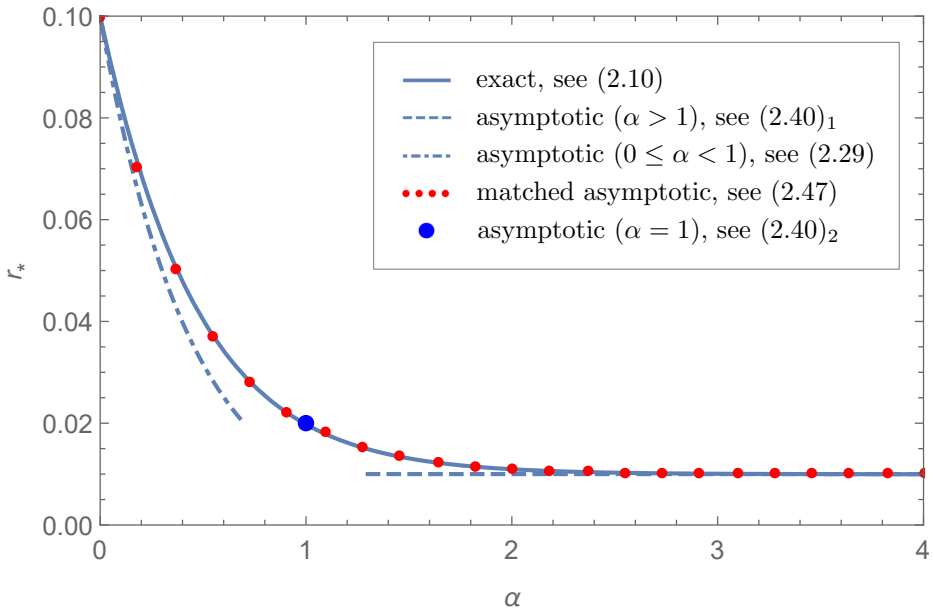

Figure 2.3: Asymptotic and exact solutions of an anti-plane problem for sinusoidal load ($\varepsilon = 0.1$, $\nu^- = 0.25$, $\nu^+ = 0.3$)

Here, blue solid lines correspond to the exact solution, dashed and dot-dashed lines display the asymptotic approximations at $\alpha > 1$ (formula $(2.22)_1$ in case of a soft coating and $(2.40)_1$ for a stiff one) and $0 \le \alpha < 1$ (formula (2.29) valid for both soft and

stiff layers), respectively, which have limited ranges of applicability. For a soft coating, case $\alpha = 1$ gives two-term approximation $(2.22)_2$, which appears to be uniformly valid over the whole range of parameter α, and the associated curve, denoted by red dots in Figure 2.3(a), is very close to the exact solution. As for a stiff layer, approximation at $\alpha = 1$, represented by formula $(2.40)_2$, is a limiting case, displayed by the blue dot in Figure 2.3(b), being valid only for this particular value of α, therefore, there is no uniformly valid approximation. We can, however, match the derived approximations through

$$\tilde{r}_* = r_*^0 \mathrm{e}^{-\frac{\alpha}{b}} + r_*^\infty \left(1 - \mathrm{e}^{-\frac{\alpha}{b}}\right), \tag{2.47}$$

where r_*^0 and r_*^∞ are dimensionless coefficients for approximations at $\alpha = 0$ and $\alpha > 1$, respectively, and b can be found using the value of r_* at $\alpha = 1$. For sinusoidal load (2.4), $b \approx 0.455$, and the related curve is plotted with red dots in Figure 2.3(b).

Chapter 3

3D deformation

Here we extend the methodology presented in the previous chapter to a full 3D problem in order to validate Winkler-Fuss hypothesis for a relatively soft layer and Kirchhoff theory for thin plates in case of the coating being stiff. Two-parametric asymptotic analysis of the equilibrium of an elastic half-space coated by a thin soft or stiff layer for a 3D setup is developed. The initial scaling is motivated by the exact solution of the plane strain problem for a vertical sinusoidal load. It is established that Winkler-Fuss hypothesis and Kirchhoff theory for thin plates are valid only for a sufficiently high contrast in stiffness of the layer and the half-space. As an alternative, a uniformly valid non-local approximation is proposed in case of a soft layer. Higher order corrections to the Winkler-Fuss formulation, such as the Pasternak model, are also studied. In the scenario, in which the Kirchhoff theory fails, other approximate formulations are introduced, reducing the original problem for a coated solid to problems for a homogeneous half-space with Neumann, mixed or effective boundary conditions along its surface. The results of the present chapter were published in [78] and [79] considering relatively soft and stiff layer, respectively.

3.1 Statement of the problem

Consider a thin linearly isotropic elastic layer ($0 \leq x_3 \leq h$) resting on an elastic half-space ($x_3 \geq h$). Let a smooth vertical static force $P = P(x_1, x_2)$ be applied at the surface of the layer, see Figure 3.1.

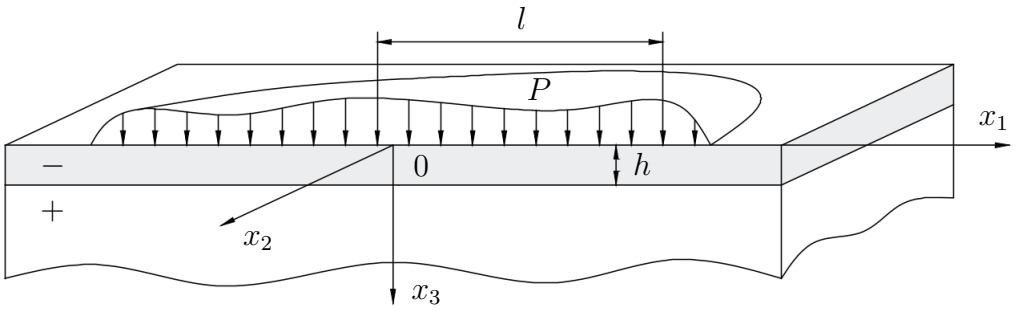

Figure 3.1: Problem statement for a 3D problem

As in Chapter 2, we use dimensionless coordinates (1.18) with governing equations (1.24) and constitutive relations (1.19) and (1.20). We also employ parameters (1.28) and (1.29), corresponding to the relative thickness and stiffness of the layer, respectively, together with relation (1.30).

The boundary conditions at $x_3 = 0$ modelling vertical loading at the upper face of the layer are

$$\sigma_{33}^{-} = -P, \qquad \sigma_{m3}^{-} = 0, \tag{3.1}$$

where $m = 1, 2$. We also impose the continuity conditions

$$u_i^{-} = u_i^{+}, \qquad \sigma_{i3}^{-} = \sigma_{i3}^{+} \tag{3.2}$$

at the interface $x_3 = h$. The decay of the spacial displacements is also assumed, i.e. $u_i^{+} \to 0$, as $x_3 \to +\infty$.

For numerous applications the most important consequence of the solution of the

stated problem is the relation between the applied load and the vertical displacement of the upper face of the layer. In case of a soft layer, similarly to the anti-plane problem presented in Chapter 2, we may expect Winkler-Fuss hypothesis to be applicable, see Section 1.2 for more detail, while in case of a stiff thin coating resting on a soft substrate, the model of a thin elastic plate may be used to describe the behaviour, see Section 1.3. In this chapter we develop a two-parametric asymptotic procedure, aiming at estimating the range of the parameter α, for which the Winkler-Fuss approximation and the theory of thin plates may be validated and mathematically justified. Refinements to this model are also derived in what follows.

3.2 Plane strain problem for a sinusoidal load

We begin with a model plane strain problem for a vertical sinusoidal force

$$P = A\mu^{-}\cos\xi_1, \tag{3.3}$$

where A is constant amplitude, see Figure 3.2.

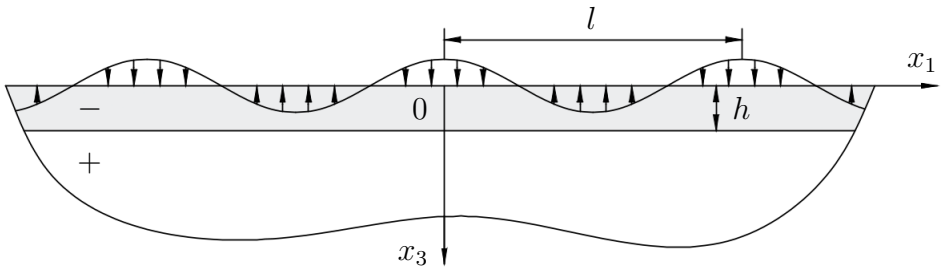

Figure 3.2: Plane problem for a sinusoidal surface load

The associated dimensionless equations of equilibrium may be taken in the form of

(1.19), (1.20) and (1.24), setting $u_2^{\pm}=0$ and $u_{s,2}^{\pm}=0$, $s=1,3$, i.e.

$$\begin{aligned}
&(\lambda^-+2\mu^-)\varepsilon^2 u^-_{1,11}+(\lambda^-+\mu^-)\varepsilon u^-_{3,13}+\mu^- u^-_{1,33}=0,\\
&\mu^-\varepsilon^2 u^-_{3,11}+(\lambda^-+\mu^-)\varepsilon u^-_{1,13}+(\lambda^-+2\mu^-)u^-_{3,33}=0,\\
&(\lambda^++2\mu^+)u^+_{1,11}+(\lambda^++\mu^+)u^+_{3,13}+\mu^+ u^+_{1,33}=0,\\
&\mu^+ u^+_{3,11}+(\lambda^++\mu^+)u^+_{1,13}+(\lambda^++2\mu^+)u^+_{3,33}=0.
\end{aligned} \tag{3.4}$$

The boundary conditions (3.1) become

$$\sigma^-_{33}=-A\mu^-\cos\xi_1, \qquad \sigma^-_{13}=0, \tag{3.5}$$

with continuity (3.2) and decay conditions.

The sought for displacement components may be presented as

$$u_1^{\pm}=f_1^{\pm}(\xi_3^{\pm})\sin\xi_1, \qquad u_3^{\pm}=f_3^{\pm}(\xi_3^{\pm})\cos\xi_1. \tag{3.6}$$

Then, on substituting (3.6) into (3.4), we have

$$\begin{aligned}
&\mu^- f_1^{-\prime\prime}(\xi_3^-)-(\lambda^-+2\mu^-)\varepsilon^2 f_1^-(\xi_3^-)-(\lambda^-+\mu^-)\varepsilon f_3^{-\prime}(\xi_3^-)=0,\\
&(\lambda^-+2\mu^-)f_3^{-\prime\prime}(\xi_3^-)+(\lambda^-+\mu^-)\varepsilon f_1^{-\prime}(\xi_3^-)-\mu^-\varepsilon^2 f_3^-(\xi_3^-)=0,\\
&\mu^+ f_1^{+\prime\prime}(\xi_3^+)-(\lambda^++2\mu^+)f_1^+(\xi_3^+)-(\lambda^++\mu^+)f_3^{+\prime}(\xi_3^+)=0,\\
&(\lambda^++2\mu^+)f_3^{+\prime\prime}(\xi_3^+)+(\lambda^++\mu^+)f_1^{+\prime}(\xi_3^+)-\mu^+ f_3^+(\xi_3^+)=0.
\end{aligned} \tag{3.7}$$

Equations (3.7) may also be rewritten as

$$a_{11}^{\pm}f_1^{\pm\prime\prime}+a_{12}^{\pm}f_1^{\pm}+a_{13}^{\pm}f_3^{\pm\prime}=0, \qquad a_{21}^{\pm}f_3^{\pm\prime\prime}+a_{22}^{\pm}f_1^{\pm\prime}+a_{23}^{\pm}f_3^{\pm}=0, \tag{3.8}$$

which after rearrangement become

$$f_1^{\pm}=-\frac{a_{11}^{\pm}}{a_{12}^{\pm}}f_1^{\pm\prime\prime}-\frac{a_{13}^{\pm}}{a_{12}^{\pm}}f_3^{\pm\prime}, \qquad f_1^{\pm\prime}=-\frac{a_{21}^{\pm}}{a_{22}^{\pm}}f_3^{\pm\prime\prime}-\frac{a_{23}^{\pm}}{a_{22}^{\pm}}f_3^{\pm}. \tag{3.9}$$

Differentiating $(3.9)_2$, substituting it into $(3.9)_1$ and differentiating again, we obtain

$$f_1^{\pm\prime}=\frac{a_{11}^{\pm}a_{21}^{\pm}}{a_{12}^{\pm}a_{22}^{\pm}}f_3^{\pm(4)}+\left(\frac{a_{11}^{\pm}a_{23}^{\pm}}{a_{12}^{\pm}a_{22}^{\pm}}-\frac{a_{13}^{\pm}}{a_{12}^{\pm}}\right)f_3^{\pm\prime\prime}, \tag{3.10}$$

which together with $(3.9)_2$ gives

$$b_1^{\pm} f_3^{\pm(4)} + b_2^{\pm} f_3^{\pm\prime\prime} + b_3^{\pm} f_3^{\pm} = 0, \tag{3.11}$$

with

$$b_1^{\pm} = \frac{a_{11}^{\pm} a_{21}^{\pm}}{a_{12}^{\pm} a_{22}^{\pm}}, \qquad b_2^{\pm} = \frac{a_{11}^{\pm} a_{23}^{\pm} - a_{13}^{\pm} a_{22}^{\pm} + a_{12}^{\pm} a_{21}^{\pm}}{a_{12}^{\pm} a_{22}^{\pm}}, \qquad b_3^{\pm} = \frac{a_{23}^{\pm}}{a_{22}^{\pm}}. \tag{3.12}$$

Coming back to the original notations, coefficients $b_i^{\pm}$ become

$$\begin{aligned} b_1^- &= -\frac{\mu^-}{\varepsilon^3(\lambda^- + \mu^-)}, & b_2^- &= \frac{2\mu^-}{\varepsilon(\lambda^- + 2\mu^-)}, & b_3^- &= -\frac{\mu^- \varepsilon}{\lambda^- + \mu^-}, \\ b_1^+ &= -\frac{\mu^+}{\lambda^+ + \mu^+}, & b_2^+ &= \frac{2\mu^+}{\lambda^+ + 2\mu^+}, & b_3^+ &= -\frac{\mu^+}{\lambda^+ + \mu^+}. \end{aligned} \tag{3.13}$$

Therefore, the solutions of (3.11) decaying at $+\infty$ take the form

$$\begin{aligned} f_3^-(\xi_3^-) &= \left(C_1 + C_2\xi_3^-\right) e^{\varepsilon\xi_3^-} + \left(C_3 + C_4\xi_3^-\right) e^{-\varepsilon\xi_3^-}, \\ f_3^+(\xi_3^+) &= \left(C_5 + C_6\xi_3^+\right) e^{-\xi_3^+}. \end{aligned} \tag{3.14}$$

Substituting the latter into (3.10), we deduce

$$\begin{aligned} f_1^-(\xi_3^-) &= e^{-\varepsilon\xi_3^-}\left[C_3 + C_4\left(\xi_3^- - C_0^-\right)\right] - e^{\varepsilon\xi_3^-}\left[C_1 + C_2\left(\xi_3^- + C_0^-\right)\right], \\ f_1^+(\xi_3^+) &= e^{-\xi_3^+}\left[C_5 + C_6\left(\xi_3^+ - \varepsilon C_0^+\right)\right], \end{aligned} \tag{3.15}$$

where $C_0^{\pm} = \dfrac{1}{\varepsilon}\left(1 + \dfrac{2\mu^{\pm}}{\lambda^{\pm} + \mu^{\pm}}\right)$. The values of C_q, $q = 1, ..., 6$, are obtained from boundary and continuity conditions (3.5) and (3.2) and given by

$$C_q = \frac{AhN_q}{D}, \tag{3.16}$$

where

$$\begin{aligned} N_1 = \;& 2\mathrm{e}^{2\varepsilon}\varepsilon^2 B_7 B_{12} + (\gamma^-)^2[B_2^+ B_{13}^-(\mu^-)^2 + 2(\gamma^+ - 2\mathrm{e}^{2\varepsilon}\varepsilon B_3^+)\mu^-\mu^+ \\ & - B_1^+ B_{13}^+(\mu^+)^2] + \gamma^-[B_1^+ B_{14}^-(\mu^+)^2 + 2(2\mathrm{e}^{2\varepsilon}\varepsilon B_4^+ - 1) - B_2^+ B_{14}^+(\mu^-)^2], \end{aligned}$$

$$
\begin{aligned}
N_2 = \; & -\mathrm{e}^{2\varepsilon}(2\varepsilon^2 B_7 B_{12} + \gamma^-[B_2^+ B_{10}^-(\mu^-)^2 - 2(\mathrm{e}^{2\varepsilon} + 2B_4^-\varepsilon)\mu^-\mu^+ \\
& -B_1^+ B_{10}^+(\mu^+)^2] - (\gamma^-)^2[B_2^+(B_9^- - 2\varepsilon^2)(\mu^-)^2 \\
& +2(\mathrm{e}^{2\varepsilon}\gamma^+ - 2B_3^-\varepsilon)\mu^-\mu^+ + B_1^+(B_4^- + \mathrm{e}^{2\varepsilon} + 2\varepsilon^2)(\mu^+)^2]), \\
N_3 = \; & -\varepsilon B_1^- B_7[B_1^- B_2^+(\mathrm{e}^{2\varepsilon}B_4^+ - 1)\mu^- + B_1^+(B_2^- + \mathrm{e}^{2\varepsilon}B_1^- B_4^+)\mu^+], \\
N_4 = \; & \varepsilon \mathrm{e}^{2\varepsilon} B_1^- B_{12}[B_1^- B_9^- \mu^- + (B_1^- B_4^- + \mathrm{e}^{2\varepsilon}B_2^-)\mu^+], \\
N_5 = \; & 2\mathrm{e}^{\varepsilon}\gamma^-\mu^-[B_1^- B_2^+(\mathrm{e}^{2\varepsilon}B_3^+ - B_3^-)\mu^- + (\mathrm{e}^{2\varepsilon}B_{11}^+ - B_{11}^-)\mu^+], \\
N_6 = \; & 2\mathrm{e}^{\varepsilon}\gamma^- B_1^+\mu^-[B_1^- B_9^- \mu^- + (B_1^- B_4^- + \mathrm{e}^{2\varepsilon}B_2^-)\mu^+],
\end{aligned}
$$

and

$$
\begin{aligned}
D = \; & 2\varepsilon[(B_1^-)^2 B_2^+(B_6 - 2\mathrm{e}^{2\varepsilon}B_5)(\mu^-)^2 + 2B_1^-[B_8^- + \mathrm{e}^{4\varepsilon}B_8^+ \\
& +\mathrm{e}^{2\varepsilon}(4B_1^-\varepsilon^2 - 2)]\mu^-\mu^+ + B_1^+[B_1^- B_2^- B_6 \\
& +2\mathrm{e}^{2\varepsilon}(B_5[1 + (\gamma^-)^2] - 4\gamma^-\varepsilon^2)](\mu^+)^2],
\end{aligned}
$$

with

$$
\begin{aligned}
& B_1^\pm = \gamma^\pm - 1, && B_6 = 1 + \mathrm{e}^{4\varepsilon}, && B_{11}^\pm = B_3^\pm \mp B_{15}^\pm, \\
& B_2^\pm = \gamma^\pm + 1, && B_7 = \mu^- - \mu^+, && B_{12} = B_2^+\mu^- + B_1^+\mu^+, \\
& B_3^\pm = 1 \pm \varepsilon, && B_8^\pm = 1 \pm \gamma^-\gamma^+, && B_{13}^\pm = \mathrm{e}^{2\varepsilon}(B_4^+ + 2\varepsilon^2) \pm 1, \\
& B_4^\pm = 1 \pm 2\varepsilon, && B_9^\pm = \mathrm{e}^{2\varepsilon} \pm B_4^\pm, && B_{14}^\pm = \mathrm{e}^{2\varepsilon}(4\varepsilon^2 \pm B_4^\pm) - 1, \\
& B_5 = 1 + 2\varepsilon^2, && B_{10}^\pm = B_9^\pm - 4\varepsilon^2, && B_{15}^\pm = \gamma^-(\varepsilon - \gamma^+ B_3^\pm) \pm \gamma^+\varepsilon.
\end{aligned}
$$

Stresses can be derived substituting displacements (3.6) with (3.14) into the corresponding expressions in (1.19) and (1.20).

Using the results together with material parameter (1.29) and relation (1.30), the leading order asymptotic behaviour of the displacements and stresses expressed in terms of small parameter ε at $\alpha \geq 0$ is given in Table 3.1 for a soft coating and in Table 3.2 for a stiff one.

It is clear that, in case of a soft layer, $u_3^- \gg u_3^+$ at $\alpha \geq 1$, i.e. the deformations

	u_1^-	u_3^-	σ_{13}^-	σ_{33}^-	σ_{11}^-	u_1^+	u_3^+	σ_{13}^+	σ_{33}^+	σ_{11}^+
$\alpha \geq 2$	ε	1	ε	1	1	$\varepsilon^{\alpha-1}$	$\varepsilon^{\alpha-1}$	1	1	1
$1 \leq \alpha \leq 2$	$\varepsilon^{\alpha-1}$	1	ε	1	1	$\varepsilon^{\alpha-1}$	$\varepsilon^{\alpha-1}$	1	1	1
$0 \leq \alpha \leq 1$	$\varepsilon^{\alpha-1}$	$\varepsilon^{\alpha-1}$	ε	1	1	$\varepsilon^{\alpha-1}$	$\varepsilon^{\alpha-1}$	1	1	1

Table 3.1: Asymptotic behaviour of displacements and stresses for a soft layer

	u_1^-	u_3^-	σ_{13}^-	σ_{33}^-	σ_{11}^-	u_1^+	u_3^+	σ_{13}^+	σ_{33}^+	σ_{11}^+
$\alpha \geq 3$	ε^{-3}	ε^{-4}	ε^{-1}	1	ε^{-2}	ε^{-4}	ε^{-4}	$\varepsilon^{\alpha-3}$	$\varepsilon^{\alpha-3}$	$\varepsilon^{\alpha-3}$
$2 \leq \alpha \leq 3$	$\varepsilon^{-\alpha}$	$\varepsilon^{-\alpha-1}$	$\varepsilon^{2-\alpha}$	1	$\varepsilon^{1-\alpha}$	$\varepsilon^{-\alpha-1}$	$\varepsilon^{-\alpha-1}$	1	1	1
$1 \leq \alpha \leq 2$	ε^{-2}	$\varepsilon^{-\alpha-1}$	1	1	ε^{-1}	$\varepsilon^{-\alpha-1}$	$\varepsilon^{-\alpha-1}$	1	1	1
$0 \leq \alpha \leq 1$	$\varepsilon^{-\alpha-1}$	$\varepsilon^{-\alpha-1}$	$\varepsilon^{1-\alpha}$	1	$\varepsilon^{-\alpha}$	$\varepsilon^{-\alpha-1}$	$\varepsilon^{-\alpha-1}$	1	1	1

Table 3.2: Asymptotic behaviour of displacements and stresses for a stiff layer

of the half-space may be neglected at leading order. Moreover, u_3^- and σ_{33}^- are of the same asymptotic order, which does not contradict the Winkler-Fuss hypothesis. For $0 \leq \alpha \leq 1$ we have $u_3^- \sim u_3^+$ and also $u_3^- \ll \sigma_{33}^-$, corresponding to a non-negligible effect of the substrate deformability. The value $\alpha = 1$ appears to be a border line value, since still $u_3^- \sim \sigma_{33}^-$, but at the same time $u_3^- \sim u_3^+$.

Now, let us consider in more detail the relation between vertical displacement u_3^- at the surface $\xi_3^- = 0$ and prescribed load (3.3), by introducing the coefficient

$$r = \frac{P}{u_3^-\big|_{\xi_3^-=0}}. \tag{3.17}$$

We have from (3.6), (3.14), (3.15) and (3.16) at leading order for a soft layer

$$r = \begin{cases} \dfrac{\lambda^- + 2\mu^-}{h}, & \alpha > 1, \\ \dfrac{2(\gamma^+ - 1)\mu^-(\lambda^- + 2\mu^-)}{h[\lambda^-\gamma^+ - 2\mu^-(1 - 2\gamma^+)]}, & \alpha = 1, \\ \dfrac{2(\gamma^+ - 1)\mu^-}{h\gamma^+}\varepsilon^{1-\alpha}, & \alpha < 1. \end{cases} \tag{3.18}$$

Hence, at $\alpha > 1$ vertical displacement u_3^- is proportional to prescribed load P. In this case, according to Winkler-Fuss hypothesis (1.31), coefficient r depends only on the thickness and elastic parameters of the layer. This result was earlier obtained in [3] for a layer with a clamped base. At the same time, at $\alpha \leq 1$ this coefficient already depends on both the parameters of the layer and the half-space and is independent of ξ_1 only for the considered sinusoidal load. It is also worth noting that at $\alpha < 1$ factor $\varepsilon^{1-\alpha}$ indicates the violation of Winkler-Fuss type behaviour.

For a stiff coating we have

$$r = \begin{cases} \dfrac{\mu^-(\gamma^- - 1)\varepsilon^4}{h\gamma^-}, & \alpha > 3, \\ \dfrac{\mu^-(\gamma^- - 1 - \gamma^+ + 7\gamma^-\gamma^+)\varepsilon^4}{3h\gamma^-(1 + \gamma^+)}, & \alpha = 3, \\ \dfrac{2\mu^-\gamma^+\varepsilon^{\alpha+1}}{h(1 + \gamma^+)}, & 1 < \alpha < 3, \\ \dfrac{\mu^-(\gamma^-(6\gamma^+ - 2) - 4\gamma^+)\varepsilon^2}{h(\gamma^-(2 + 3\gamma^+) - 2(1 + \gamma^+))}, & \alpha = 1, \\ \dfrac{2\mu^-(\gamma^+ - 1)\varepsilon^{\alpha+1}}{h\gamma^+}, & \alpha < 1. \end{cases} \tag{3.19}$$

As a result, the case $\alpha > 3$, when the coefficient r is independent of the parameters of substrate, is clearly observed. This points out that the equation of plate bending may be expected at leading order as a relation involving vertical displacement u_3^- and the applied load P. Note again, that the ratio does not involve ξ_1 since the considered applied load is sinusoidal. In general, it is a function of ξ_1.

3.3 Asymptotic analysis for a soft layer

Now we are in a position to develop a more general procedure, using the data in Table 3.1 as a motivation for the scaling exploited in the asymptotic procedure for a soft layer below, addressing all of the cases corresponding to the classification in this Table.

3.3.1 Case $\alpha \geq 2$ $\left(\mu \lesssim \varepsilon^2\right)$

First, we scale the displacements and stresses according to the data in the first row of the Table. Thus, we have for the layer

$$\begin{aligned} &u_m^- = h\varepsilon u_m^{-*}, \qquad \sigma_{12}^- = \mu^-\varepsilon^2\sigma_{12}^{-*}, \qquad \sigma_{ii}^- = \mu^-\sigma_{ii}^{-*}, \\ &u_3^- = hu_3^{-*}, \qquad \sigma_{m3}^- = \mu^-\varepsilon\sigma_{m3}^{-*}, \end{aligned} \tag{3.20}$$

where the quantities with the asterisk in superscript are assumed to be of the same asymptotic order, and, as before, $m = 1, 2$. In the present section, similarly to Chapter 2, the applied load is scaled as in (2.15). In view of (3.20), governing equations $(1.24)_1$ and (1.19) may be rewritten as

$$\begin{aligned} &\sigma_{mm,m}^{-*} + \varepsilon^2\sigma_{12,n}^{-*} + \sigma_{m3,3}^{-*} = 0, \\ &\varepsilon^2(\sigma_{13,1}^{-*} + \sigma_{23,2}^{-*}) + \sigma_{33,3}^{-*} = 0, \\ &\sigma_{mm}^{-*} = \varepsilon^2(\gamma^- u_{m,m}^{-*} + (\gamma^- - 2)u_{n,n}^{-*}) + (\gamma^- - 2)u_{3,3}^{-*}, \\ &\sigma_{33}^{-*} = \varepsilon^2(\gamma^- - 2)(u_{1,1}^{-*} + u_{2,2}^{-*}) + \gamma^- u_{3,3}^{-*}, \\ &\sigma_{12}^{-*} = u_{1,2}^{-*} + u_{2,1}^{-*}, \\ &\sigma_{m3}^{-*} = u_{m,3}^{-*} + u_{3,m}^{-*}, \end{aligned} \tag{3.21}$$

with comma denoting now differentiation with respect to dimensionless variables ξ_i.

Here and below, the scaling for the half-space is given by

$$u_i^+ = h\varepsilon^{\alpha-1}u_i^{+*}, \qquad \sigma_{ij}^+ = \mu^-\sigma_{ij}^{+*}, \tag{3.22}$$

which, substituting into $(1.24)_2$ and (1.20), gives

$$\begin{aligned}
&\sigma^{+*}_{i1,1} + \sigma^{+*}_{i2,2} + \sigma^{+*}_{i3,3} = 0,\\
&\sigma^{+*}_{mm} = \gamma^{+} u^{+*}_{m,m} + (\gamma^{+} - 2)(u^{+*}_{n,n} + u^{+*}_{3,3}),\\
&\sigma^{+*}_{33} = \gamma^{+} u^{+*}_{3,3} + (\gamma^{+} - 2)(u^{+*}_{1,1} + u^{+*}_{2,2}),\\
&\sigma^{+*}_{12} = u^{+*}_{1,2} + u^{+*}_{2,1},\\
&\sigma^{+*}_{m3} = u^{+*}_{m,3} + u^{+*}_{3,m}.
\end{aligned} \tag{3.23}$$

We also have from (3.1)

$$\sigma^{-*}_{33} = -p^{*}, \qquad \sigma^{-*}_{m3} = 0 \tag{3.24}$$

at $\xi^{-}_{3} = 0$, and from (3.2)

$$u^{-*}_{m} = \varepsilon^{\alpha-2} u^{+*}_{m}, \qquad u^{-*}_{3} = \varepsilon^{\alpha-1} u^{+*}_{3}, \qquad \varepsilon\sigma^{-*}_{m3} = \sigma^{+*}_{m3}, \qquad \sigma^{-*}_{33} = \sigma^{+*}_{33} \tag{3.25}$$

at $\xi^{-}_{3} = 1$.

It is clear from (3.25) that $u^{-*}_{m} \gg u^{+*}_{m}$ at $\alpha > 2$ while $u^{-*}_{m} \sim u^{+*}_{m}$ at $\alpha = 2$. In what follows we tackle each of these subcases separately.

Subcase $\alpha > 2$ $(\mu \ll \varepsilon^{2})$

Let us begin with the analysis of the layer by expanding the displacement and stress components in asymptotic series as

$$\begin{pmatrix} u^{-*}_{i} \\ \sigma^{-*}_{ij} \end{pmatrix} = \begin{pmatrix} u^{-(0)}_{i} \\ \sigma^{-(0)}_{ij} \end{pmatrix} + \varepsilon^{\beta} \begin{pmatrix} u^{-(1)}_{i} \\ \sigma^{-(1)}_{ij} \end{pmatrix} + \ldots, \tag{3.26}$$

where

$$\beta = \begin{cases} 2, & \alpha \geq 3, \\ \alpha - 1, & 1 < \alpha \leq 3. \end{cases} \tag{3.27}$$

At leading order, we have from (3.21)

$$\begin{aligned}
&\sigma^{-(0)}_{mm,m} + \sigma^{-(0)}_{m3,3} = 0,\\
&\sigma^{-(0)}_{33,3} = 0,\\
&\sigma^{-(0)}_{mm} = (\gamma^- - 2) u^{-(0)}_{3,3},\\
&\sigma^{-(0)}_{33} = \gamma^- u^{-(0)}_{3,3},\\
&\sigma^{-(0)}_{12} = u^{-(0)}_{1,2} + u^{-(0)}_{2,1},\\
&\sigma^{-(0)}_{m3} = u^{-(0)}_{m,3} + u^{-(0)}_{3,m},
\end{aligned} \tag{3.28}$$

subject to

$$\sigma^{-(0)}_{33} = -p^*, \qquad \sigma^{-(0)}_{m3} = 0, \tag{3.29}$$

and

$$u^{-(0)}_i = 0, \qquad \sigma^{+(0)}_{m3} = 0, \qquad \sigma^{-(0)}_{33} = \sigma^{+(0)}_{33} \tag{3.30}$$

at $\xi^-_3 = 0$ and $\xi^-_3 = 1$, respectively.

First, from $(3.28)_2$, satisfying boundary condition $(3.29)_1$, we deduce

$$\sigma^{-(0)}_{33} = -p^*. \tag{3.31}$$

Then, $(3.28)_4$ and $(3.30)_1$ imply

$$u^{-(0)}_3 = \frac{1}{\gamma^-}\left(1 - \xi^-_3\right) p^*, \tag{3.32}$$

which at $\xi^-_3 = 0$ validates the Winkler-Fuss hypothesis, see (1.31) in Section 1.2 and also the discussion presented in Subsection 3.3.6.

Next, we find the rest of the displacements and stresses. In particular, $(3.28)_3$ yields

$$\sigma^{-(0)}_{mm} = -\vartheta p^*, \tag{3.33}$$

where

$$\vartheta = 1 - \frac{2}{\gamma^-}. \tag{3.34}$$

Now, substituting (3.33) into $(3.28)_1$ and satisfying $(3.29)_2$, we arrive at

$$\sigma_{m3}^{-(0)} = \vartheta \xi_3^- \frac{\partial p^*}{\partial \xi_m}. \tag{3.35}$$

Then, using (3.35), $(3.28)_6$, and (3.30), we infer

$$u_m^{-(0)} = \left(\frac{\eta}{8} (\xi_3^-)^2 - \frac{\xi_3^-}{\gamma^-} + \frac{3}{2\gamma^-} - \frac{1}{2} \right) \frac{\partial p^*}{\partial \xi_m}, \tag{3.36}$$

where

$$\eta = 4 \left(1 - \frac{1}{\gamma^-} \right). \tag{3.37}$$

Finally, combining the latter with $(3.28)_5$, we have

$$\sigma_{12}^{-(0)} = \left(\frac{\eta}{4} (\xi_3^-)^2 - \frac{2\xi_3^-}{\gamma^-} + \frac{3}{\gamma^-} - 1 \right) \frac{\partial^2 p^*}{\partial \xi_1 \partial \xi_2}. \tag{3.38}$$

Subcase $\alpha = 2$ $(\mu \sim \varepsilon^2)$

Here we start from same leading order equations (3.28) and boundary conditions (3.29) for the layer, while the continuity conditions at $\xi_3^- = 1$ are now given by

$$u_m^{-(0)} = u_m^{+(0)}, \qquad u_3^{-(0)} = 0, \qquad \sigma_{m3}^{+(0)} = 0, \qquad \sigma_{33}^{-(0)} = \sigma_{33}^{+(0)}. \tag{3.39}$$

As above, quantities $\sigma_{33}^{-(0)}, u_3^{-(0)}, \sigma_{mm}^{-(0)}$ and $\sigma_{m3}^{-(0)}$ are expressed by (3.31) – (3.35), respectively. Then, using (3.35) and $(3.28)_6$, we deduce

$$u_m^{-(0)} = \left(\frac{\eta}{8} (\xi_3^-)^2 - \frac{\xi_3^-}{\gamma^-} + \frac{3}{2\gamma^-} - \frac{1}{2} \right) \frac{\partial p^*}{\partial \xi_m} + u_m^{-(0)}\big|_{\xi_3^- = 1}. \tag{3.40}$$

Thus, contrary to the subcase $\alpha > 2$, the effect of the substrate on horizontal displacements $u_m^{-(0)}$ now appears at leading order because of $(3.39)_1$. This is also true for shear stress $\sigma_{12}^{-(0)}$, for which we get from $(3.28)_5$ and (3.40)

$$\sigma_{12}^{-(0)} = \left(\frac{\eta}{4} (\xi_3^-)^2 - \frac{2\xi_3^-}{\gamma^-} + \frac{3}{\gamma^-} - 1 \right) \frac{\partial^2 p^*}{\partial \xi_1 \partial \xi_2} + \left(\frac{\partial u_1^{-(0)}}{\partial \xi_2} + \frac{\partial u_2^{-(0)}}{\partial \xi_1} \right) \Bigg|_{\xi_3^- = 1}. \tag{3.41}$$

However, the leading order relation between $u_3^{-(0)}$ and $\sigma_{33}^{-(0)}$ is still given by Winkler-Fuss formula (3.32).

3.3.2 Case $1 \leq \alpha < 2$ $\left(\varepsilon^2 \lesssim \mu \ll \varepsilon\right)$

The scaling for the layer now takes the form

$$\begin{aligned} &u_m^- = h\varepsilon^{\alpha-1}u_m^{-*}, \qquad &&\sigma_{12}^- = \mu^-\varepsilon^\alpha\sigma_{12}^{-*}, \qquad &&\sigma_{ii}^- = \mu^-\sigma_{ii}^{-*}, \\ &u_3^- = hu_3^{-*}, \qquad &&\sigma_{m3}^- = \mu^-\varepsilon\sigma_{m3}^{-*}. \end{aligned} \tag{3.42}$$

As a result, governing equations $(1.24)_1$ and (1.19) can be written as

$$\begin{aligned} &\sigma_{mm,m}^{-*} + \varepsilon^\alpha\sigma_{12,n}^{-*} + \sigma_{m3,3}^{-*} = 0, \\ &\varepsilon^2(\sigma_{13,1}^{-*} + \sigma_{23,2}^{-*}) + \sigma_{33,3}^{-*} = 0, \\ &\sigma_{mm}^{-*} = \varepsilon^\alpha(\gamma^- u_{m,m}^{-*} + (\gamma^- - 2)u_{n,n}^{-*}) + (\gamma^- - 2)u_{3,3}^{-*}, \\ &\sigma_{33}^{-*} = \varepsilon^\alpha(\gamma^- - 2)(u_{1,1}^{-*} + u_{2,2}^{-*}) + \gamma^- u_{3,3}^{-*}, \\ &\sigma_{12}^{-*} = u_{1,2}^{-*} + u_{2,1}^{-*}, \\ &\sigma_{m3}^{-*} = \varepsilon^{\alpha-2}u_{m,3}^{-*} + u_{3,m}^{-*}. \end{aligned} \tag{3.43}$$

Boundary conditions (3.24) stay the same, whereas the continuity conditions at $\xi_3^- = 1$ become

$$u_m^{-*} = u_m^{+*}, \qquad u_3^{-*} = \varepsilon^{\alpha-1}u_3^{+*}, \qquad \varepsilon\sigma_{m3}^{-*} = \sigma_{m3}^{+*}, \qquad \sigma_{33}^{-*} = \sigma_{33}^{+*}. \tag{3.44}$$

Below we consider separately the subcases $1 < \alpha < 2$ and $\alpha = 1$.

Subcase $1 < \alpha < 2$ $(\varepsilon^2 \ll \mu \ll \varepsilon)$

At leading order, we have for the layer

$$\begin{aligned}
&\sigma^{-(0)}_{mm,m} + \sigma^{-(0)}_{m3,3} = 0,\\
&\sigma^{-(0)}_{33,3} = 0,\\
&\sigma^{-(0)}_{mm} = (\gamma^- - 2)u^{-(0)}_{3,3},\\
&\sigma^{-(0)}_{33} = \gamma^- u^{-(0)}_{3,3},\\
&\sigma^{-(0)}_{12} = u^{-(0)}_{1,2} + u^{-(0)}_{2,1},\\
&u^{-(0)}_{m,3} = 0,
\end{aligned} \tag{3.45}$$

subject to boundary conditions (3.29) and the following continuity conditions at $\xi_3^- = 1$

$$u_m^{-(0)} = u_m^{+(0)}, \qquad u_3^{-(0)} = 0, \qquad \sigma_{m3}^{+(0)} = 0, \qquad \sigma_{33}^{-(0)} = \sigma_{33}^{+(0)}. \tag{3.46}$$

As in Subsection 3.3.1, quantities $\sigma_{33}^{-(0)}, u_3^{-(0)}, \sigma_{mm}^{-(0)}$ and $\sigma_{m3}^{-(0)}$ are given by (3.31) – (3.35), respectively. Also, formulae $(3.45)_6$ and $(3.45)_5$ yield

$$u_m^{-(0)} = u_m^{-(0)}\big|_{\xi_3^-=1}, \tag{3.47}$$

and

$$\sigma_{12}^{-(0)} = \left(\frac{\partial u_1^{-(0)}}{\partial \xi_2} + \frac{\partial u_2^{-(0)}}{\partial \xi_1}\right)\Bigg|_{\xi_3^-=1}. \tag{3.48}$$

Here, in contrast to (3.40) and (3.41), quantities $u_m^{-(0)}$ and $\sigma_{12}^{-(0)}$ in (3.47) and (3.48) depend only upon substrate deformations.

Subcase $\alpha = 1$ $(\mu \sim \varepsilon)$

Now the leading order equations for the layer are again given by (3.45), subject to boundary conditions (3.29), with the continuity conditions at $\xi_3^- = 1$ taking the form

$$u_i^{-(0)} = u_i^{+(0)}, \qquad \sigma_{m3}^{+(0)} = 0, \qquad \sigma_{33}^{-(0)} = \sigma_{33}^{+(0)}. \tag{3.49}$$

Remarkably, even though $\alpha = 1$, i.e. $\mu = \dfrac{\mu^-}{\mu^+} \sim \dfrac{h}{l} = \varepsilon$, hence $\mu^- \ll \mu^+$, the half-space is still not stiff enough to behave as an absolutely rigid substrate; compare $(3.46)_2$ and $(3.49)_1$ at $i = 3$. Therefore, we cannot expect the validity of the Winkler-Fuss hypothesis.

As before, the quantity of $\sigma_{33}^{-(0)}$ is given by (3.31), whereas, as it follows from $(3.45)_4$ and $(3.29)_1$,

$$u_3^{-(0)} = \frac{p^*}{\gamma^-}(1 - \xi_3^-) + u_3^{-(0)}\Big|_{\xi_3^-=1}. \tag{3.50}$$

This relation demonstrates that vertical displacement $u_3^{-(0)}$ is no longer proportional to prescribed load p^* due to presence of an extra term in the right hand side, corresponding to the substrate effect, see $(3.49)_1$ at $i = 3$. Thus, the Winkler-Fuss approximation is not valid even at leading order.

Finally, quantities $\sigma_{mm}^{-(0)}$, $\sigma_{m3}^{-(0)}$, $u_m^{-(0)}$ and $\sigma_{12}^{-(0)}$ now satisfy formulae (3.33), (3.35), (3.47) and (3.48), respectively, given in the previous subsections.

3.3.3 Case $0 \leq \alpha < 1$ $(\varepsilon \lesssim \mu \ll 1)$

The scaling for the layer is

$$u_i^- = h\varepsilon^{\alpha-1}u_i^{-*}, \qquad \sigma_{12}^- = \mu^-\varepsilon^\alpha\sigma_{12}^{-*}, \qquad \sigma_{ii}^- = \mu^-\sigma_{ii}^{-*}, \qquad \sigma_{m3}^- = \mu^-\varepsilon\sigma_{m3}^{-*}. \tag{3.51}$$

Consequently, governing equations $(1.24)_1$ and (1.19) become

$$\begin{aligned}
&\sigma^{-*}_{mm,m} + \varepsilon^{\alpha}\sigma^{-*}_{12,n} + \sigma^{-*}_{m3,3} = 0,\\
&\varepsilon^{2}\sigma^{-*}_{13,1} + \varepsilon^{2}\sigma^{-*}_{23,2} + \sigma^{-*}_{33,3} = 0,\\
&\varepsilon^{1-\alpha}\sigma^{-*}_{mm} = \varepsilon(\gamma^{-}u^{-*}_{m,m} + (\gamma^{-}-2)u^{-*}_{n,n}) + (\gamma^{-}-2)u^{-*}_{3,3},\\
&\varepsilon^{1-\alpha}\sigma^{-*}_{33} = \varepsilon(\gamma^{-}-2)(u^{-*}_{1,1} + u^{-*}_{2,2}) + \gamma^{-}u^{-*}_{3,3},\\
&\sigma^{-*}_{12} = u^{-*}_{1,2} + u^{-*}_{2,1},\\
&\varepsilon^{2-\alpha}\sigma^{-*}_{m3} = u^{-*}_{m,3} + \varepsilon u^{-*}_{3,m},
\end{aligned} \tag{3.52}$$

subject to boundary conditions (3.24). The continuity conditions at $\xi_3^- = 1$ can be written as

$$u_i^{-*} = u_i^{+*}, \qquad \varepsilon\sigma^{-*}_{m3} = \sigma^{+*}_{m3}, \qquad \sigma^{-*}_{33} = \sigma^{+*}_{33}. \tag{3.53}$$

At leading order, we get from (3.52) and (3.53)

$$\begin{aligned}
&\sigma^{-(0)}_{mm,m} + \varepsilon^{\alpha}\sigma^{-(0)}_{12,n} + \sigma^{-(0)}_{m3,3} = 0,\\
&\sigma^{-(0)}_{33,3} = 0,\\
&u^{-(0)}_{i,3} = 0,\\
&\sigma^{-(0)}_{12} = u^{-(0)}_{1,2} + u^{-(0)}_{2,1},
\end{aligned} \tag{3.54}$$

where term $\sigma^{-(0)}_{12,n}$ can be neglected at $0 < \alpha < 1$, and

$$u_i^{-(0)} = u_i^{+(0)}, \qquad \sigma^{+(0)}_{m3} = 0, \qquad \sigma^{-(0)}_{33} = \sigma^{+(0)}_{33}. \tag{3.55}$$

Integrating $(3.54)_2$ and satisfying $(3.29)_1$, we arrive again at (3.31) for $\sigma^{-(0)}_{33}$. Next, $(3.54)_3$ results in

$$u_i^{-(0)} = u_i^{-(0)}\Big|_{\xi_3^- = 1}. \tag{3.56}$$

All the displacements of the layer are now strongly affected by the presence of the half-space, according to boundary condition $(3.55)_1$.

3.3.4 Higher order corrections

Below, we derive higher order corrections to the relation between vertical displacement of the upper face of the layer $u_3^-\big|_{\xi_3^-=0}$ and applied load P, expressing the studied Winkler-Fuss hypothesis. We restrict ourselves to the range $\alpha > 1$, in which it is valid at leading order. The form of asymptotic expansion (3.26) involving parameter β, see (3.27), motivates a separate treatment of cases $\alpha > 3$, $\alpha = 3$ and $1 < \alpha < 3$.

Case $\alpha > 3$ $(\mu \ll \varepsilon^3)$

Over this parameter range, the sought for correction is $O(\varepsilon^2)$, see (3.26) and (3.27). Then, governing equations $(3.21)_2$ and $(3.21)_4$ become

$$\begin{aligned} &\sigma_{13,1}^{-(0)} + \sigma_{23,2}^{-(0)} + \sigma_{33,3}^{-(1)} = 0, \\ &\sigma_{33}^{-(1)} = (\gamma^- - 2)\left(u_{1,1}^{-(0)} + u_{2,2}^{-(0)}\right) + \gamma^- u_{3,3}^{-(1)}, \end{aligned} \tag{3.57}$$

subject to the boundary condition at $\xi_3^- = 0$

$$\sigma_{33}^{-(1)} = 0, \tag{3.58}$$

and the continuity condition at $\xi_3^- = 1$

$$u_3^{-(1)} = 0. \tag{3.59}$$

Thus, at $\alpha > 3$ the interface between the layer and the half-space may be treated as a clamped one not only at leading order, but also at the next one.

Using $(3.57)_1$, (3.35), and (3.58), we deduce

$$\sigma_{33}^{-(1)} = \frac{2 - \gamma^-}{2\gamma^-} (\xi_3^-)^2 \tilde{\Delta}_{12} p^*, \tag{3.60}$$

where

$$\tilde{\Delta}_{12} = \frac{\partial^2}{\partial \xi_1^2} + \frac{\partial^2}{\partial \xi_2^2} \tag{3.61}$$

is a 2D Laplace operator in ξ_1 and ξ_2. Then, substituting (3.36) into $(3.57)_2$, and taking into account (3.59), we obtain

$$u_3^{-(1)} = \frac{(2-\gamma^-)(\xi_3^- - 1)}{6(\gamma^-)^2}\left[6 - 3\xi_3^- + \gamma^-(\xi_3^- - 2 + (\xi_3^-)^2)\right]\tilde{\Delta}_{12}p^*. \tag{3.62}$$

Case $\alpha = 3$ $(\mu \sim \varepsilon^3)$

Equations (3.57) and boundary condition (3.58) are now complemented by the continuity condition

$$u_3^{-(1)} = u_3^{+(0)}. \tag{3.63}$$

As a result, we have same expression (3.60) for $\sigma_{33}^{-(1)}$, whereas $u_3^{-(1)}$ becomes

$$u_3^{-(1)} = \frac{(2-\gamma^-)(\xi_3^- - 1)}{6(\gamma^-)^2}\left[6 - 3\xi_3^- + \gamma^-(\xi_3^- - 2 + (\xi_3^-)^2)\right]\tilde{\Delta}_{12}p^* + u_3^{-(1)}\Big|_{\xi_3^-=1}, \tag{3.64}$$

where the last term in the right hand side is given by (3.63).

Case $1 < \alpha < 3$ $(\varepsilon^3 \ll \mu \ll \varepsilon)$

In this case the sought for correction is $O(\varepsilon^{\alpha-1})$. Therefore,

$$\begin{aligned} \sigma_{33,3}^{-(1)} &= 0, \\ \sigma_{33}^{-(1)} &= \gamma^- u_{3,3}^{-(1)}, \end{aligned} \tag{3.65}$$

leading to

$$\sigma_{33}^{-(1)} = 0, \tag{3.66}$$

and

$$u_3^{-(1)} = u_3^{-(1)}\Big|_{\xi_3^-=1}. \tag{3.67}$$

Hence, the next order correction is entirely affected by substrate deformation.

3.3.5 Approximate formulation for a half-space

As it follows from the analysis above, in some cases in order to find stresses and displacements of the layer, interfacial displacements $u_i^{-(0)}\Big|_{\xi_3^-=1}$ and $u_3^{-(1)}\Big|_{\xi_3^-=1}$ should be derived. Similarly to Subsection 2.3.5 in the previous chapter, an approximate formulation for a half-space may be introduced which allows to obtain these values.

Vertical displacement $\sigma_{33}^{-(0)}$ is constant across the thickness of the layer for any value of parameter α, see (3.31), therefore, the applied load can be transmitted to the interface. In view of continuity conditions (3.30), (3.39), (3.46), (3.49) and (3.53), a simpler problem for a homogeneous half-space ($\xi_3^+ > 0$) can be formulated with the following boundary conditions at $\xi_3^+ = 0$

$$\sigma_{33}^{+} = -P, \qquad \sigma_{m3}^{+} = 0. \tag{3.68}$$

Thus, leading order interfacial displacements $u_i^{-(0)}\Big|_{\xi_3^-=1}$, involved, for instance, in (3.40), (3.47) and (3.50), and $u_3^{-(1)}\Big|_{\xi_3^-=1}$ in (3.64) and (3.67), can be found from the solution of the aforementioned problem. For a sinusoidal load (3.3), it is given in Section 3.5 as Case 1. For an arbitrary load the solution can be derived, for example, by substituting given vertical stress in (3.31), into a convolution with the Boussinesq's solution, see [112].

3.3.6 Discussion

Asymptotic analysis above proves that the Winkler-Fuss hypothesis is valid at leading order at $\alpha > 1$ ($\mu \ll \varepsilon$), see (3.32) at $\xi_3^- = 0$. In dimensional form it is given by (1.31) with coefficient r coinciding with its exact value in the first row in (3.18).

The correction to the Winkler-Fuss model depends upon the value of parameter α over range $\alpha > 1$. In particular, at $\alpha > 3$ ($\mu \ll \varepsilon^3$), we have a two-term asymptotic formula, see (3.32) and (3.62) at $\xi_3^- = 0$. It is

$$w_0 = \frac{P}{r} + \frac{T}{r^2}\Delta_{12}P, \tag{3.69}$$

where Δ_{12} is introduced in (1.33), $w_0 = u_3^-\big|_{x_3=0}$ is the deflection of the surface of the layer and

$$T = \frac{h(5\gamma^- - (\gamma^-)^2 - 6)\mu^-}{3}. \tag{3.70}$$

Expression (3.70) for coefficient T shows that the deformation of the half-space does not influence the calculated correction. It is also clear that the latter is of relative order $O(\varepsilon^2)$. The two-term formula above can also be rewritten in symbolic form as

$$P = \frac{rw_0}{1 + \dfrac{T}{r}\Delta_{12}} \approx rw_0 - T\Delta_{12}w_0, \tag{3.71}$$

corresponding to the Pasternak elastic foundation, see (1.32) in Section 1.2 and also [74, 129, 137].

In case $\alpha = 3$ ($\mu \sim \varepsilon^3$), it might be seen from (3.32) and (3.64) that the associated correction involves a term expressing the effect of the half-space, namely

$$w_0 = \frac{P}{r} + \frac{T}{r^2}\Delta_{12}P + w_h, \tag{3.72}$$

or again

$$P \approx r(w_0 - w_h) - T\Delta_{12}w_0, \tag{3.73}$$

where displacement of the interface $w_h = u_3^-\big|_{x_3=h}$ is also of order $O(\varepsilon^2)$ according to Table 3.1 and asymptotic relations (3.22).

For $1 < \alpha < 3$ ($\varepsilon^3 \ll \mu \ll \varepsilon$), see (3.32) and (3.67), the last term in (3.72) is greater than the second one, resulting in the two-term asymptotic formula

$$P = r(w_0 - w_h). \tag{3.74}$$

where $w_h = O(\varepsilon^{\alpha-1})$. Displacement w_h in (3.72) – (3.74), may be found from a simpler problem for a homogeneous half-space $x_3 \geq h$ formulated in Subsection 3.3.5.

As it has already been mentioned, the Winkler-Fuss hypothesis fails at leading order at $0 \leq \alpha \leq 1$ ($\varepsilon \ll \mu \lesssim 1$). In particular, it is violated even at $\mu = \dfrac{\mu^-}{\mu^+} \sim \varepsilon = \dfrac{h}{l}$, which is still a relatively large contrast, as it follows from (3.50) at $\alpha = 1$, and also confirmed by comparison with the exact solution, see the second line in (3.18).

Formula (3.74) can be also written as

$$P = r\delta w, \tag{3.75}$$

where $\delta w = w_0 - w_h$. It is worth noting that outside the range of validity of the Winkler-Fuss hypothesis at $\alpha = 1$, the leading order solution will also take the form of (3.75), in which $w_0 \sim w_h \sim \dfrac{P}{r}$, see (3.50) at $\xi_3^- = 0$.

Finally, we remark that at $0 \leq \alpha < 1$ (3.75) becomes

$$\delta w = 0, \tag{3.76}$$

reflecting almost uniform variation of the transverse displacement across the thickness of the layer. This approximation is also valid at non-contrast limit $\alpha = 0$. Interfacial value w_h at $0 \leq \alpha \leq 1$ again may be found at leading order from the problem for a homogeneous half-space as in formulae (3.72) – (3.74) above.

3.4 Asymptotic analysis for a stiff layer

In this section we develop an asymptotic scheme for a relatively stiff layer. The scaling required for this procedure now follows from the orders of displacements and stresses presented in Table 3.2.

3.4.1 Case $\alpha \geq 3$ $\left(\mu \lesssim \varepsilon^3\right)$

First, we scale the displacements and stresses for the layer using the data in the first row of Table 3.2. Therefore, we have

$$\begin{aligned} &u_m^- = h\varepsilon^{-3}u_m^{*-}, \qquad &&\sigma_{mm}^- = \mu^-\varepsilon^{-2}\sigma_{mm}^{*-}, \qquad &&\sigma_{12}^- = \mu^-\varepsilon^{-2}\sigma_{12}^{*-}, \\ &u_3^- = h\varepsilon^{-4}u_3^{*-}, \qquad &&\sigma_{33}^- = \mu^-\sigma_{33}^{*-}, \qquad &&\sigma_{m3}^- = \mu^-\varepsilon^{-1}\sigma_{m3}^{*-}. \end{aligned} \tag{3.77}$$

Again, we assume all quantities with the asterisk in superscript to be of the same asymptotic order. In view of (3.77), governing equations $(1.24)_1$ and (1.19) become

$$\begin{aligned} &\sigma_{i1,1}^{*-} + \sigma_{i2,2}^{*-} + \sigma_{i3,3}^{*-} = 0, \\ &\varepsilon^2\sigma_{mm}^{*-} = \varepsilon^2\gamma^- u_{m,m}^{*-} + \varepsilon^2(\gamma^- - 2)u_{n,n}^{*-} + (\gamma^- - 2)u_{3,3}^{*-}, \\ &\varepsilon^4\sigma_{33}^{*-} = \varepsilon^2(\gamma^- - 2)u_{1,1}^{*-} + \varepsilon^2(\gamma^- - 2)u_{2,2}^{*-} + \gamma^- u_{3,3}^{*-}, \\ &\sigma_{12}^{*-} = u_{1,2}^{*-} + u_{2,1}^{*-}, \\ &\varepsilon^2\sigma_{m3}^{*-} = u_{m,3}^{*-} + u_{3,m}^{*-}. \end{aligned} \tag{3.78}$$

Eliminating the term $u_{3,3}^{*-}$ from $(3.78)_2$ and $(3.78)_3$, we deduce

$$\sigma_{mm}^{*-}\gamma^- - \varepsilon^2(\gamma^- - 2)\sigma_{33}^{*-} = 4(\gamma^- - 1)u_{m,m}^{*-} + 2(\gamma^- - 2)u_{n,n}^{*-}. \tag{3.79}$$

Using the scaling for the half-space given by

$$u_i^+ = h\varepsilon^{-4}u_i^{*+}, \qquad \sigma_{ij}^+ = \mu^-\varepsilon^{\alpha-3}\sigma_{ij}^{*+}, \tag{3.80}$$

equations $(1.24)_2$ and (1.20) may be rewritten as

$$\begin{aligned}
&\sigma^{*+}_{i1,1} + \sigma^{*+}_{i2,2} + \sigma^{*+}_{i3,3} = 0,\\
&\sigma^{*+}_{mm} = \gamma^{+} u^{*+}_{m,m} + (\gamma^{+} - 2)(u^{*+}_{n,n} + u^{*+}_{3,3}),\\
&\sigma^{*+}_{33} = \gamma^{+} u^{*+}_{3,3} + (\gamma^{+} - 2)(u^{*+}_{1,1} + u^{*+}_{2,2}),\\
&\sigma^{*+}_{12} = u^{*+}_{1,2} + u^{*+}_{2,1},\\
&\sigma^{*+}_{m3} = u^{*+}_{m,3} + u^{*+}_{3,m}.
\end{aligned} \tag{3.81}$$

Boundary and continuity conditions (3.1) and (3.2) take the form

$$\sigma^{*-}_{33} = -p^{*}, \qquad \sigma^{*-}_{m3} = 0 \tag{3.82}$$

at $\xi^{-}_{3} = 0$, and

$$\varepsilon u^{*-}_{m} = u^{*+}_{m}, \qquad u^{*-}_{3} = u^{*+}_{3}, \qquad \sigma^{*-}_{m3} = \varepsilon^{\alpha-2}\sigma^{*+}_{m3}, \qquad \sigma^{*-}_{33} = \varepsilon^{\alpha-3}\sigma^{*+}_{33}. \tag{3.83}$$

at $\xi^{-} = 1$.

In (3.83), $\sigma^{*-}_{33} \gg \sigma^{*+}_{33}$ at $\alpha > 3$ whereas $\sigma^{*-}_{33} \sim \sigma^{*+}_{33}$ at $\alpha = 3$, hence, we consider these subcases separately.

Subcase $\alpha > 3$ $(\mu \ll \varepsilon^{3})$

We expand the displacements and stresses of the layer in asymptotic series

$$\begin{pmatrix} u^{*-}_{i} \\ \\ \sigma^{*-}_{ij} \end{pmatrix} = \begin{pmatrix} u^{-(0)}_{i} \\ \\ \sigma^{-(0)}_{ij} \end{pmatrix} + \dots . \tag{3.84}$$

Hence, at leading order, we get from (3.78)

$$\begin{aligned}
&\sigma_{i1,1}^{-(0)} + \sigma_{i2,2}^{-(0)} + \sigma_{i3,3}^{-(0)} = 0,\\
&u_{3,3}^{-(0)} = 0,\\
&\sigma_{12}^{-(0)} = u_{1,2}^{-(0)} + u_{2,1}^{-(0)},\\
&u_{m,3}^{-(0)} + u_{3,m}^{-(0)} = 0,\\
&\sigma_{mm}^{-(0)} = \eta u_{m,m}^{-(0)} + 2\vartheta u_{n,n}^{-(0)},
\end{aligned} \tag{3.85}$$

subject to the boundary conditions at $\xi_3^- = 0$

$$\sigma_{33}^{-(0)} = -p^*, \qquad \sigma_{m3}^{-(0)} = 0, \tag{3.86}$$

and the continuity conditions at $\xi_3^- = 1$

$$u_m^{+(0)} = 0, \qquad u_3^{-(0)} = u_3^{+(0)}, \qquad \sigma_{i3}^{-(0)} = 0, \tag{3.87}$$

where ϑ and η are defined in (3.34) and (3.37), respectively.

First, $(3.85)_2$ implies

$$u_3^{-(0)} = W_p, \tag{3.88}$$

where W_p is an arbitrary function of variables ξ_1 and ξ_2 representing the dimensionless deflection of the layer. Then, on integrating $(3.85)_4$, we deduce

$$u_m^{-(0)} = -\xi_3^- \frac{\partial W_p}{\partial \xi_m} + F_1, \tag{3.89}$$

where $F_1 = F_1(\xi_1, \xi_2)$. Substituting the latter into $(3.85)_3$, $(3.85)_5$, using $(3.85)_1$ and satisfying conditions $(3.86)_2$ and $(3.87)_3$, we infer

$$F_1 = \frac{1}{2}\frac{\partial W_p}{\partial \xi_m}. \tag{3.90}$$

Therefore,

$$u_m^{-(0)} = \frac{\partial W_p}{\partial \xi_m}\left(\frac{1}{2} - \xi_3^-\right), \tag{3.91}$$

and

$$\begin{aligned}
\sigma_{mm}^{-(0)} &= \left(\frac{1}{2} - \xi_3^-\right)\left(\eta\frac{\partial^2 W_p}{\partial\xi_m^2} + 2\vartheta\frac{\partial^2 W_p}{\partial\xi_n^2}\right), \\
\sigma_{12}^{-(0)} &= (1-2\xi_3^-)\frac{\partial^2 W_p}{\partial\xi_1\partial\xi_2}, \\
\sigma_{m3}^{-(0)} &= \frac{\eta}{2}\xi_3^-(\xi_3^- - 1)\left(\frac{\partial^3 W_p}{\partial\xi_m^3} + \frac{\partial^3 W_p}{\partial\xi_m\partial\xi_n^2}\right).
\end{aligned} \tag{3.92}$$

Finally, from $(3.92)_3$ and $(3.85)_1$, and satisfying the continuity condition $(3.87)_3$, we obtain for the vertical stress

$$\sigma_{33}^{-(0)} = -\frac{\eta}{12}\left[(\xi_3^-)^2(2\xi_3^- - 3) + 1\right]\tilde{\Delta}_{12}^2 W_p, \tag{3.93}$$

where

$$\tilde{\Delta}_{12}^2 = \frac{\partial^4}{\partial\xi_1^4} + 2\frac{\partial^4}{\partial\xi_1^2\partial\xi_2^2} + \frac{\partial^4}{\partial\xi_2^4} \tag{3.94}$$

Using the condition $(3.86)_1$ at $\xi_3^- = 0$, we have

$$\frac{\eta}{12}\tilde{\Delta}_{12}^2 W_p = p^*, \tag{3.95}$$

which in dimensional form coincides with the equation (1.34) of plate bending with $P_r = 0$.

Subcase $\alpha = 3$ $(\mu \sim \varepsilon^3)$

Here, we begin with the same leading order governing equations for the layer (3.85) and boundary conditions (3.86), while continuity conditions at $\xi_3^- = 1$ take the form

$$u_m^{+(0)} = 0, \qquad u_3^{-(0)} = u_3^{+(0)}, \qquad \sigma_{m3}^{-(0)} = 0, \qquad \sigma_{33}^{-(0)} = \sigma_{33}^{+(0)}. \tag{3.96}$$

Following a similar procedure, the quantities $u_3^{-(0)}, u_m^{-(0)}$ are found as (3.88), (3.91), respectively, and $\sigma_{mm}^{-(0)}, \sigma_{12}^{-(0)}\sigma_{m3}^{-(0)}$ as (3.92). Then, from $(3.85)_1$, we obtain

$$\sigma_{33}^{-(0)} = -\frac{\eta}{12}(\xi_3^-)^2(2\xi_3^- - 3)\tilde{\Delta}_{12}^2 W_p + F_2, \tag{3.97}$$

where F_2 is an arbitrary function of ξ_1 and ξ_2. The vertical stress at the interface is given by

$$\sigma_{33}^{-(0)}\Big|_{\xi_3^-=1} = \frac{\eta}{12}\tilde{\Delta}_{12}^2 W_p + F_2. \tag{3.98}$$

Due to continuity condition $(3.96)_4$ at $\xi_3^- = 1$ we get

$$F_2 = \sigma_{33}^{+(0)}\Big|_{\xi_3^-=1} - \frac{\eta}{12}\tilde{\Delta}_{12}^2 W_p. \tag{3.99}$$

Thus,

$$\sigma_{33}^{-(0)} = -\frac{\eta}{12}((\xi_3^-)^2(2\xi_3^- - 3) + 1)\tilde{\Delta}_{12}^2 W_p + \sigma_{33}^{+(0)}\Big|_{\xi_3^-=1}, \tag{3.100}$$

which, satisfying $(3.86)_1$ at $\xi_3^- = 0$, implies

$$\frac{\eta}{12}\tilde{\Delta}_{12}^2 W_p = p^* + \sigma_{33}^{+(0)}\Big|_{\xi_3^-=1}. \tag{3.101}$$

The equation above demonstrates that at $\alpha = 3$ the plate bending theory is still valid, but in contrast to the subcase $\alpha > 3$, the half-space reaction P_r is now nonzero.

3.4.2 Case $2 \le \alpha < 3$ $\left(\varepsilon^3 \lesssim \mu \ll \varepsilon^2\right)$

The scaling for the layer is now given by (see row 2 in Table 3.2)

$$\begin{aligned} &u_m^- = h\varepsilon^{-\alpha}u_m^{*-}, && \sigma_{mm}^- = \mu^-\varepsilon^{1-\alpha}\sigma_{mm}^{*-}, && \sigma_{12}^- = \mu^-\varepsilon^{1-\alpha}\sigma_{12}^{*-}, \\ &u_3^- = h\varepsilon^{-\alpha-1}u_3^{*-}, && \sigma_{33}^- = \mu^-\sigma_{33}^{*-}, && \sigma_{m3}^- = \mu^-\varepsilon^{2-\alpha}\sigma_{m3}^{*-}. \end{aligned} \tag{3.102}$$

Hence, due to (3.102), equations $(1.24)_1$ and (1.19) become

$$\begin{aligned} &\sigma_{m1,1}^{*-} + \sigma_{m2,2}^{*-} + \sigma_{m3,3}^{*-} = 0, \\ &\varepsilon^{3-\alpha}(\sigma_{13,1}^{*-} + \sigma_{23,2}^{*-}) + \sigma_{33,3}^{*-} = 0, \\ &\varepsilon^2\sigma_{mm}^{*-} = \varepsilon^2\gamma^- u_{m,m}^{*-} + \varepsilon^2(\gamma^- - 2)u_{n,n}^{*-} + (\gamma^- - 2)u_{3,3}^{*-}, \\ &\varepsilon^{\alpha+1}\sigma_{33}^{*-} = \varepsilon^2(\gamma^- - 2)u_{1,1}^{*-} + \varepsilon^2(\gamma^- - 2)u_{2,2}^{*-} + \gamma^- u_{3,3}^{*-}, \\ &\sigma_{12}^{*-} = u_{1,2}^{*-} + u_{2,1}^{*-}, \\ &\varepsilon^2\sigma_{m3}^{*-} = u_{m,3}^{*-} + u_{3,m}^{*-}. \end{aligned} \tag{3.103}$$

Similarly to the previous Subsection 3.4.1, we deduce from $(3.103)_3$ and $(3.103)_4$

$$\sigma^{*-}_{mm}\gamma^- - \varepsilon^{\alpha-1}(\gamma^- - 2)\sigma^{*-}_{33} = 4(\gamma^- - 1)u^{*-}_{m,m} + 2(\gamma^- - 2)u^{*-}_{n,n}. \tag{3.104}$$

The scaling for the half-space here and below takes the form

$$u^+_i = h\varepsilon^{-\alpha-1}u^{*+}_i, \qquad \sigma^+_{ij} = \mu^-\sigma^{*+}_{ij}, \tag{3.105}$$

leading to equations (3.81).

Boundary conditions are once again represented as (3.82) and the continuity conditions are

$$\varepsilon u^{*-}_m = u^{*+}_m, \qquad u^{*-}_3 = u^{*+}_3, \qquad \sigma^{*-}_{m3} = \varepsilon^{\alpha-2}\sigma^{*+}_{m3}, \qquad \sigma^{*-}_{33} = \sigma^{*+}_{33}. \tag{3.106}$$

Below, we deal with the subcases $2 < \alpha < 3$ and $\alpha = 2$ separately.

Subcase $2 < \alpha < 3$ $(\varepsilon^3 \ll \mu \ll \varepsilon^2)$

The leading order governing equations are

$$\begin{aligned}
&\sigma^{-(0)}_{m1,1} + \sigma^{-(0)}_{m2,2} + \sigma^{-(0)}_{m3,3} = 0,\\
&\sigma^{-(0)}_{33,3} = 0,\\
&u^{-(0)}_{3,3} = 0,\\
&\sigma^{-(0)}_{12} = u^{-(0)}_{1,2} + u^{-(0)}_{2,1},\\
&u^{-(0)}_{m,3} + u^{-(0)}_{3,m} = 0,\\
&\sigma^{-(0)}_{mm} = \eta u^{-(0)}_{m,m} + 2\vartheta u^{-(0)}_{n,n},
\end{aligned} \tag{3.107}$$

subject to boundary conditions (3.86), and the following continuity conditions at $\xi^-_3 = 1$

$$u^{+(0)}_m = 0, \qquad u^{-(0)}_3 = u^{+(0)}_3, \qquad \sigma^{-(0)}_{m3} = 0, \qquad \sigma^{-(0)}_{33} = \sigma^{+(0)}_{33}. \tag{3.108}$$

As in Subsection 3.4.1, the quantities $u_3^{-(0)}$, $u_m^{-(0)}$ are found in the form (3.88), (3.91), respectively, and $\sigma_{mm}^{-(0)}$, $\sigma_{12}^{-(0)}$, $\sigma_{m3}^{-(0)}$ are obtained as (3.92). Then, integrating $(3.107)_2$ with respect to ξ_3^- and satisfying $(3.86)_1$, we derive

$$\sigma_{33}^{-(0)} = -p^*. \tag{3.109}$$

It is clear from (3.109) that in this case the applied load p^* is transmitted to the interface and is no longer connected with the layer deflection directly. Thus, the value of the deflection and, subsequently, the rest of the stresses and displacements, strongly depend on the value of the interfacial displacement $u_3^{+(0)}$, due to $(3.108)_2$, which indicates violation of the plate bending theory.

Subcase $\alpha = 2$ $(\mu \sim \varepsilon^2)$

The leading order equations are again given by (3.107) with boundary conditions (3.86), and the continuity conditions at $\xi_3^- = 1$ are written as

$$u_m^{+(0)} = 0, \qquad u_3^{-(0)} = u_3^{+(0)}, \qquad \sigma_{i3}^{-(0)} = \sigma_{i3}^{+(0)}, \tag{3.110}$$

leading to vertical displacement $u_3^{-(0)}$ and stress $\sigma_{33}^{-(0)}$ expressed as (3.88) and (3.109), respectively. Using $(3.107)_5$, we deduce

$$\begin{aligned} u_1^{-(0)} &= -\xi_3^- \frac{\partial W_p}{\partial \xi_1} + F_3, \\ u_2^{-(0)} &= -\xi_3^- \frac{\partial W_p}{\partial \xi_2} + F_4, \end{aligned} \tag{3.111}$$

where F_3 and F_4 are arbitrary functions of ξ_1 and ξ_2. Therefore, $(3.107)_6$ implies

$$\begin{aligned} \sigma_{11}^{-(0)} &= \eta \left(\frac{\partial F_3}{\partial \xi_1} - \xi_3^- \frac{\partial^2 W_p}{\partial \xi_1^2} \right) + 2\vartheta \left(\frac{\partial F_4}{\partial \xi_2} - \xi_3^- \frac{\partial^2 W_p}{\partial \xi_2^2} \right), \\ \sigma_{22}^{-(0)} &= \eta \left(\frac{\partial F_4}{\partial \xi_2} - \xi_3^- \frac{\partial^2 W_p}{\partial \xi_2^2} \right) + 2\vartheta \left(\frac{\partial F_3}{\partial \xi_1} - \xi_3^- \frac{\partial^2 W_p}{\partial \xi_1^2} \right), \end{aligned} \tag{3.112}$$

and $(3.107)_4$ yields

$$\sigma_{12}^{-(0)} = -2\xi_3^- \frac{\partial^2 W_p}{\partial \xi_1 \xi_2} + \frac{\partial F_3}{\partial \xi_2} + \frac{\partial F_4}{\partial \xi_1}. \tag{3.113}$$

From $(3.107)_1$, taking into account (3.112) and (3.113), and satisfying $(3.86)_2$, we arrive at

$$\begin{aligned}
\sigma_{13}^{-(0)} &= \frac{\eta}{2}(\xi_3^-)^2 \left[\frac{\partial^3 W_p}{\partial \xi_1^3} + \frac{\partial^3 W_p}{\partial \xi_1 \partial \xi_2^2}\right] - \xi_3^- \left(\eta \frac{\partial^2 F_3}{\partial \xi_1^2} + (\eta - 1)\frac{\partial^2 F_4}{\partial \xi_1 \partial \xi_2} + \frac{\partial^2 F_3}{\partial \xi_2^2}\right), \\
\sigma_{23}^{-(0)} &= \frac{\eta}{2}(\xi_3^-)^2 \left[\frac{\partial^3 W_p}{\partial \xi_1^2 \partial \xi_2} + \frac{\partial^3 W_p}{\partial \xi_2^3}\right] - \xi_3^- \left(\eta \frac{\partial^2 F_4}{\partial \xi_2^2} + (\eta - 1)\frac{\partial^2 F_3}{\partial \xi_1 \partial \xi_2} + \frac{\partial^2 F_4}{\partial \xi_1^2}\right),
\end{aligned} \tag{3.114}$$

where functions F_3 and F_4 can be found from solving the problem for the half-space and using continuity conditions $(3.110)_3$.

3.4.3 Case $1 \leq \alpha < 2$ $\left(\varepsilon^2 \lesssim \mu \ll \varepsilon\right)$

The scaling for the layer is taken as

$$\begin{aligned}
&u_m^- = h\varepsilon^{-2} u_m^{*-}, \qquad && \sigma_{12}^- = \mu^- \varepsilon^{-1} \sigma_{12}^{*-}, \qquad && u_3^- = h\varepsilon^{-\alpha-1} u_3^{*-}, \\
&\sigma_{i3}^- = \mu^- \sigma_{m3}^{*-}, && \sigma_{mm}^- = \mu^- \varepsilon^{-1} \sigma_{mm}^{*-}.
\end{aligned} \tag{3.115}$$

Substituting the latter into governing equations $(1.24)_1$ and (1.19), we have

$$\begin{aligned}
&\sigma_{m1,1}^{*-} + \sigma_{m2,2}^{*-} + \sigma_{m3,3}^{*-} = 0, \\
&\varepsilon(\sigma_{13,1}^{*-} + \sigma_{23,2}^{*-}) + \sigma_{33,3}^{*-} = 0, \\
&\varepsilon^\alpha \sigma_{mm}^{*-} = \varepsilon^\alpha \gamma^- u_{m,m}^{*-} + \varepsilon^\alpha(\gamma^- - 2) u_{n,n}^{*-} + (\gamma^- - 2) u_{3,3}^{*-}, \\
&\varepsilon^{\alpha+1} \sigma_{33}^{*-} = \varepsilon^\alpha(\gamma^- - 2) u_{1,1}^{*-} + \varepsilon^\alpha(\gamma^- - 2) u_{2,2}^{*-} + \gamma^- u_{3,3}^{*-}, \\
&\sigma_{12}^{*-} = u_{1,2}^{*-} + u_{2,1}^{*-}, \\
&\varepsilon^2 \sigma_{m3}^{*-} = u_{m,3}^{*-} + \varepsilon^{2-\alpha} u_{3,m}^{*-},
\end{aligned} \tag{3.116}$$

with the following additional equation obtained from $(3.116)_3$ and $(3.116)_4$

$$\sigma_{mm}^{*-} \gamma^- - \varepsilon(\gamma^- - 2)\sigma_{33}^{*-} = 4(\gamma^- - 1) u_{m,m}^{*-} + 2(\gamma^- - 2) u_{n,n}^{*-}, \tag{3.117}$$

this being similar to (3.79) and (3.104).

The boundary conditions are taken as (3.82), whereas the continuity conditions at $\xi_3^- = 1$ are

$$\varepsilon^{\alpha-1} u_m^{*-} = u_m^{*+}, \qquad u_3^{*-} = u_3^{*+}, \qquad \sigma_{i3}^{*-} = \sigma_{i3}^{*+}. \tag{3.118}$$

We again treat subcases $1 < \alpha < 2$ and $\alpha = 1$ separately.

Subcase $1 < \alpha < 2$ $(\varepsilon^2 \ll \mu \ll \varepsilon)$

Leading order equations are

$$\begin{aligned}
&\sigma_{m1,1}^{-(0)} + \sigma_{m2,2}^{-(0)} + \sigma_{m3,3}^{-(0)} = 0,\\
&\sigma_{33,3}^{-(0)} = 0,\\
&u_{3,3}^{-(0)} = 0,\\
&\sigma_{12}^{-(0)} = u_{1,2}^{-(0)} + u_{2,1}^{-(0)},\\
&u_{m,3}^{-(0)} = 0,\\
&\sigma_{mm}^{-(0)} = \eta u_{m,m}^{-(0)} + 2\vartheta u_{n,n}^{-(0)},
\end{aligned} \tag{3.119}$$

subject to boundary conditions (3.86) and the continuity conditions at $\xi_3^- = 1$

$$u_m^{+(0)} = 0, \qquad u_3^{-(0)} = u_3^{+(0)}, \qquad \sigma_{i3}^{-(0)} = \sigma_{i3}^{+(0)}. \tag{3.120}$$

As before, $u_3^{-(0)}$ and $\sigma_{33}^{-(0)}$ are expressed as (3.88) and (3.109). It follows from $(3.119)_5$ and $(3.125)_1$ that

$$\begin{aligned}
u_1^{-(0)} &= F_5,\\
u_2^{-(0)} &= F_6,
\end{aligned} \tag{3.121}$$

resulting in

$$\begin{aligned}
\sigma_{11}^{-(0)} &= \eta \frac{\partial F_5}{\partial \xi_1} + 2\vartheta \frac{\partial F_6}{\partial \xi_2},\\
\sigma_{22}^{-(0)} &= \eta \frac{\partial F_6}{\partial \xi_2} + 2\vartheta \frac{\partial F_5}{\partial \xi_1},
\end{aligned} \tag{3.122}$$

and

$$\sigma_{12}^{-(0)} = \frac{\partial F_5}{\partial \xi_2} + \frac{\partial F_6}{\partial \xi_1}, \tag{3.123}$$

where F_5 and F_6 are arbitrary functions of ξ_1 and ξ_2. Finally, from $(3.119)_1$, satisfying $(3.86)_2$, we infer

$$\begin{aligned} \sigma_{13}^{-(0)} &= -\xi_3^- \left(\eta \frac{\partial^2 F_5}{\partial \xi_1^2} + (\eta - 1) \frac{\partial^2 F_6}{\partial \xi_1 \partial \xi_2} + \frac{\partial^2 F_5}{\partial \xi_2^2} \right), \\ \sigma_{23}^{-(0)} &= -\xi_3^- \left(\eta \frac{\partial^2 F_6}{\partial \xi_2^2} + (\eta - 1) \frac{\partial^2 F_5}{\partial \xi_1 \partial \xi_2} + \frac{\partial^2 F_6}{\partial \xi_1^2} \right). \end{aligned} \tag{3.124}$$

Here, functions F_5 and F_6 can again be derived from the continuity conditions $(3.120)_3$.

Subcase $\alpha = 1$ $(\mu \sim \varepsilon)$

Now the leading order governing equations and the boundary conditions are taken as (3.119) and (3.86), respectively, and the continuity conditions at $\xi_3^- = 1$ are

$$u_i^{-(0)} = u_i^{+(0)}, \qquad \sigma_{i3}^{-(0)} = \sigma_{i3}^{+(0)}. \tag{3.125}$$

As above, $u_3^{-(0)}$ and $\sigma_{33}^{-(0)}$ are given by (3.88) and (3.109), respectively, while $(3.119)_5$ and $(3.125)_1$ imply

$$u_m^{-(0)} = u_m^{+(0)}\big|_{\xi_3^- = 1}. \tag{3.126}$$

Hence,

$$\begin{aligned} \sigma_{mm}^{-(0)} &= \left(\eta \frac{\partial u_m^{+(0)}}{\partial \xi_m} + 2\vartheta \frac{\partial u_n^{+(0)}}{\partial \xi_n} \right)\Bigg|_{\xi_3^- = 1}, \\ \sigma_{12}^{-(0)} &= \left(\frac{\partial u_1^{+(0)}}{\partial \xi_2} + \frac{\partial u_2^{+(0)}}{\partial \xi_1} \right)\Bigg|_{\xi_3^- = 1}. \end{aligned} \tag{3.127}$$

Thus, from $(3.119)_1$, and satisfying $(3.86)_2$, we arrive at

$$\sigma_{m3}^{-(0)} = -\xi_3^- \left(\eta \frac{\partial^2 u_m^{+(0)}}{\partial \xi_m^2} + (\eta - 1) \frac{\partial^2 u_n^{+(0)}}{\partial \xi_1 \partial \xi_2} + \frac{\partial^2 u_m^{+(0)}}{\partial \xi_n^2} \right)\Bigg|_{\xi_3^- = 1}. \tag{3.128}$$

3.4.4 Case $0 \leq \alpha < 1$ $(\varepsilon \lesssim \mu \ll 1)$

The scaling for the layer is

$$\begin{aligned} &u_i^- = h\varepsilon^{-\alpha-1}u_i^{*-}, \qquad &&\sigma_{12}^- = \mu^-\varepsilon^{-\alpha}\sigma_{12}^{*-}, \qquad &&\sigma_{33}^- = \mu^-\sigma_{33}^{*-}, \\ &\sigma_{mm}^- = \mu^-\varepsilon^{-\alpha}\sigma_{mm}^{*-}, \qquad &&\sigma_{m3}^- = \mu^-\varepsilon^{1-\alpha}\sigma_{m3}^{*-}. \end{aligned} \tag{3.129}$$

As a result, the governing equations $(1.24)_1$ and (1.19) become

$$\begin{aligned} &\sigma_{m1,1}^{*-} + \sigma_{m2,2}^{*-} + \sigma_{m3,3}^{*-} = 0, \\ &\varepsilon^{2-\alpha}(\sigma_{13,1}^{*-} + \sigma_{23,2}^{*-}) + \sigma_{33,3}^{*-} = 0, \\ &\varepsilon\sigma_{mm}^{*-} = \varepsilon\gamma^- u_{m,m}^{*-} + \varepsilon(\gamma^- - 2)u_{n,n}^{*-} + (\gamma^- - 2)u_{3,3}^{*-}, \\ &\varepsilon^{\alpha+1}\sigma_{33}^{*-} = \varepsilon(\gamma^- - 2)u_{1,1}^{*-} + \varepsilon(\gamma^- - 2)u_{2,2}^{*-} + \gamma^- u_{3,3}^{*-}, \\ &\sigma_{12}^{*-} = u_{1,2}^{*-} + u_{2,1}^{*-}, \\ &\varepsilon^2\sigma_{m3}^{*-} = u_{m,3}^{*-} + \varepsilon u_{3,m}^{*-}, \end{aligned} \tag{3.130}$$

together with the equation

$$\sigma_{mm}^{*-}\gamma^- - \varepsilon^\alpha(\gamma^- - 2)\sigma_{33}^{*-} = 4(\gamma^- - 1)u_{m,m}^{*-} + 2(\gamma^- - 2)u_{n,n}^{*-}, \tag{3.131}$$

subject to boundary conditions (3.82) and the continuity conditions at $\xi_3^- = 1$

$$u_i^{*-} = u_i^{*+}, \qquad \sigma_{m3}^{*-} = \varepsilon^{\alpha-1}\sigma_{m3}^{*+}, \qquad \sigma_{33}^{*-} = \sigma_{33}^{*+}. \tag{3.132}$$

At leading order the governing equations are

$$\begin{aligned} &\sigma_{m1,1}^{-(0)} + \sigma_{m2,2}^{-(0)} + \sigma_{m3,3}^{-(0)} = 0, \\ &\sigma_{33,3}^{-(0)} = 0, \\ &u_{3,3}^{-(0)} = 0, \\ &\sigma_{12}^{-(0)} = u_{1,2}^{-(0)} + u_{2,1}^{-(0)}, \\ &u_{m,3}^{-(0)} = 0, \\ &\sigma_{mm}^{-(0)} - \varepsilon^\alpha\vartheta\sigma_{33}^{-(0)} = \eta u_{m,m}^{-(0)} + 2\vartheta u_{n,n}^{-(0)}, \end{aligned} \tag{3.133}$$

where term $\sigma_{33}^{-(0)}$ can be neglected at $0 < \alpha < 1$, with boundary conditions (3.86) and the continuity conditions at $\xi_3^- = 1$

$$u_i^{-(0)} = u_i^{+(0)}, \qquad \sigma_{m3}^{+(0)} = 0, \qquad \sigma_{33}^{-(0)} = \sigma_{33}^{+(0)}. \tag{3.134}$$

The stated problem leads to the results for the displacements and vertical stress given by (3.88), (3.126) and (3.109).

3.4.5 Approximate formulations for a half-space

The analysis of the relation between the applied force p^* and the deflection of the layer W_p considered above demonstrates that the classical equation of plate bending arises only at a relatively high contrast ($\alpha \geq 3$ or $\mu \lesssim \varepsilon^3$), see (3.95) and (3.101). Moreover, (3.95) is completely independent of the half-space presence, therefore, the value of the deflection W_p can be easily obtained.

At the same time, at $\alpha \leq 3$, it is not possible to treat the layer and the half-space separately, therefore, in order to find the deflection W_p, the problem for the half-space should be also solved. We can, however, formulate boundary conditions at the surface of the half-space instead of solving the full original problem for a layered solid.

At $\alpha = 3$, using continuity conditions (3.96) along with equation (3.101), the sought for effective boundary conditions at $\xi_3^+ = 0$ for the half-space take the form

$$u_m^{+(0)} = 0, \qquad \sigma_{33}^{+(0)} = \frac{\eta}{12}\tilde{\Delta}_{12}^2 u_3^{+(0)}|_{\xi_3^+=0} - p^*. \tag{3.135}$$

Thus, the normal stress is expressed through the vertical displacement at the surface; in doing so, the operator in the right hand side of (3.135) corresponds to the Kirchhoff plate theory.

At $0 \leq \alpha < 3$, the vertical force applied at the upper face of the layer can be transmitted to the interface, see (3.109). Therefore, at $1 < \alpha < 3$, using continuity conditions (3.108), (3.110) and (3.120), we arrive at the following mixed boundary conditions along the surface of the half-space $\xi_3^+ = 0$

$$u_m^{+(0)} = 0, \qquad \sigma_{33}^{+(0)} = -p^*. \tag{3.136}$$

At $\alpha = 1$, taking into account expression (3.128) for shear stresses and continuity conditions (3.125), the effective boundary conditions at $\xi_3^+ = 0$ become

$$\sigma_{33}^{+(0)} = -p^*, \qquad \sigma_{m3}^{+(0)} = -\left(\eta \frac{\partial^2 u_m^{+(0)}}{\partial \xi_m^2} + (\eta - 1)\frac{\partial^2 u_n^{+(0)}}{\partial \xi_1 \partial \xi_2} + \frac{\partial^2 u_m^{+(0)}}{\partial \xi_n^2}\right)\Bigg|_{\xi_3^+=0}. \tag{3.137}$$

Here, the shear stresses are expressed through the horisontal displacements at the surface. These conditions were previously studied in [36] and [160] for a non-contrast case.

Finally, at $0 \leq \alpha < 1$, due to continuity conditions (3.134), we get boundary conditions (3.68) formulated in Subsection 3.3.5.

Transverse displacement $u_3^{-(0)}$ is always uniform at leading order across the thickness of the layer, i.e. $u_3^{-(0)} = W_p$, see (3.88). Thus, due to continuity conditions $(3.108)_2$, $(3.110)_2$, $(3.120)_2$, $(3.125)_1$, $(3.134)_1$, we have

$$W_p = u_3^{+(0)}|_{\xi_3^+=0}. \tag{3.138}$$

Therefore, in case of $\alpha \leq 3$, the value of the deflection of the layer follows from solutions of the simpler problems for the half-space with the boundary conditions formulated above applied along its surface. For plane strain problem with sinusoidal load (3.3) they are presented in Section 3.5.

3.5 BVPs for a homogeneous half-space

Consider a homogeneous elastic half-space ($\xi_3^+ \geq 0$) subject to the boundary conditions presented in Table 3.3, where P is a vertical sinusoidal load defined in (3.3).

The equations of the formulated plane strain problem and the solution are given by $(3.4)_3$, $(3.4)_4$ and (3.6) with functions $(3.14)_2$ and $(3.15)_2$, where C_0^+ is taken as $(3.16)_1$, and the values of the coefficients C_5 and C_6, corresponding to the appropriate boundary conditions, are presented in Table 3.3, together with the rest of the displacement and stress components at the surface $\xi_3^+ = 0$. In the Table, $D_1 = \gamma^- - 1 - \gamma^+ + 7\gamma^-\gamma^+$, $D_2 = \gamma^-(2 + 3\gamma^+) - 2(1 + \gamma^+)$ and $D_3 = \gamma^-(3\gamma^+ - 1) - 2\gamma^+$.

3.6 Validation of asymptotic results

In this section we justify the derived asymptotic results by numerical comparison with the exact solution of the plane problem for sinusoidal load (3.3) applied at the surface $x_3 = 0$ or $\xi_3^- = 0$. In doing so, we study the normalized coefficient

$$r_* = \frac{h}{\mu^-} r, \tag{3.139}$$

where r is defined in (3.17).

The related exact solution takes the form

$$r_* = \frac{Ah}{C_1 + C_2} \tag{3.140}$$

with constants C_1 and C_2 given by (3.16), see Section 3.2.

In case of a soft layer, the asymptotic formulae are given in (3.72) – (3.76), where interfacial displacement w_h, as it was discussed above, can be obtained from a simpler

	Case 1	Case 2	Case 3	Case 4
Boundary conditions for a homogeneous half-space				
σ_{33}^+	$-P$	$\dfrac{\eta\mu^+}{12a}\dfrac{\partial^4 u_3^+}{\partial\xi_1^4}\Big\vert_{\xi_3^+=0} - P$	$-P$	$-P$
u_1^+	–	0	0	–
σ_{13}^+	0	–	–	$-\dfrac{\eta\mu^+}{l}\dfrac{\partial^2 u_1^+}{\partial\xi_1^2}\Big\vert_{\xi_3^+=0}$
Coefficients in $(3.14)_2$ and $(3.15)_2$				
$\dfrac{c_5\mu^+}{Aa\mu^-}$	$\dfrac{\gamma^+}{2(\gamma^+-1)}$	$\dfrac{3\gamma^-(\gamma^++1)}{D_1}$	$\dfrac{\gamma^++1}{2\gamma^+}$	$\dfrac{D_2}{2D_3}$
$\dfrac{c_6\mu^+}{Aa\mu^-}$	$\dfrac{1}{2}$	$\dfrac{3\gamma^-(\gamma^+-1)}{D_1}$	$\dfrac{\gamma^+-1}{2\gamma^+}$	$\dfrac{(3\gamma^--2)(\gamma^+-1)}{2D_3}$
Displacement and stress components at the surface $\xi_3^+=0$				
$\dfrac{u_1^+\mu^+}{Aa\mu^-\sin\xi_1}$	$-\dfrac{1}{2(\gamma^+-1)}$	–	–	$\dfrac{\gamma^-}{2(\gamma^-+2\gamma^+-3\gamma^-\gamma^+)}$
$\dfrac{u_3^+\mu^+}{Aa\mu^-\cos\xi_1}$	$\dfrac{\gamma^+}{2(\gamma^+-1)}$	$\dfrac{3\gamma^-(\gamma^++1)}{D_1}$	$\dfrac{\gamma^++1}{2\gamma^+}$	$\dfrac{D_2}{2D_3}$
$\dfrac{\sigma_{13}^+}{A\mu^-\sin\xi_1}$	–	$-\dfrac{6\gamma^-}{D_1}$	$-\dfrac{1}{\gamma^+}$	$-\dfrac{2(\gamma^--1)}{D_3}$
$\dfrac{\sigma_{33}^+}{A\mu^-\cos\xi_1}$	–	$-\dfrac{6\gamma^-\gamma^+}{D_1}$	–	–

Table 3.3: BVPs for a homogeneous half-space

problem for a half-space with load (3.3) applied at its surface, see Subsection 3.3.5 and Section 3.5. Therefore, using Case 1 in Table 3.3, we get

$$r_* = \begin{cases} \gamma^-, \quad \text{formula (1.31) with } r \text{ from the first line in (3.18)}, \\ \dfrac{3l^2(\gamma^-)^2}{3l^2\gamma^- - h^2(5\gamma^- - (\gamma^-)^2 - 6)}, \quad \text{formula (3.69)}, \\ \dfrac{2h\mu^+\gamma^-(\gamma^+-1)}{l\gamma^-\gamma^+\mu^- + 2h\mu^+(\gamma^+-1)}, \quad \text{formula (3.74)}, \\ \dfrac{2h\mu^+(\gamma^+-1)}{l\gamma^+\mu^-}, \quad \text{formula (3.76)}. \end{cases} \tag{3.141}$$

For a stiff layer, we use asymptotic relation (3.95) for $\alpha > 3$, and the solutions

of plane problems in Table 3.3 for $0 \leq \alpha \leq 3$, see Subsection 3.4.5 and Section 3.5 for more detail. Thus, the expression for the coefficient r coincides with leading order exact solution (3.19).

Numerical results are presented in Figures 3.3 and 3.4 for a soft and a stiff coating, respectively, in which $\alpha = \log_\varepsilon \mu$ and also $\nu^- = 0.25$, $\nu^+ = 0.3$, and $\varepsilon = h/l = 0.1$.

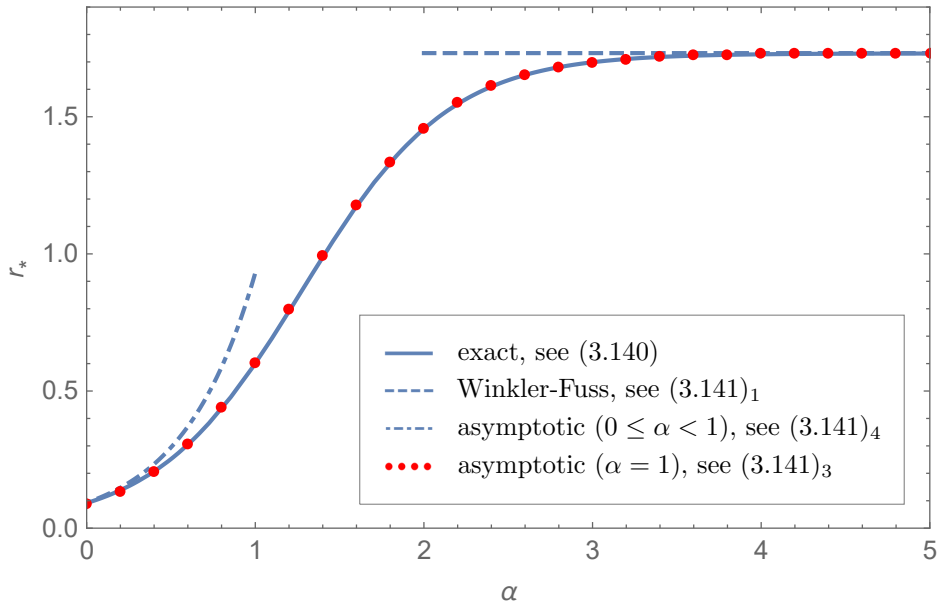

Figure 3.3: Approximate and exact solutions for sinusoidal load for a soft layer ($\varepsilon = 0.1$, $\nu^- = 0.25$, $\nu^+ = 0.3$)

In Figure 3.3 the exact solution is plotted with solid line, while the graphs corresponding to the Winkler-Fuss hypothesis (the first line in (3.141)) and the formula in the forth line in (3.141) (which is based on the assumption of uniform variation of the transverse displacement across the thickness of the layer) are displayed by dashed and dot-dashed lines, respectively. The Figure shows that two aforementioned formulae have limited ranges of applicability. At the same time, the formula in the third line of (3.141) appears to be uniformly valid, and the associated curve denoted by red dots in

the Figure coincide with that for the exact solution. We also mention that the deviation of the straight line corresponding to the Pasternak model, see the second line in (3.141), from that for the Winkler-Fuss one is only 0.07%.

(a) $0 \le \alpha \le 1.5$

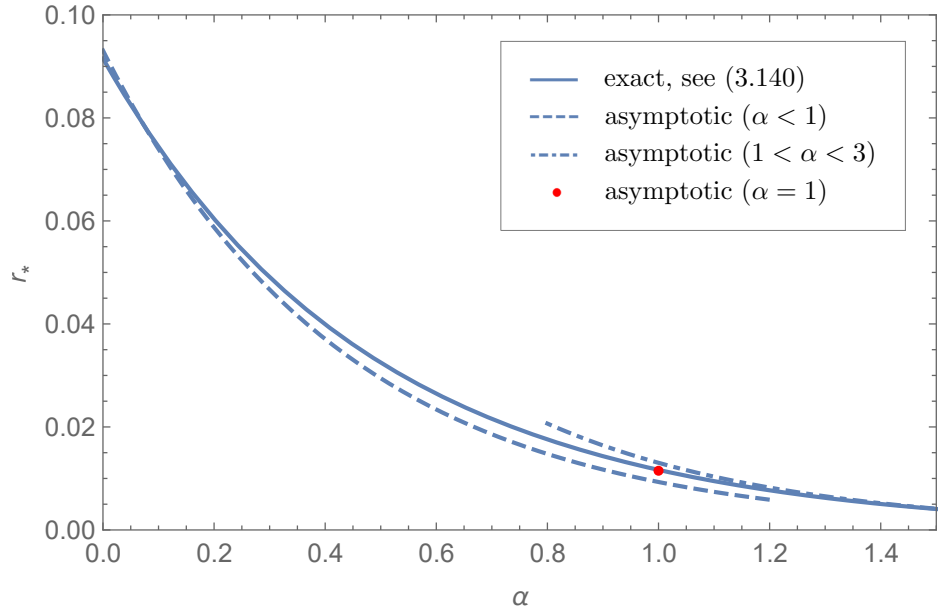

(b) $2.5 \le \alpha \le 5.5$

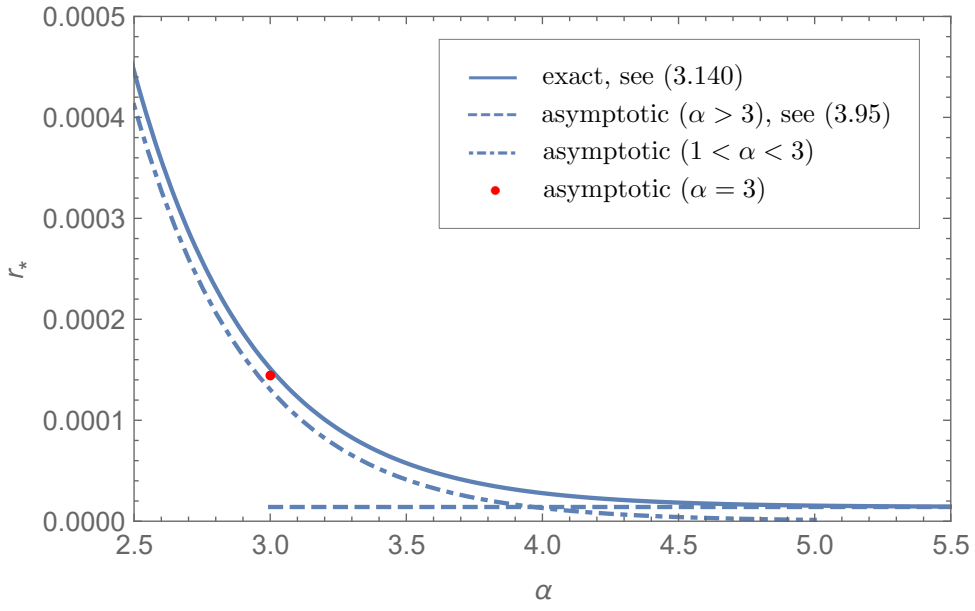

Figure 3.4: Approximate and exact solutions for sinusoidal load for a stiff layer ($\varepsilon = 0.1$, $\nu^- = 0.25$, $\nu^+ = 0.3$)

In Figure 3.4 the exact solution is also depicted by solid line, whereas the graphs related to the developed asymptotic approximations are represented by dashed and dot-dashed lines. The asymptotic results for limiting cases $\alpha = 1$ and $\alpha = 3$ are denoted by red dots in Figures 3.4(a) and 3.4(b), respectively. The region $1.5 < \alpha < 2.5$ is not shown since the difference between the associated asymptotic approximation and the exact solution is virtually indistinguishable.

Chapter 4

Higher order effective boundary conditions

In this chapter we consider a 3D dynamic problem for a solid covered by a thin coating with the absence of contrast in stiffness of the layer and the substrate. Higher order effective boundary conditions are derived for a coated half-space. Comparison with the long wavelength expansion of the exact solutions of plane and anti-plane time-harmonic problems for the coating demonstrates the validity of the proposed formulation. At the same time the corrections to the simplest leading order effective conditions, earlier obtained in the widely cited paper [22], are proven to be asymptotically inconsistent. The results were published in [80].

4.1 Statement of the problem

We consider a dynamic problem for a linearly elastic isotropic layer of thickness h occupying the area $0 \leq x_3 \leq h$, lying on an elastic half-space $x_3 \geq h$. The prescribed vertical dynamic force $P = P(x_1, x_2, t)$ is acting on the free surface of the layer, see Figure 3.1.

As in Chapter 3, the boundary and continuity conditions may be taken as (3.1)

and (3.2), respectively, with the decay conditions, but the dimensionless governing equations for the dynamic problem are given by (1.22) together with the constitutive relations (1.19) and (1.20). Note, that dimensionless coordinates and time follow from (1.18) and (1.21), respectively.

The leading order effective boundary conditions on the surface of the substrate, modelling the effect of the coating, can be written as, see (3.18) in [36],

$$\begin{aligned}
&\sigma_{33}^{+} = \rho^{-} h \frac{\partial^2 u_3^{+}}{\partial t^2} - P, \\
&\sigma_{m3}^{+} = \rho^{-} h \left[\frac{\partial^2 u_m^{+}}{\partial t^2} - (c_2^{-})^2 \left(\frac{\partial^2 u_m^{+}}{\partial x_n^2} + \eta \frac{\partial^2 u_m^{+}}{\partial x_m^2} + (\eta - 1) \frac{\partial^2 u_n^{+}}{\partial x_m \partial x_n} \right) \right],
\end{aligned} \tag{4.1}$$

where γ^{-} and η are defined in (1.12) and (3.37), respectively, and $m, n = 1, 2$, $m \neq n$. In absence of surface loading ($P = 0$) these conditions coincide with those in [160] derived starting from the 2D theory of plate extension. The comparisons made in [36] with [103] also provide an illustration of the asymptotic consistency of the leading order effective boundary conditions obtained in [160]. The developments in [22], see also [127] treating a similar anisotropic problem, claim that the effective conditions (4.1) ignore several essential h-terms. The formulae (35) and (36) in [22] rewritten in the notation specified in this section, similarly to [36], can be presented as

$$\begin{aligned}
\sigma_{33}^{+} = \quad & \rho^{-} h \frac{\partial^2 u_3^{+}}{\partial t^2} \underline{- h \left(\frac{\partial \sigma_{m3}^{+}}{\partial x_m} + \frac{\partial \sigma_{n3}^{+}}{\partial x_n} \right)}, \\
\sigma_{m3}^{+} = \quad & \rho^{-} h \left[\frac{\partial^2 u_m^{+}}{\partial t^2} \underline{- (c_2^{-})^2 \left(\frac{\partial^2 u_m^{+}}{\partial x_n^2} + \eta \frac{\partial^2 u_m^{+}}{\partial x_m^2} \right.} \left. + (\eta - 1) \frac{\partial^2 u_n^{+}}{\partial x_m \partial x_n} \right) \right] \underline{- h \vartheta \frac{\partial \sigma_{33}^{+}}{\partial x_m}},
\end{aligned} \tag{4.2}$$

where ϑ is introduced in (3.34). The underlined terms in formulae (4.2) do not appear

in the effective conditions (4.1). The former may be also transformed to

$$\begin{aligned}
\sigma_{33}^{+} = \;& \rho^{-}h\frac{\partial^2 u_3^{+}}{\partial t^2} - \rho^{-}h^2\left[\frac{\partial^3 u_m^{+}}{\partial t^2\partial x_m} + \frac{\partial^3 u_n^{+}}{\partial t^2\partial x_n} - (c_2^{-})^2\left(\frac{\partial^3 u_m^{+}}{\partial x_m\partial x_n^2} + \frac{\partial^3 u_n^{+}}{\partial x_m^2\partial x_n}\right.\right.\\
& \left.\left.+\eta\left[\frac{\partial^3 u_m^{+}}{\partial x_m^3} + \frac{\partial^3 u_n^{+}}{\partial x_n^3}\right] + (\eta-1)\left[\frac{\partial^3 u_n^{+}}{\partial x_m^2\partial x_n} + \frac{\partial^3 u_m^{+}}{\partial x_m\partial x_n^2}\right]\right)\right]\\
& +h^2\vartheta\left(\frac{\partial^2\sigma_{33}^{+}}{\partial x_m^2} + \frac{\partial^2\sigma_{33}^{+}}{\partial x_n^2}\right), \qquad (4.3)\\
\sigma_{m3}^{+} = \;& \rho^{-}h\left[\frac{\partial^2 u_m^{+}}{\partial t^2} - (c_2^{-})^2\left(\frac{\partial^2 u_m}{\partial x_n^2} + \eta\frac{\partial^2 u_m^{+}}{\partial x_m^2} + (\eta-1)\frac{\partial^2 u_n^{+}}{\partial x_m\partial x_n}\right)\right]\\
& -h^2\vartheta\left(\rho^{-}\frac{\partial^3 u_3^{+}}{\partial t^2\partial x_m} - \left[\frac{\partial^2\sigma_{m3}^{+}}{\partial x_m^2} + \frac{\partial^2\sigma_{n3}^{+}}{\partial x_m\partial x_n}\right]\right).
\end{aligned}$$

It is already clear at this stage that all extra h^2-terms in (4.3) can be neglected at leading order. In what follows, this observation is asymptotically justified. We also show below that h^2-terms in (4.3) are not identical to a proper asymptotic correction to (4.1).

4.2 Asymptotic analysis

The aim of the study is to determine an asymptotic correction to the leading order effective boundary conditions (4.1), in order to address consistency of (4.2), or equivalently, (4.3). Here we implement an asymptotic procedure similar to [36], modifying it slightly according to a more recent treatment in [30]. As usual, we study the boundary value problem for an elastic coating with the Dirichlet boundary conditions

$$u_i^{-} = v_i \qquad (4.4)$$

at the interface $x_3 = h$, where $v_i = v_i(x_1, x_2, t)$ denote prescribed displacements, see Figure 4.1.

We assume that the thickness of the coating h is small compared to typical wave length l, therefore, we employ a small geometric parameter given by (1.28). According

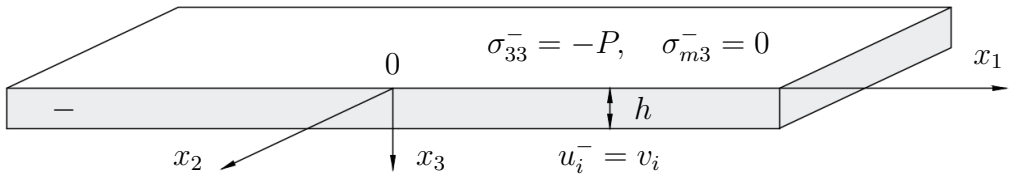

Figure 4.1: Boundary value problem for a thin coating

to the conventional asymptotic procedure, e.g. [3], [36], and references therein, we adopt the scaling

$$\begin{aligned} &u_i^- = l u_i^{-*}, \qquad && \sigma_{mm}^- = \mu^- \sigma_{mm}^{-*}, \qquad && P = \mu^- \varepsilon p^* \\ &v_i = l v_i^*, && \sigma_{i3}^- = \mu^- \varepsilon \sigma_{i3}^{-*}, && \sigma_{12}^- = \mu^- \sigma_{12}^{-*}, \end{aligned} \tag{4.5}$$

where as before all quantities with the asterisk in superscript are assumed to be of the same asymptotic order.

The equations $(1.22)_1$ and the constitutive relations (1.19), become

$$\begin{aligned} &\sigma_{mm,m}^{-*} + \sigma_{12,n}^{-*} + \sigma_{m3,3}^{-*} = u_{m,\tau\tau}^{-*}, \\ &\sigma_{33,3}^{-*} + \varepsilon \left(\sigma_{13,1}^{-*} + \sigma_{23,2}^{-*} \right) = u_{3,\tau\tau}^{-*}, \\ &\sigma_{12}^{-*} = u_{1,2}^{-*} + u_{2,1}^{-*}, \\ &\varepsilon \sigma_{mm}^{-*} = (\gamma^- - 2) u_{3,3}^{-*} + \varepsilon \left(\gamma^- u_{m,m}^{-*} + (\gamma^- - 2) u_{n,n}^{-*} \right), \\ &\varepsilon^2 \sigma_{m3}^{-*} = u_{m,3}^{-*} + \varepsilon u_{3,m}^{-*}, \\ &\varepsilon^2 \sigma_{33}^{-*} = \gamma^- u_{3,3}^{-*} + \varepsilon (\gamma^- - 2) \left(u_{1,1}^{-*} + u_{2,2}^{-*} \right), \end{aligned} \tag{4.6}$$

with the transformed boundary conditions

$$\begin{aligned} &\sigma_{33}^{-*} = -p^*, \qquad && \sigma_{m3}^{-*} = 0, \qquad && \xi_3^- = 0, \\ &u_i^{-*} = v_i^*, && \xi_3^- = 1. \end{aligned} \tag{4.7}$$

First, expressing $u_{3,3}^{-*}$ from $(4.6)_6$ and substituting the result into $(4.6)_4$, we obtain

$$\sigma_{mm}^{-*} = \eta u_{m,m}^{-*} + 2\vartheta u_{n,n}^{-*} + \vartheta \varepsilon \sigma_{33}^{-*}. \tag{4.8}$$

Next, we expand the displacements and stresses as

$$\begin{pmatrix} u_i^{-*} \\ \\ \sigma_{ij}^{-*} \end{pmatrix} = \begin{pmatrix} u_i^{-(0)} \\ \\ \sigma_{ij}^{-(0)} \end{pmatrix} + \varepsilon \begin{pmatrix} u_i^{-(1)} \\ \\ \sigma_{ij}^{-(1)} \end{pmatrix} + \varepsilon^2 \begin{pmatrix} u_i^{(2)} \\ \\ \sigma_{ij}^{(2)} \end{pmatrix} + \dots . \tag{4.9}$$

Substituting the latter into the equations (4.6) and (4.8), we have at leading order

$$\begin{aligned} &\sigma_{mm,m}^{-(0)} + \sigma_{12,n}^{-(0)} + \sigma_{m3,3}^{-(0)} = u_{m,\tau\tau}^{-(0)}, \\ &\sigma_{33,3}^{-(0)} = u_{3,\tau\tau}^{-(0)}, \\ &\sigma_{12}^{-(0)} = u_{1,2}^{-(0)} + u_{2,1}^{-(0)}, \\ &u_{i,3}^{-(0)} = 0, \\ &\sigma_{mm}^{-(0)} = \eta u_{m,m}^{-(0)} + 2\vartheta u_{n,n}^{-(0)}, \end{aligned} \tag{4.10}$$

with the boundary conditions

$$\begin{aligned} &\sigma_{33}^{-(0)} = -p^*, \qquad \sigma_{m3}^{-(0)} = 0, \qquad \xi_3^- = 0, \\ &u_i^{-(0)} = v_i^*, \qquad \xi_3^- = 1. \end{aligned} \tag{4.11}$$

Integrating the leading order equations (4.10) and accounting for the boundary conditions (4.11), we get

$$\begin{aligned} u_i^{-(0)} &= v_i^*, \\ \sigma_{33}^{-(0)} &= \xi_3^- \frac{\partial^2 v_3^*}{\partial \tau^2} - p^*, \\ \sigma_{mm}^{-(0)} &= \eta \frac{\partial v_m^*}{\partial \xi_m} + 2\vartheta \frac{\partial v_n^*}{\partial \xi_n}, \\ \sigma_{m3}^{-(0)} &= \xi_3^- \left[\frac{\partial^2 v_m^*}{\partial \tau^2} - \frac{\partial^2 v_m^*}{\partial \xi_n^2} - \eta \frac{\partial^2 v_m^*}{\partial \xi_m^2} - (\eta - 1) \frac{\partial^2 v_n^*}{\partial \xi_m \xi_n} \right]. \end{aligned} \tag{4.12}$$

Note, that leading order equations above, as in was discussed in Subsection 3.4.5, represent effective boundary conditions (3.137) for a static problem with contrast in stiffness of the layer and the half-space.

At next asymptotic order, the governing equations take the form

$$\begin{aligned}
&\sigma^{-(1)}_{mm,m} + \sigma^{-(1)}_{12,n} + \sigma^{-(1)}_{m3,3} = u^{-(1)}_{m,\tau\tau},\\
&\sigma^{-(1)}_{33,3} + \sigma^{-(0)}_{13,1} + \sigma^{-(0)}_{23,2} = u^{-(1)}_{3,\tau\tau},\\
&\sigma^{-(1)}_{12} = u^{-(1)}_{1,2} + u^{-(1)}_{2,1},\\
&\sigma^{-(0)}_{mm} = (\gamma^- - 2)\left(u^{-(1)}_{3,3} + u^{-(0)}_{n,n}\right) + \gamma^- u^{-(0)}_{m,m},\\
&u^{-(1)}_{m,3} + u^{-(0)}_{3,m} = 0,\\
&\gamma^- u^{-(1)}_{3,3} + (\gamma^- - 2)\left(u^{-(0)}_{1,1} + u^{-(0)}_{2,2}\right) = 0,\\
&\sigma^{-(1)}_{mm} = \eta u^{-(1)}_{m,m} + \vartheta\left(2u^{-(1)}_{n,n} + \sigma^{-(0)}_{33}\right),
\end{aligned} \tag{4.13}$$

with the boundary conditions

$$\begin{aligned}
&\sigma^{-(1)}_{i3} = 0, \qquad \xi^-_3 = 0,\\
&u^{-(1)}_{i} = 0, \qquad \xi^-_3 = 1.
\end{aligned} \tag{4.14}$$

First, we obtain from $(4.13)_5$ and $(4.13)_6$, respectively, satisfying $(4.14)_2$

$$u^{-(1)}_m = (1-\xi^-_3)\frac{\partial v^*_3}{\partial \xi_m}, \tag{4.15}$$

and

$$u^{-(1)}_3 = \vartheta(1-\xi^-_3)\left(\frac{\partial v^*_1}{\partial \xi_1} + \frac{\partial v^*_2}{\partial \xi_2}\right). \tag{4.16}$$

Then, using $(4.13)_3$, we have

$$\sigma^{-(1)}_{12} = 2(1-\xi^-_3)\frac{\partial^2 v^*_3}{\partial \xi_1 \partial \xi_2}. \tag{4.17}$$

Next, we deduce from $(4.13)_2$ and $(4.14)_1$

$$\begin{aligned}
\sigma^{-(1)}_{33} = \; & \frac{\xi^-_3}{\gamma^-}\left((\xi^-_3 - 2 + \gamma^- - \xi^-_3\gamma^-)\left[\frac{\partial^3 v^*_1}{\partial\xi_1\partial\tau^2} + \frac{\partial^3 v^*_2}{\partial\xi_2\partial\tau^2}\right]\right.\\
& \left. + 2\xi^-_3(\gamma^- - 1)\left[\frac{\partial^3 v^*_1}{\partial\xi_1\partial\xi_2^2} + \frac{\partial^3 v^*_2}{\partial\xi_1^2\partial\xi_2} + \frac{\partial^3 v^*_1}{\partial\xi_1^3} + \frac{\partial^3 v^*_2}{\partial\xi_2^3}\right]\right).
\end{aligned} \tag{4.18}$$

As a result, $(4.13)_7$ becomes

$$\sigma^{-(1)}_{mm} = \; 2(1-\xi^-_3)\left[(\vartheta+1)\frac{\partial^2 v^*_3}{\partial\xi_m^2} + \vartheta\frac{\partial^2 v^*_3}{\partial\xi_n^2}\right] + \vartheta\left[\xi^-_3\frac{\partial^2 v^*_3}{\partial\tau^2} - p^*\right]. \tag{4.19}$$

Therefore, $(4.13)_1$ implies

$$\begin{aligned}\sigma_{m3}^{-(1)} = \; & -\xi_3^- \left[\left(\xi_3^- - 1 - \frac{\xi_3^-}{\gamma^-} \right) \frac{\partial^3 v_3^*}{\partial \xi_m \partial \tau^2} - (\vartheta + 1)(\xi_3^- - 2) \right. \\ & \left. \left(\frac{\partial^3 v_3^*}{\partial \xi_m \partial \xi_n^2} + \frac{\partial^3 v_3^*}{\partial \xi_m^3} \right) - \vartheta \frac{\partial p^*}{\partial \xi_m} \right].\end{aligned} \tag{4.20}$$

Finally, substituting the leading order formulae $(4.12)_2$ and $(4.12)_4$ and $O(\varepsilon)$ corrections (4.18) and (4.20) into the expansions (4.9), we arrive at

$$\begin{aligned}\sigma_{33}^{-*} = \; & \xi_3^- \frac{\partial^2 v_3^*}{\partial \tau^2} - p^* + \varepsilon \frac{\xi_3^-}{\gamma^-} \left[(\xi_3^- - 2 + \gamma^- - \xi_3^- \gamma^-) \left(\frac{\partial^3 v_1^*}{\partial \xi_1 \partial \tau^2} + \frac{\partial^3 v_2^*}{\partial \xi_2 \partial \tau^2} \right) \right. \\ & \left. + 2\xi_3^- (\gamma^- - 1) \left(\frac{\partial^3 v_1^*}{\partial \xi_1 \partial \xi_2^2} + \frac{\partial^3 v_2^*}{\partial \xi_1^2 \partial \xi_2} + \frac{\partial^3 v_1^*}{\partial \xi_1^3} + \frac{\partial^3 v_2^*}{\partial \xi_2^3} \right) \right] + ..., \\ \sigma_{m3}^{-*} = \; & \xi_3^- \left[\frac{\partial^2 v_m^*}{\partial \tau^2} - \frac{\partial^2 v_m^*}{\partial \xi_n^2} - \eta \frac{\partial^2 v_m^*}{\partial \xi_m^2} - (\eta - 1) \frac{\partial^2 v_n^*}{\partial \xi_m \xi_n} \right] \\ & - \varepsilon \xi_3^- \left[\left(\xi_3^- - 1 - \frac{\xi_3^-}{\gamma^-} \right) \frac{\partial^3 v_3^*}{\partial \xi_m \partial \tau^2} - (\vartheta + 1)(\xi_3^- - 2) \right. \\ & \left. \left(\frac{\partial^3 v_3^*}{\partial \xi_m \partial \xi_n^2} + \frac{\partial^3 v_3^*}{\partial \xi_m^3} \right) - \vartheta \frac{\partial p^*}{\partial \xi_m} \right] + \dots .\end{aligned} \tag{4.21}$$

The continuity of the displacements and stresses at the interface $x_3 = h$, see (3.2) and (4.4), readily result in refined effective boundary conditions for the substrate $x_3 \geq h$. In the original variables they take the form

$$\begin{aligned}\sigma_{33}^{+} = \; & \rho^- h \frac{\partial^2 u_3^+}{\partial t^2} - P + \frac{\rho^- h^2}{\gamma^-} \left[2(c_2^-)^2 (\gamma^- - 1) \left(\frac{\partial^3 u_1^+}{\partial x_1 \partial x_2^2} + \frac{\partial^3 u_2^+}{\partial x_1^2 \partial x_2} \right. \right. \\ & \left. \left. + \frac{\partial^3 u_1^+}{\partial x_1^3} + \frac{\partial^3 u_2^+}{\partial x_2^3} \right) - \left(\frac{\partial^3 u_1^+}{\partial x_1 \partial t^2} + \frac{\partial^3 u_2^+}{\partial x_2 \partial t^2} \right) \right], \\ \sigma_{m3}^{+} = \; & \rho^- h \left[\frac{\partial^2 u_m^+}{\partial t^2} - (c_2^-)^2 \left(\frac{\partial^2 u_m^+}{\partial x_n^2} + \eta \frac{\partial^2 u_m^+}{\partial x_m^2} + (\eta - 1) \frac{\partial^2 u_n^+}{\partial x_m \partial x_n} \right) \right] + \frac{\rho^- h^2}{\gamma^-} \\ & \left[\frac{\partial^3 u_3^+}{\partial x_m \partial t^2} + 2(c_2^-)^2 (1 - \gamma^-) \left(\frac{\partial^3 u_3^+}{\partial x_m \partial x_n^2} + \frac{\partial^3 u_3^+}{\partial x_m^3} \right) \right] + h\vartheta \frac{\partial P}{\partial x_m}.\end{aligned} \tag{4.22}$$

Comparing these formulae at $P = 0$ with (4.3) we can see that higher order h^2-terms do not coincide.

4.3 Comparison with the exact solutions

In order to validate the asymptotic results obtained in the previous section, let us compare them with the long wave length expansion of the exact solutions of plane and

anti-plane time-harmonic problems for the coating.

4.3.1 Plane strain problem

First, let us consider a time-harmonic plane strain problem for the coating over the plane Ox_1x_3. In this case the displacements u_s^-, $s = 1, 3$ can be taken as (1.14) with the related equations of motion (1.16) and (1.17). The solutions are sought for in the form

$$\varphi = f(x_3)\mathrm{e}^{ik(x_1-ct)}, \qquad \psi_m = 0, \qquad \psi_3 = g(x_3)\mathrm{e}^{ik(x_1-ct)}. \tag{4.23}$$

Substituting the latter into (1.16) and (1.17), we deduce

$$f(x_3) = A_1\mathrm{e}^{kx_3\alpha^-} + A_2\mathrm{e}^{-kx_3\alpha^-}, \qquad g(x_3) = A_3\mathrm{e}^{kx_3\beta^-} + A_4\mathrm{e}^{-kx_3\beta^-}, \tag{4.24}$$

where A_d, $d = 1, 2, 3, 4$, are arbitrary constants, α^- and β^- are defined in (1.65).

We consider a traction free upper face ($P = 0$), i.e. at $x_3 = 0$

$$\sigma_{s3}^- = 0, \qquad s = 1, 3, \tag{4.25}$$

imposing the boundary conditions (4.4) at the lower face $x_3 = h$ with

$$v_s = hB_s\mathrm{e}^{ik(x_1-ct)}, \tag{4.26}$$

where B_s are certain prescribed values.

On satisfying the boundary conditions, we have

$$\begin{pmatrix} i\alpha^- & -i\alpha^- & \Upsilon^2 & \Upsilon^2 \\ \Upsilon^2 & \Upsilon^2 & -i\beta^- & i\beta^- \\ ik\mathrm{e}^{kh\alpha^-} & ik\mathrm{e}^{-kh\alpha^-} & \beta^-k\mathrm{e}^{kh\beta^-} & -\beta^-k\mathrm{e}^{-kh\beta^-} \\ \alpha^-k\mathrm{e}^{kh\alpha^-} & -\alpha^-k\mathrm{e}^{-kh\alpha^-} & -ik\mathrm{e}^{kh\beta^-} & -ik\mathrm{e}^{-kh\beta^-} \end{pmatrix} \begin{pmatrix} A_1 \\ A_2 \\ A_3 \\ A_4 \end{pmatrix} = \begin{pmatrix} 0 \\ 0 \\ hB_1 \\ hB_3 \end{pmatrix} \tag{4.27}$$

where $\Upsilon = \sqrt{1 - \frac{1}{2}\frac{c^2}{(c_2^-)^2}}$, and coefficients A_d expressed through the given constants B_s are

$$A_1 = h\frac{N_1}{D}, \quad A_2 = \mathrm{e}^{kh\alpha^-} h\frac{N_2}{D}, \quad A_3 = -h\frac{N_3}{D}, \quad A_4 = -\mathrm{e}^{kh\beta^-} h\frac{N_4}{D},$$

where

$$\begin{aligned}
N_1 = \; & iB_1\left(\mathrm{e}^{kh\alpha^-}(D_1\alpha^-\beta^- + D_2\Upsilon^4) - 2\mathrm{e}^{kh\beta^-}\alpha^-\beta^-\Upsilon^2\right) \\
& -B_3\beta^-\left(\mathrm{e}^{kh\alpha^-}(D_2\alpha^-\beta^- + D_1\Upsilon^4) - 2\mathrm{e}^{kh\beta^-}\Upsilon^2\right), \\
N_2 = \; & iB_1\left(D_1\alpha^-\beta^- - 2\mathrm{e}^{kh(\alpha^-+\beta^-)}\alpha^-\beta^-\Upsilon^2 - \Upsilon^4 D_2\right) \\
& +B_3\beta^-\left(D_1\Upsilon^4 - D_2\alpha^-\beta^- - 2\mathrm{e}^{kh(\alpha^-+\beta^-)}\Upsilon^2\right), \\
N_3 = \; & iB_3\left(\mathrm{e}^{kh\beta^-}(D_3\alpha^-\beta^- + D_4\Upsilon^4) - 2\mathrm{e}^{kh\alpha^-}\alpha^-\beta^-\Upsilon^2\right) \\
& +B_1\alpha^-\left(\mathrm{e}^{kh\beta^-}(D_4\alpha^-\beta^- + D_3\Upsilon^4) - 2\mathrm{e}^{kh\alpha^-}\Upsilon^2\right), \\
N_4 = \; & iB_3\left(D_3\alpha^-\beta^- - 2\mathrm{e}^{kh(\alpha^-+\beta^-)}\alpha^-\beta^-\Upsilon^2 - \Upsilon^4 D_4\right) \\
& -B_1\alpha^-\left(D_3\Upsilon^4 - D_4\alpha^-\beta^- - 2\mathrm{e}^{kh(\alpha^-+\beta^-)}\Upsilon^2\right),
\end{aligned}$$

and

$$D = k\left[8\mathrm{e}^{kh(\alpha^-+\beta^-)}\alpha^-\beta^-\Upsilon^2 + D_2D_4[(\alpha^-)^2(\beta^-)^2 + \Upsilon^4] - D_1D_3\alpha^-\beta^-(1+\Upsilon^4)\right],$$

with

$$D_1 = 1 + \mathrm{e}^{2kh\beta^-}, \quad D_2 = 1 - \mathrm{e}^{2kh\beta^-}, \quad D_3 = 1 + \mathrm{e}^{2kh\alpha^-}, \quad D_4 = 1 - \mathrm{e}^{2kh\alpha^-}.$$

Then, substituting (4.23) and (4.24) into (1.14), we get

$$\begin{aligned}
u_1^- &= k\left[\beta^-(A_3\mathrm{e}^{2kx_3\beta^-} - A_4)\mathrm{e}^{-kx_3\beta^-} + i(A_1\mathrm{e}^{2kx_3\alpha^-} + A_2)\mathrm{e}^{-kx_3\alpha^-}\right], \\
u_3^- &= k\left[\alpha^-(A_1\mathrm{e}^{2kx_3\alpha^-} - A_2)\mathrm{e}^{-kx_3\alpha^-} - i(A_3\mathrm{e}^{2kx_3\beta^-} + A_4)\mathrm{e}^{-kx_3\beta^-}\right].
\end{aligned} \tag{4.28}$$

Here and below the factor $\mathrm{e}^{ik(x_1-ct)}$ is omitted. Next, using the expressions above and the constitutive relations (1.19), we have for the stresses at $x_3 = h$

$$\begin{aligned}
\sigma_{33}^- &= 2\mu^- k^2\left[\Upsilon^2(A_1\mathrm{e}^{2kh\alpha^-} + A_2)\mathrm{e}^{-kh\alpha^-} - i\beta^-(A_3\mathrm{e}^{2kh\beta^-} - A_4)\mathrm{e}^{-kh\beta^-}\right], \\
\sigma_{13}^- &= 2\mu^- k^2\left[\Upsilon^2(A_3\mathrm{e}^{2kh\beta^-} + A_4)\mathrm{e}^{-kh\beta^-} + i\alpha^-(A_1\mathrm{e}^{2kh\alpha^-} - A_2)\mathrm{e}^{-kh\alpha^-}\right].
\end{aligned} \tag{4.29}$$

The last expressions can be expanded into asymptotic series in the small parameter $\varepsilon = kh \ll 1$ ($l = k^{-1}$ in (1.28)) to get

$$\begin{aligned}
\frac{\sigma_{33}^-}{\varepsilon^2\mu^-} &= -B_3(\zeta^-)^2 - iB_1\left(2 - \frac{2+(\zeta^-)^2}{\gamma^-}\right)\varepsilon + ..., \\
\frac{\sigma_{13}^-}{\varepsilon^2\mu^-} &= B_1\left[\eta - (\zeta^-)^2\right] + iB_3\left(2 - \frac{2+(\zeta^-)^2}{\gamma^-}\right)\varepsilon - \frac{B_1}{3} \\
&\quad \left(20 + (\zeta^-)^2\left[(\zeta^-)^2 - 8\right] + \frac{6(\zeta^-)^2 - 44}{\gamma^-} + \frac{4\left[(\zeta^-)^2 + 6\right]}{(\gamma^-)^2}\right)\varepsilon^2 + ...,
\end{aligned} \tag{4.30}$$

where the dimensionless velocity ζ^- is introduced in (1.25).

The asymptotic effective conditions (4.22) for the same displacements (4.26) prescribed at the lower face, become

$$\begin{aligned}
\sigma_{33}^- &= k^2h^2\rho^-\left(-B_3c^2 - iB_1kh\left[2(c_2^-)^2 - \frac{2(c_2^-)^2 + c^2}{\gamma^-}\right]\right), \\
\sigma_{13}^- &= k^2h^2\rho^-\left(B_1\left[(c_2^-)^2\eta - c^2\right] + iB_3kh\left[2(c_2^-)^2 - \frac{2(c_2^-)^2 + c^2}{\gamma^-}\right]\right),
\end{aligned} \tag{4.31}$$

or, rewritten in terms of ε and ζ^-,

$$\begin{aligned}
\frac{\sigma_{33}^-}{\varepsilon^2\mu^-} &= -B_3(\zeta^-)^2 - iB_1\left[2 - \frac{2+(\zeta^-)^2}{\gamma^-}\right]\varepsilon, \\
\frac{\sigma_{13}^-}{\varepsilon^2\mu^-} &= B_1\left[\eta - (\zeta^-)^2\right] + iB_3\left[2 - \frac{2+(\zeta^-)^2}{\gamma^-}\right]\varepsilon.
\end{aligned} \tag{4.32}$$

These formulae coincide with the two-term expansion of the exact solution (4.30). Thus, the validity of the asymptotic results in Section 4.2 is confirmed.

Let us now test the conditions in [22] in a similar manner. In case of the displacements (4.26) the relation (4.2) takes the form

$$\begin{aligned}
\sigma_{33}^- &= -\frac{h^2\rho^-\left(iB_1k^3h\left[4(c_2^-)^2 - c^2\right] + B_3c^2k^2\right)}{1 + k^2h^2\vartheta}, \\
\sigma_{13}^- &= \frac{h^2\rho^-\left(B_1k^2\left[4(c_2^-)^2(1-\gamma^-) - c^2\right] + iB_3kh\vartheta\right)}{1 + k^2h^2\vartheta},
\end{aligned} \tag{4.33}$$

or, expanding the latter in ε,

$$\begin{aligned}
\frac{\sigma_{33}^-}{\varepsilon^2\mu^-} &= -B_3(\zeta^-)^2 - iB_1\left[\eta - (\zeta^-)^2\right]\varepsilon + B_3(\zeta^-)^2\vartheta\varepsilon^2 + ..., \\
\frac{\sigma_{13}^-}{\varepsilon^2\mu^-} &= B_1\left[\eta - (\zeta^-)^2\right] + iB_3(\zeta^-)^2\vartheta\varepsilon + B_1\vartheta\left[(\zeta^-)^2 - \eta\right]\varepsilon^2 + ...
\end{aligned} \tag{4.34}$$

These conditions coincide with the asymptotic expansion of the exact solution (4.30) only at leading order. This means that the effect of the underlined terms in (4.2) appears only at next order; in doing so, it is different from $O(\varepsilon)$ correction in the asymptotic expansion (4.30). As an illustration, in Figure 4.2 for $\nu^- = 0.3$ we plot the normalized coefficients χ^E_{s3} and χ^B_{s3}, $s = 1, 3$, at ε-terms in (4.30) and (4.34), respectively. They are

$$\chi^E_{s3} = 2 - \frac{2 + (\zeta^-)^2}{\gamma^-}, \qquad \chi^B_{33} = \eta - (\zeta^-)^2, \qquad \chi^B_{13} = (\zeta^-)^2 \vartheta. \tag{4.35}$$

4.3.2 Anti-plane problem

Let us now proceed with an anti-plane problem. In this case the equation of motion is taken as (1.76) and the boundary condition at the upper face $x_3 = 0$ is given by

$$\sigma^-_{23} = 0. \tag{4.36}$$

Similarly to (4.26), the boundary condition at the lower face $x_3 = h$ takes the form

$$u^-_2 = hB_2 \mathrm{e}^{ik(x_1 - ct)}, \tag{4.37}$$

where B_2 is also a certain prescribed value. As in Subsection 1.4.5, the displacement u^-_2 can be taken as (1.79) leading to the solution $(1.81)_1$. Satisfying boundary conditions (4.36) and (4.37), we obtain

$$A = 0, \qquad B = \frac{hB_2}{\cos(\alpha^- kh)}, \tag{4.38}$$

resulting in

$$u^-_2 = \frac{hB_2 \cos(\alpha^- k x_3)}{\cos(\alpha^- kh)}, \tag{4.39}$$

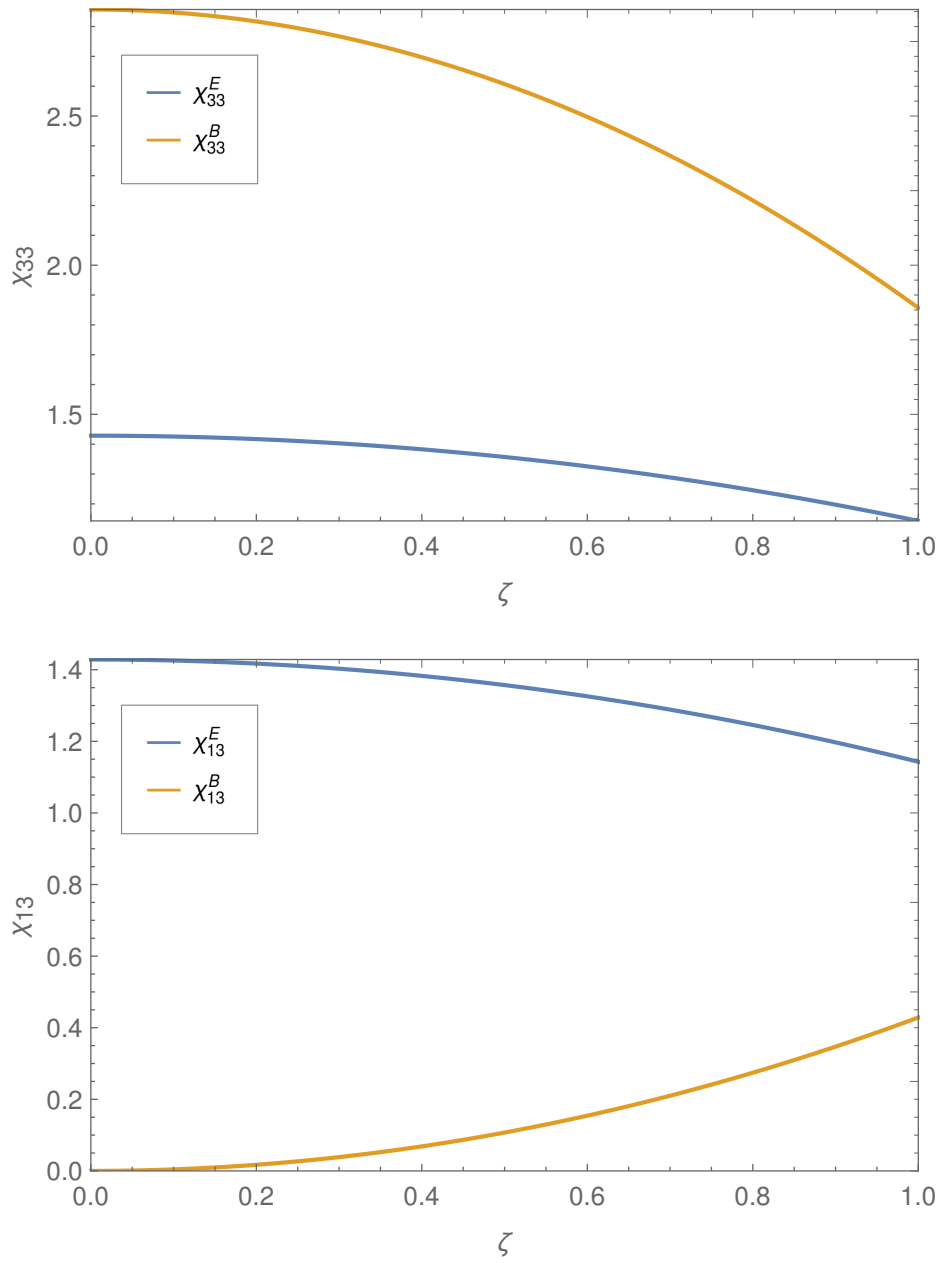

Figure 4.2: Comparison of coefficients at ε-terms ($\nu^- = 0.3$)

and

$$\sigma^-_{23} = -\frac{hB_2 k\alpha^- \mu^- \sin(\alpha^- k x_3)}{\cos(\alpha^- kh)}, \tag{4.40}$$

with the factor $e^{ik(x_1 - ct)}$ omitted here and below.

Employing small parameter $\varepsilon = kh$ and dimensionless velocity ζ^- for stress (4.40)

at the boundary $x_3 = h$, and expanding it in asymptotic series, we deduce

$$\frac{\sigma_{23}^-}{\varepsilon^2\mu^-} = B_2\left(1 - \frac{1}{3}\left[1-(\zeta^-)^2\right]\varepsilon^2 + \frac{2}{15}\left[1-(\zeta^-)^2\right]^2\varepsilon^4 + ...\right)\left[1-(\zeta^-)^2\right]. \tag{4.41}$$

Taking into account that the prescribed displacement u_2^- are given by (4.37) and $u_s^- = 0$, the asymptotic results $(4.22)_2$ become

$$\sigma_{23}^- = B_2 h^2 k^2 \rho^- \left[(c_2^-)^2 - c^2\right], \tag{4.42}$$

or, rewritten in terms of ε and ζ^-,

$$\frac{\sigma_{23}^-}{\varepsilon^2\mu^-} = B_2\left[1-(\zeta^-)^2\right]. \tag{4.43}$$

This expression coincide with the leading order of the exact solution (4.41), which confirms the validity of the leading order asymptotic results. The next asymptotic order term of the above formula is equal to 0, since it only depends on u_3, which is equal to 0 for an anti-plane problem, see $(4.22)_2$. It is also confirmed by the exact solution results (4.41), where the next asymptotic order term is also equal to 0. The next order correction in (4.41) is of order ε^2, therefore, in order to compare it with the asymptotic solution, the $O(\varepsilon^2)$ correction should be obtained.

Chapter 5

Rayleigh-type waves

In this chapter we are aiming at a multiparametric treatment of a dynamic problem for a coated elastic half-space with a clamped surface. The focus is on the analysis of localised waves that do not exist on a clamped homogeneous half-space. Non-traditional effective boundary conditions along the substrate surface incorporating the effect of the coating are derived using a long-wave high-frequency procedure. The derived conditions are implemented within the framework of the earlier developed specialised formulation for surface waves, resulting in a perturbation of the shortened equation of surface motion in the form of an integral or pseudo-differential operator. Non-uniform asymptotic formula for the speeds of the sought for Rayleigh-type waves, failing near zero frequency and the thickness resonances of a layer with both clamped faces, follow from the aforementioned perturbed equation. Asymptotic results are compared with the numerical solutions of the full dispersion relation for a clamped coated half-space. A similarity with Love-type waves proves to be useful for interpreting numerical data.

5.1 Statement of the problem

Consider an isotropic elastic layer of thickness h occupying the area $-h \leqslant x_3 \leqslant 0$ with clamped surface, lying on a half-space $x_3 \geqslant 0$, see Figure 5.1.

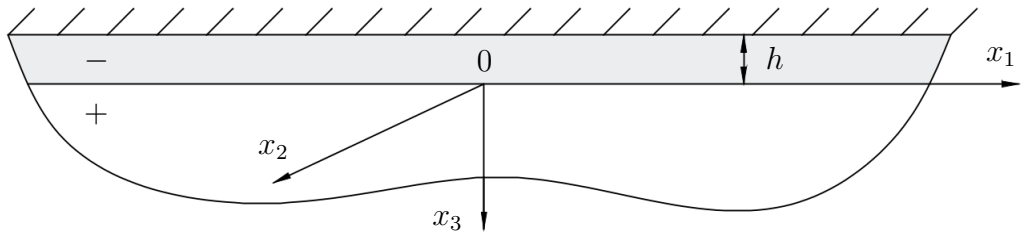

Figure 5.1: A clamped coated half-space

The equations of motion and the constitutive relations follow from (1.1) and (1.8), respectively. The boundary condition modelling the clamped surface of the layer ($x_3 = -h$) can be written as

$$u_i^- = 0. \tag{5.1}$$

As before, we specify continuity conditions (3.2) at $x_3 = 0$.

We also assume that the layer is softer than the half-space, employing, therefore, material parameter μ introduced in the first row of (1.29).

5.2 Anti-plane problem

Let us first consider anti-plane problem associated with Love waves. In this case, boundary conditions (5.1) take the form

$$u_2^- = 0. \tag{5.2}$$

The solution of the stated problem follows from the one presented in Subsection

1.4.5 for a coated half-space with a free surface. Accounting for clamped boundary condition (5.2) the dispersion relation becomes

$$\tan(kh\beta^-) + \frac{\mu\beta^-}{\beta^+} = 0. \tag{5.3}$$

Employing the dimensionless variables ζ^+, Ω^+ and K given in (1.25), the numerical illustrations of dispersion relation (5.3) with

$$\rho = 0.6, \qquad \nu^- = 0.3, \qquad \nu^+ = 0.25, \tag{5.4}$$

where ρ is introduced in (1.23), are presented for different values of the relative stiffness μ in Figure 5.2. Here, blue solid curves represent dispersion relations, yellow and green dashed lines correspond to the shear wave speeds of the substrate $\zeta^+ = 1$ or $c = c_2^+$ and the coating $\zeta^+ = \sqrt{\dfrac{\mu}{\rho}}$ or $c = c_2^-$, respectively.

First of all, it is observed from Figure 5.2 that as the contrast decreases (μ is getting closer to unity), the shear wave fronts of the layer and the half-space become closer to each other. At the same time, the solution lies between the dashed lines. Thus, this confirms that the Love wave exists if the shear wave speed of the half-space exceeds that of the layer, i.e. $c_2^- < c_2^+$, or, in other words, if the relative stiffness is less than the relative density, i.e. $\mu < \rho$.

The initial points of the modes are denoted with red dots in Figure 5.2. They are located on the line corresponding to the shear wave speed of the half-space $c = c_2^+$, therefore, for these points $\beta^+ \to 0$ and, according to (5.3), $\tan(kh\beta^-) \to \infty$. Hence, their coordinates follow from

$$\Omega_0^+ = K_0 = \frac{\pi z}{2\sqrt{\dfrac{\rho}{\mu} - 1}}, \qquad z = 1, 3, 5, \dots . \tag{5.5}$$

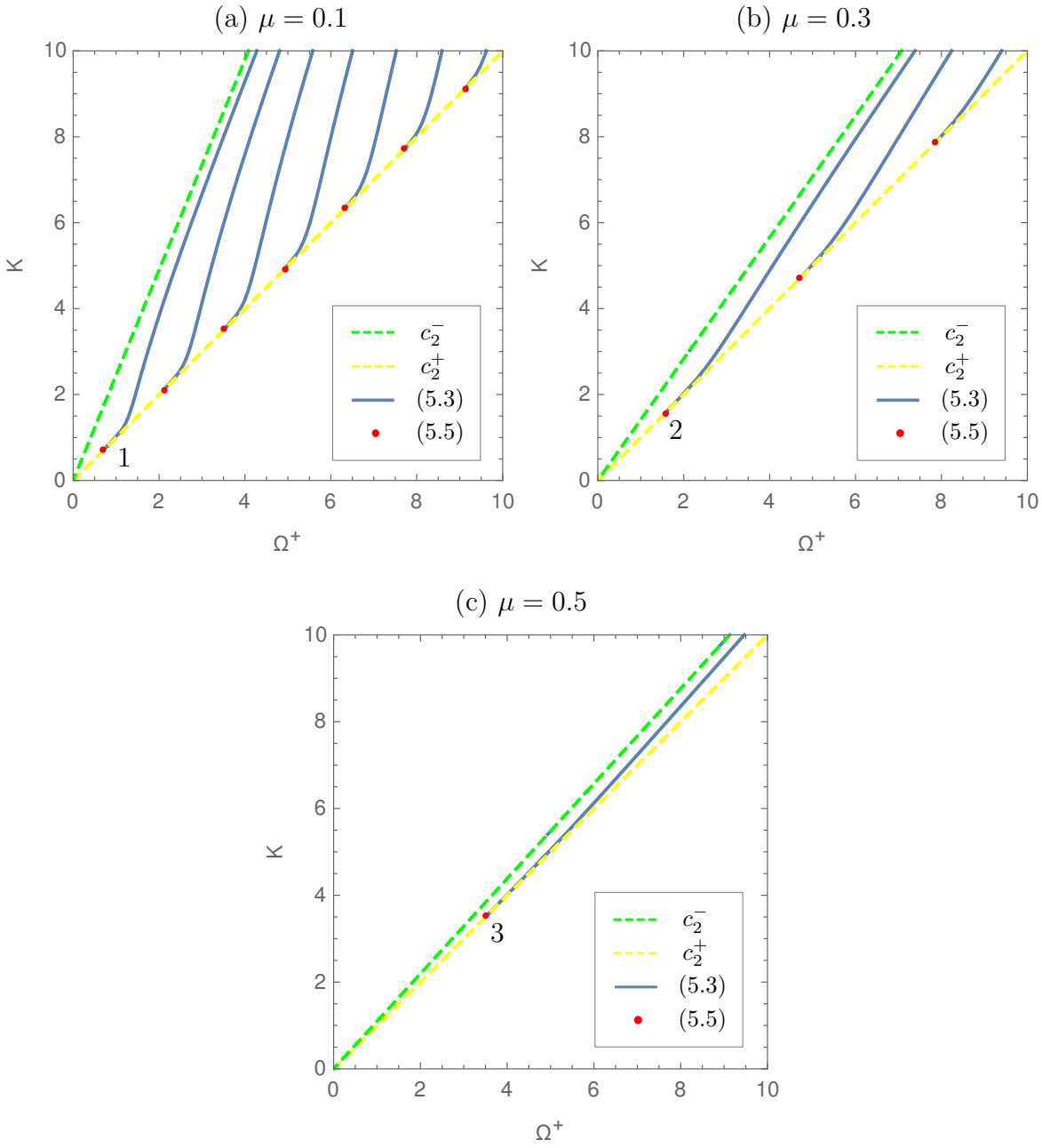

Figure 5.2: Dispersion curves for Love-type waves for several types of contrast ($\rho = 0.6$, $\nu^- = 0.3$, $\nu^+ = 0.25$)

Moreover, it is worth noting that an initial point of a fundamental mode is closer to the vicinity of zero for more pronounced contrast (smaller value of μ), compare points 1, 2 and 3, which is consistent with (5.5).

It is also possible to find approximations for $K \gg 1$. As K gets larger, the phase

velocity tends to the shear wave speed of the coating, i.e., $c \to c_2^-$, thus, $\beta^- \to 0$ and, following from (5.3), $\tan(kh\beta^-) \to 0$. As a result, we have

$$\Omega^+ \sim \sqrt{\frac{\mu(\pi^2 y^2 + K^2)}{\rho}}, \qquad y = 1, 2, 3, ..., \qquad K \gg 1. \tag{5.6}$$

5.3 Plane strain problem

Let us now proceed with the plane strain problem for which boundary conditions (5.1) take the form

$$u_s^- = 0, \tag{5.7}$$

together with continuity conditions (3.2) at the interface $x_3 = 0$ specified as

$$u_s^- = u_s^+, \qquad \sigma_{s3}^- = \sigma_{s3}^+. \tag{5.8}$$

The wave potentials may be found in the form

$$\begin{aligned} \varphi^- &= [A_1 \cos(\alpha^- k x_3) + A_2 \sin(\alpha^- k x_3)]\mathrm{e}^{ik(x_1 - ct)}, \qquad \varphi^+ = A_5 \mathrm{e}^{ik(x_1 - ct) - \alpha^+ k x_3}, \\ \psi^- &= [A_3 \cos(\beta^- k x_3) + A_4 \sin(\beta^- k x_3)]\mathrm{e}^{ik(x_1 - ct)}, \qquad \psi^+ = A_6 \mathrm{e}^{ik(x_1 - ct) - \beta^+ k x_3}, \end{aligned} \tag{5.9}$$

where A_q, $q = 1, ..., 6$, are arbitrary constants, α^- and β^- are introduced in (1.65), α^+ and β^+ are defined in (1.38).

Substituting (5.9) into (1.14) and (1.8) and then into boundary and continuity conditions (5.7) and (5.8), respectively, we derive a dispersion relation in the form

$$\det \mathbf{A} = 0, \tag{5.10}$$

with the following non-zero components

$$\begin{aligned}
&a_{11} = -ic_\alpha^-, && a_{12} = is_\alpha^-, && a_{13} = \beta^- s_\beta^-, && a_{14} = \beta^- c_\beta^-,\\
&a_{21} = \alpha^- s_\alpha^-, && a_{22} = \alpha^- c_\alpha^-, && a_{23} = ic_\beta^-, && a_{24} = -is_\beta^-,\\
&a_{34} = -\beta^-, && a_{36} = -\beta^+, && a_{42} = \alpha^-, && a_{45} = \alpha^+,\\
&a_{51} = \mu\eta^-, && a_{54} = 2i\beta^-\mu, && a_{55} = -\eta^+, && a_{56} = 2i\beta^+,\\
&a_{62} = 2i\alpha^-\mu && a_{63} = -\mu\chi_\beta^-, && a_{65} = 2i\alpha^+, && a_{66} = \chi_\beta^+,
\end{aligned} \tag{5.11}$$

and

$$a_{31} = -a_{35} = a_{43} = -a_{46} = i. \tag{5.12}$$

In the above,

$$\begin{aligned}
&s_\alpha^- = \sin(kh\alpha^-), && c_\alpha^- = \cos(kh\alpha^-), && s_\beta^- = \sin(kh\beta^-),\\
&c_\beta^- = \cos(kh\beta^-), && \chi_\alpha^\pm = 1 \mp (\alpha^\pm)^2, && \chi_\beta^\pm = 1 \pm (\beta^\pm)^2,\\
&\eta^\pm = 2 - \chi_\alpha^\pm(\kappa^\pm)^2.
\end{aligned} \tag{5.13}$$

Now we are in a position to perform qualitative analysis of dispersion relation (5.10) depending on the value of material parameter μ similarly to the previous section. In doing so, taking into account dimensionless variables (1.25), we present numerical illustrations of dispersion relation (5.10) with (5.4) for different values of relative stiffness μ, see Figure 5.3. Here, blue solid lines again depict exact dispersion curves, yellow and green dashed lines represent the shear wave speeds of the substrate $c = c_2^+$ and the coating $c = c_2^-$, respectively.

First of all, we can comment on existence of surface waves. Similarly to the Love-type waves considered in Section 5.2, the surface wave exists if the shear wave speed of the half-space is greater than that of the layer ($c_2^- < c_2^+$), or, again, if the relative stiffness is less than the relative density ($\mu < \rho$).

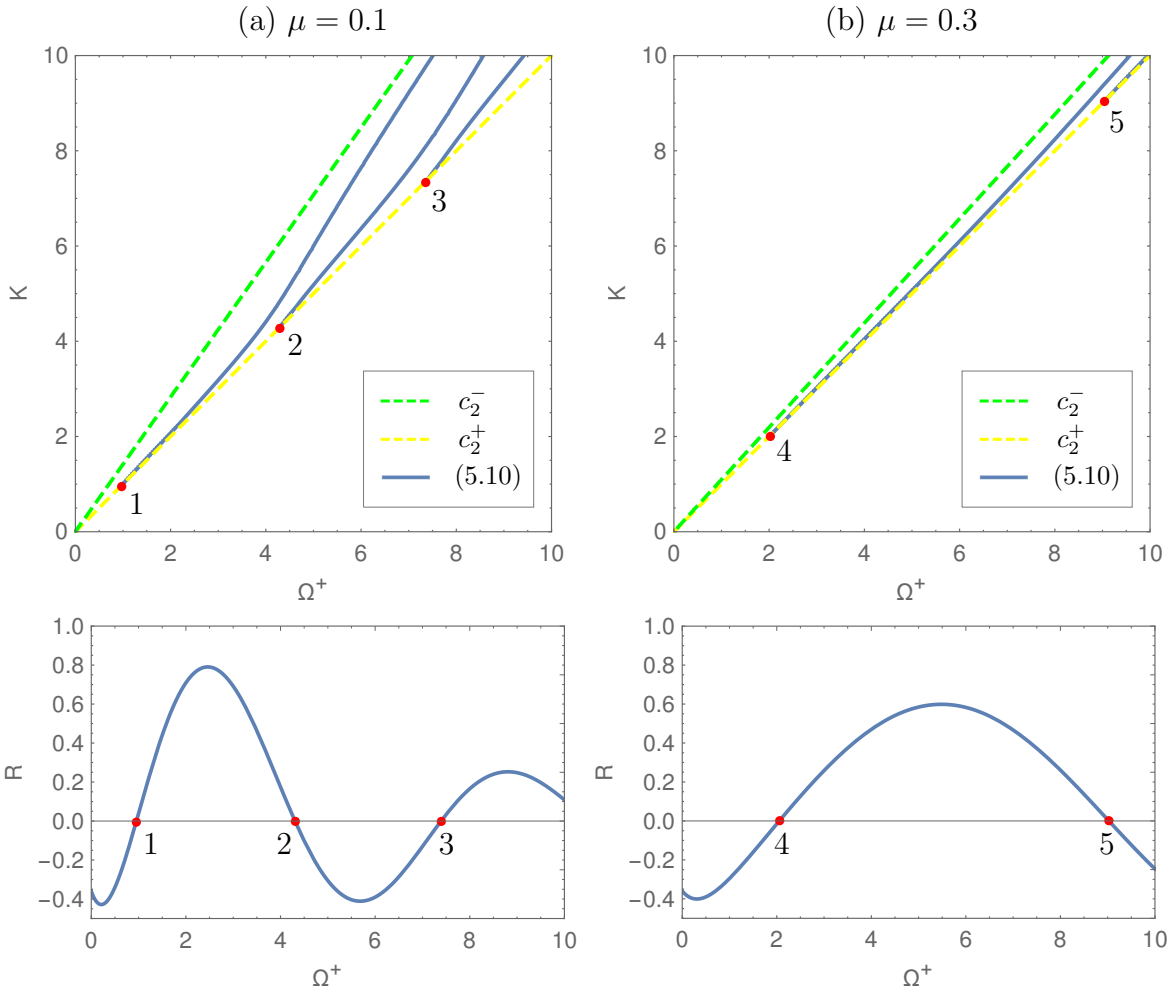

Figure 5.3: Dispersion curves for Rayleigh-type waves and associated functions $R(\Omega^+)$ ($\rho = 0.6$, $\nu^- = 0.3$, $\nu^+ = 0.25$)

The analysis of the initial points of the modes denoted by red dots in Figure 5.3 is less straightforward compared to that for Love-type waves. Here it is more difficult to obtain a particular expression for the coordinates of these points, since the dispersion relation is more cumbersome. We can, however, at least reduce the determinant currently depending on Ω^+ and K to a function of dimensionless frequency only. In doing so, we substitute $c = c_2^+$ into the determinant $\mathbf{A}$, obtaining, therefore, the following function

$$R(\Omega^+) = \det\mathbf{A}|_{c=c_2^+}\,. \tag{5.14}$$

Hence, the positions of the initial points 1, 2, 3, 4 and 5 correspond to zeros of the one-parametric function $R(\Omega^+)$, see Figure 5.3.

Finally, approximations for $K \gg 1$ also follow from (5.6) obtained for the Love-type waves, see Section 5.2. The numerical plots of these together with the dispersion relation (5.10) for $\mu = 0.1$ are shown in Figure 5.4, represented by blue solid and green dashed lines, respectively.

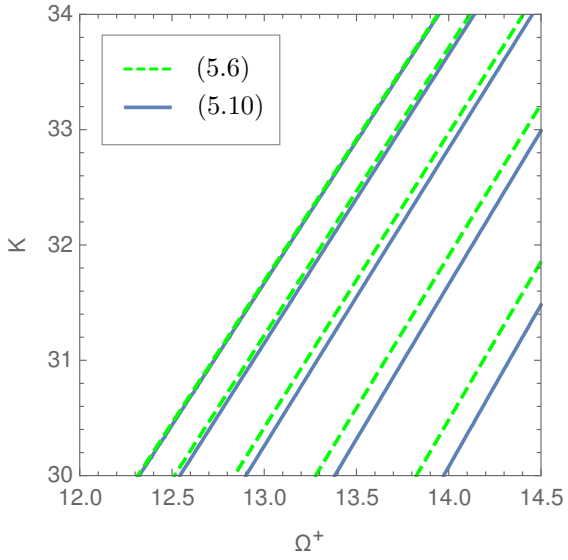

Figure 5.4: Short-wave behaviour of Rayleigh-type waves ($\mu = 0.1$)

If contrast in stiffness of the layer and the half-space is rather high, we may expect Rayleigh wave front to appear except for the thickness resonances frequencies. Indeed, the plot for the dispersion relation (5.10) for $\mu = 0.001$ presented in Figure 5.5 is consistent with the above. In this Figure, blue curves correspond to the dispersion relation (5.10), while a pink dashed line represents the Rayleigh wave speed $c = c_R$, see Subsection 1.4.1 for more detail. Yellow and green dashed lines depict stretch and shear thickness resonance frequencies, respectively, which, in dimensionless form, are

expressed as

$$\Omega_{st}^{+} = \sqrt{\frac{\mu}{\rho}}\kappa^{-}\pi y, \qquad \Omega_{sh}^{+} = \sqrt{\frac{\mu}{\rho}}\pi y, \qquad y = 1, 2, 3, \dots . \tag{5.15}$$

Similarly to the thickness resonances for Rayleigh-Lamb waves, see Subsection 1.4.4, (5.15) correspond to the eigenvalues of the problems for a layer (1.75), but with clamped faces ($u_s^- = 0$) instead of traction free ones ($u_{s,3}^- = 0$).

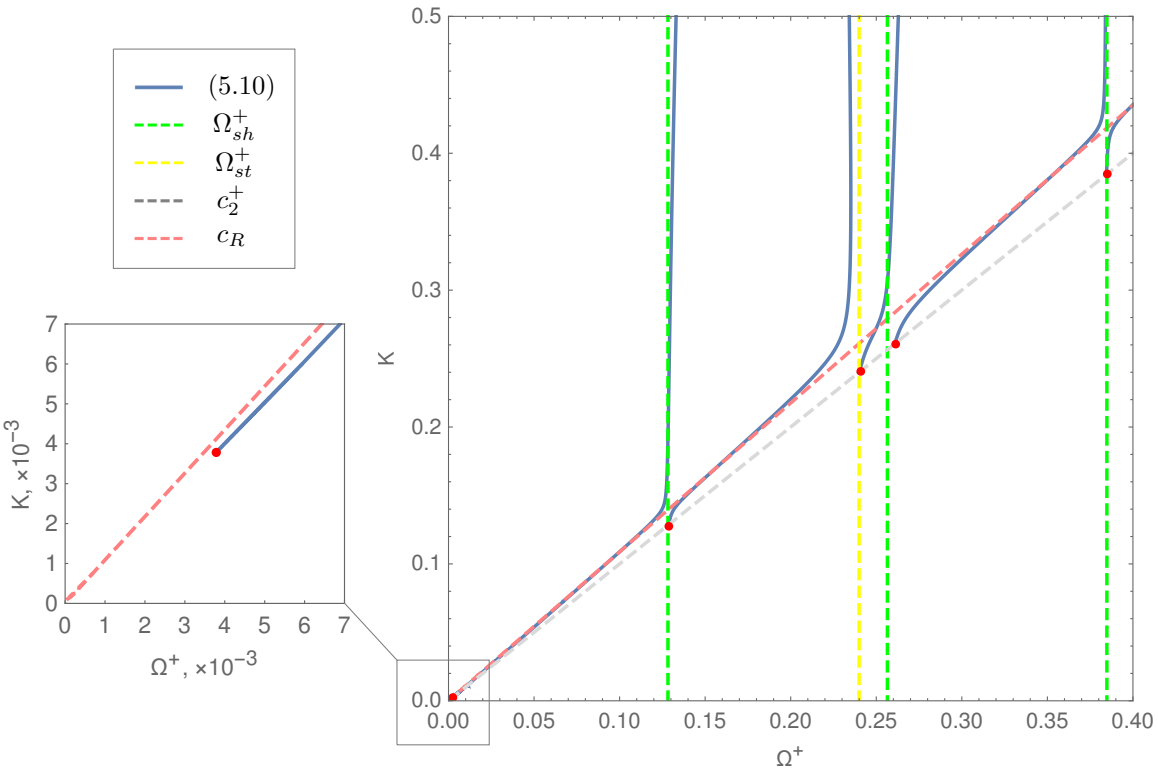

Figure 5.5: Dispersion curves for Rayleigh-type waves for high-contrast setup ($\mu = 0.001$).

The fact that the Rayleigh wave front is clearly observed inspires approximation of the exact dispersion relation (5.10) using the hyperbolic-elliptic model for the Rayleigh wave field, see Subsection 1.4.3. The asymptotic procedures required for the approximation are presented in the following section in plane strain formulation.

5.4 Asymptotic formulation for the layer and model for the half-space

In order to proceed with the asymptotic model, we first need to obtain the effective boundary conditions modelling the presence of the layer, similarly to Chapter 4, and then, use them as surface stresses for the half-space.

5.4.1 Asymptotic procedure for a layer

Let us start with considering the problem for the layer separately from the substrate. As in Chapter 4, we impose Dirichlet boundary conditions as (4.4) at the lower face $x_3 = 0$.

We begin with defining the dimensionless coordinates and variables. We employ ξ_1 defined in (1.18), ξ_3^- taken as

$$\xi_3^- = \frac{x_3 + h}{h}, \tag{5.16}$$

and Ω^- introduced in (1.25). Thus, the basic relations are written as $(1.26)_1$ and (1.19).

We assume the thickness of the layer to be small, therefore, we introduce small parameter (1.28).

Similar to the previous chapters, we adopt the asymptotic scaling as

$$u_s^- = hu_s^{*-}, \qquad \sigma_{ss}^- = \mu^- \sigma_{ss}^{*-}, \qquad \sigma_{13}^- = \mu^- \sigma_{13}^{*-}, \qquad v_s = hv_s^*, \tag{5.17}$$

and we also consider the dimensionless frequency Ω^- to be of order one, i.e. $\Omega^- \sim 1$. It is worth noting that usually, the dimensionless frequency is considered to be small ($\Omega^- \ll 1$) which leads to the approximation for the fundamental mode only.

Here, we set it to be of order one to tackle higher orders as well. The low-frequency approximation in this case can be easily obtained taking the limit of the resulting stresses as $\Omega^- \to 0$.

In view of (5.17), governing equations $(1.26)_1$ and (1.19) are rewritten as

$$\begin{aligned}
&\varepsilon\sigma^{*-}_{s1,1} + \sigma^{*-}_{s3,3} + (\Omega^-)^2 u^{*-}_s = 0,\\
&\sigma^{*-}_{11} = \varepsilon\gamma^- u^{*-}_{1,1} + (\gamma^- - 2)u^{*-}_{3,3},\\
&\sigma^{*-}_{33} = \varepsilon(\gamma^- - 2)u^{*-}_{1,1} + \gamma^- u^{*-}_{3,3},\\
&\sigma^{*-}_{13} = u^{*-}_{1,3} + \varepsilon u^{*-}_{3,1},
\end{aligned} \tag{5.18}$$

subject to boundary conditions (5.7) and (4.4) given by

$$\begin{aligned}
&u^{*-}_s = 0, \qquad \xi^-_3 = 0,\\
&u^{*-}_s = v^*_s, \qquad \xi^-_3 = 1.
\end{aligned} \tag{5.19}$$

We expand the scaled displacement and stress components in asymptotic series as

$$\begin{pmatrix} u^{*-}_s \\ \sigma^{*-}_{ss} \\ \sigma^{*-}_{13} \end{pmatrix} = \begin{pmatrix} u^{-(0)}_s \\ \sigma^{-(0)}_{ss} \\ \sigma^{-(0)}_{13} \end{pmatrix} + \dots . \tag{5.20}$$

Therefore, at leading order we have

$$\begin{aligned}
&\sigma^{-(0)}_{i3,3} + (\Omega^-)^2 u^{-(0)}_i = 0,\\
&\sigma^{-(0)}_{11} = (\gamma^- - 2)u^{-(0)}_{3,3},\\
&\sigma^{-(0)}_{33} = \gamma^- u^{-(0)}_{3,3},\\
&\sigma^{-(0)}_{13} = u^{-(0)}_{1,3},
\end{aligned} \tag{5.21}$$

with the following boundary conditions

$$\begin{aligned}
&u^{-(0)}_i = 0, \qquad \xi^-_3 = 0,\\
&u^{-(0)}_i = v^*_i, \qquad \xi^-_3 = 1.
\end{aligned} \tag{5.22}$$

First, from $(5.21)_3$ we obtain

$$\sigma_{33}^{-(0)} = \gamma^- \frac{\partial u_3^{-(0)}}{\partial \xi_3^-}. \tag{5.23}$$

Substituting (5.23) into $(5.21)_1$, we deduce the second order differential equation

$$\gamma^- \frac{\partial^2 u_3^{-(0)}}{\partial (\xi_3^-)^2} + u_3^{-(0)} (\Omega^-)^2 = 0, \tag{5.24}$$

the solution of which is given by

$$u_3^{-(0)} = C_1 \sin\left(\frac{\Omega^-}{\kappa^-}\xi_3^-\right) + C_2 \cos\left(\frac{\Omega^-}{\kappa^-}\xi_3^-\right). \tag{5.25}$$

Using boundary conditions (5.22) we derive

$$C_1 = \frac{v_3^*}{\sin\left(\dfrac{\Omega^-}{\kappa^-}\right)}, \qquad C_2 = 0, \tag{5.26}$$

hence,

$$u_3^{-(0)} = \frac{v_3^*}{\sin\left(\dfrac{\Omega^-}{\kappa^-}\right)} \sin\left(\frac{\Omega^-}{\kappa^-}\xi_3^-\right). \tag{5.27}$$

Following the same procedure for $u_1^{-(0)}$, we get

$$u_1^{-(0)} = \frac{v_1^*}{\sin(\Omega^-)} \sin(\Omega^- \xi_3^-). \tag{5.28}$$

Finally, we arrive at

$$\sigma_{33}^{-(0)} = \frac{\kappa^- \Omega^- v_3^*}{\sin\left(\dfrac{\Omega^-}{\kappa^-}\right)} \cos\left(\frac{\Omega^-}{\kappa^-}\xi_3^-\right), \tag{5.29}$$

and

$$\sigma_{13}^{-(0)} = \frac{\Omega^- v_1^*}{\sin(\Omega^-)} \cos(\Omega^- \xi_3^-). \tag{5.30}$$

Note, that for obtained stresses (5.29) and (5.30) the thickness variation is not polynomial, but sinusoidal, which is a characteristic of a high-frequency approximation.

Due to continuity conditions $(3.2)_2$, the aforementioned stresses taken at the interface $\xi_3^- = 1$ or $x_3 = 0$ result in effective boundary conditions for the substrate $x_3 \geq 0$. In the dimensional variables they are

$$\begin{aligned} \sigma_{33}^+ &= \kappa^- \omega \sqrt{\rho^- \mu^-} v_3 \cot\left(\frac{\omega h}{c_2^- \kappa^-}\right), \\ \sigma_{13}^+ &= \omega \sqrt{\rho^- \mu^-} v_1 \cot\left(\frac{\omega h}{c_2^-}\right). \end{aligned} \tag{5.31}$$

where v_s are displacements of the surface of the half-space, i.e.

$$v_s = u_s^+ \tag{5.32}$$

at $x_3 = 0$. These conditions appear to be non-traditional, corresponding to high-frequency long-wave phenomena failing at

$$\sin\left(\frac{\omega h}{c_2^- \kappa^-}\right) = 0 \qquad \text{or} \qquad \sin\left(\frac{\omega h}{c_2^-}\right) = 0, \tag{5.33}$$

which represent thickness resonances (5.15).

Having effective boundary conditions (5.31) modelling the presence of the layer, we can now proceed with applying the hyperbolic-elliptic model for the Rayleigh wave field, using these conditions as surface stresses for the half-space.

5.4.2 Low-frequency model

Let us first find a low-frequency approximation, i.e. $\omega \to 0$, corresponding to the fundamental mode of the dispersion relation. As it was discussed above, we take the limit of effective boundary conditions (5.31) as $\omega \to 0$. Thus, (5.31) yields

$$\sigma_{33}^+ = \frac{\gamma^- \mu^-}{h} v_3, \qquad \sigma_{13}^+ = \frac{\mu^-}{h} v_1. \tag{5.34}$$

We employ the hyperbolic-elliptic model presented in Subsection 1.4.3, in particular, we concentrate on wave equation (1.61) combining both vertical and horizontal components of elastic potential φ^+.

The displacements of the surface of the half-space v_s in (5.34) may be taken as (1.52), and the Cauchy-Riemann identity for wave equation $(1.44)_1$ takes the form

$$\varphi^+_{,3} = -\alpha_R H(\varphi^+_{,1}), \tag{5.35}$$

therefore, accounting for (1.53), we have

$$\begin{aligned} Q_1 &= -\alpha_R \frac{\gamma^- \mu^-}{h}\left(1 - \frac{2}{1+\beta_R^2}\right) H(\varphi^+_{,1}), \\ H(Q_2) &= \frac{\mu^-}{h}\left(1 - \frac{1+\beta_R^2}{2}\right) H(\varphi^+_{,1}). \end{aligned} \tag{5.36}$$

Substituting the latter into wave equation (1.61) together with (1.56) and (1.60), we obtain

$$\Box_R \varphi^+ = \frac{\mu}{h}\Gamma H(\varphi^+_{,1}), \tag{5.37}$$

where $\Box_R$ is introduced in (1.55) and

$$\Gamma = -\frac{\beta_R(\beta_R^2-1)\left(1+2\beta_R^2+\beta_R^4+4\alpha_R^2\gamma^-\right)}{8\left[\beta_R^2+\alpha_R^2(1-2\beta_R^2)+\alpha_R\beta_R(\beta_R^4-1)\right]}. \tag{5.38}$$

We consider the waves to be time-harmonic, i.e. $\varphi^+ \sim \mathrm{e}^{ik(x_1-ct)}$, hence, the dispersion relation follows from (5.37) as

$$\frac{c^2}{c_R^2} - \frac{\mu\Gamma c}{\omega h} - 1 = 0, \tag{5.39}$$

which fails at $\omega \to 0$ contrary to the dispersion relation obtained in a low-frequency limit for a coated half-space with traction free surface, see (5.4) in [36] with $P = 0$. The latter, rewritten in current notation, is given by

$$\Box_R \varphi^+ = bhH(\varphi^+_{,111}), \tag{5.40}$$

which for the time-harmonic waves becomes

$$\frac{c^2}{c_R^2} + \frac{bh\omega}{c} - 1 = 0. \tag{5.41}$$

In the above,

$$b = \frac{\mu(1-\beta_R^2)}{2\mathfrak{B}}\left[\left(1-(\beta_R^-)^2\right)(\alpha_R+\beta_R)-\beta_R\eta\right] \tag{5.42}$$

with $\mathfrak{B}$ and η introduced in (1.56) and (3.37), respectively, and

$$\beta_R^- = \sqrt{1-\frac{c_R^2}{(c_2^-)^2}}. \tag{5.43}$$

Dispersion relation (5.39), however, is still useful, especially in case of high contrast.

Introducing dimensionless velocity ζ^+ and frequency Ω^+ defined in (1.25), and dimensionless Rayleigh wave speed given by

$$\zeta_R = \frac{c_R}{c_2^+}, \tag{5.44}$$

we can rewrite dispersion relation (5.39) as

$$\frac{(\zeta^+)^2}{\zeta_R^2} - \mu\Gamma\frac{\zeta^+}{\Omega^+} - 1 = 0. \tag{5.45}$$

We consider material parameter μ to be small, meaning that the layer is much softer than the half-space, and expand the wave speed in asymptotic series as

$$\zeta^+ = \zeta^{+(0)} + \mu\zeta^{+(1)} + \dots. \tag{5.46}$$

In view of (5.46), dispersion relation (5.45) becomes

$$\frac{(\zeta^{+(0)}+\mu\zeta^{+(1)})^2}{\zeta_R^2} - \mu\Gamma\frac{\zeta^{+(0)}+\mu\zeta^{+(1)}}{\Omega^+} - 1 = 0. \tag{5.47}$$

Therefore, at leading order, we have

$$\zeta^{+(0)} = \zeta_R. \tag{5.48}$$

At next order, we get

$$\frac{2\zeta^{+(0)}\zeta^{+(1)}}{\zeta_R^2} - \Gamma\frac{\zeta^{+(0)}}{\Omega^+} = 0, \tag{5.49}$$

resulting in

$$\zeta^{+(1)} = \frac{\Gamma}{2\Omega^+}\zeta_R^2. \tag{5.50}$$

Finally, substituting (5.48) and (5.50) into (5.46), we obtain an approximation for dimensionless velocity in a low-frequency formulation

$$\zeta^+ = \zeta_R + \frac{\mu\Gamma}{2\Omega^+}\zeta_R^2 + \dots . \tag{5.51}$$

Note, that this approximation is non-uniform, since it fails at $\Omega^+ \to 0$.

5.4.3 High-frequency model

Let us now consider effective boundary conditions (5.31) corresponding to high-frequency limit. Similarly to the previous subsection, we derive for (5.31)

$$\begin{aligned} Q_1 &= -\alpha_R\kappa^-\omega\sqrt{\rho^-\mu^-}\cot\left(\frac{\omega h}{c_2^-\kappa^-}\right)\left(1-\frac{2}{1+\beta_R^2}\right)H(\varphi_{,1}),\\ H(Q_2) &= \omega\sqrt{\rho^-\mu^-}\cot\left(\frac{\omega h}{c_2^-}\right)\left(1-\frac{1+\beta_R^2}{2}\right)H(\varphi_{,1}), \end{aligned} \tag{5.52}$$

which after substitution into (1.61) with (1.56) and (1.60) imply

$$\Box_R\varphi^+ = \frac{\omega\sqrt{\rho^-\mu^-}}{\mu^+}\Gamma H(\varphi_{,1}^+), \tag{5.53}$$

where

$$\Gamma = -\frac{\beta_R(\beta_R^2-1)\left[(1+\beta_R^2)^2\cot\left(\dfrac{\omega h}{c_2^-}\right)+4\alpha_R^2\kappa^-\cot\left(\dfrac{\omega h}{\kappa^- c_2^-}\right)\right]}{8\left[\beta_R^2+\alpha_R^2(1-2\beta_R^2)+\alpha_R\beta_R(\beta_R^4-1)\right]}. \tag{5.54}$$

For time-harmonic waves, (5.53) takes the form

$$\frac{c^2}{c_R^2} - \sqrt{\mu\rho}\frac{\Gamma c}{c_2^+} - 1 = 0, \tag{5.55}$$

which in dimensionless form is given by

$$\frac{(\zeta^+)^2}{\zeta_R^2} - \sqrt{\mu\rho}\Gamma\zeta^+ - 1 = 0. \tag{5.56}$$

We again consider μ to be small and expand the wave speed in asymptotic series as

$$\zeta^+ = \zeta^{+(0)} + \sqrt{\mu}\zeta^{+(1)} + \dots . \tag{5.57}$$

Hence, dispersion relation (5.56) becomes

$$\frac{(\zeta^{+(0)} + \sqrt{\mu}\zeta^{+(1)})^2}{\zeta_R^2} - \sqrt{\mu\rho}\Gamma(\zeta^{+(0)} + \sqrt{\mu}\zeta^{+(1)}) - 1 = 0, \tag{5.58}$$

having leading order phase velocity given by (5.48). At next order, (5.58) yields

$$\frac{2\zeta^{+(0)}\zeta^{+(1)}}{\zeta_R^2} - \sqrt{\rho}\Gamma\zeta^{+(0)} = 0, \tag{5.59}$$

leading to

$$\zeta^{+(1)} = \frac{\sqrt{\rho}\Gamma}{2}\zeta_R^2. \tag{5.60}$$

As a result, we arrive at a non-uniform approximation for dimensionless velocity at a high-frequency limit

$$\zeta^+ = \zeta_R + \frac{\sqrt{\mu\rho}\Gamma}{2}\zeta_R^2 + ..., \tag{5.61}$$

where the source of non-uniformity is the coefficient Γ, since $\Gamma \to \infty$ at thickness resonances (5.15).

5.5 Numerical comparison of the asymptotic results with the exact solution

In this section we numerically compare the derived asymptotic approximations for a wave speed (5.51) and (5.61), corresponding to low- and high-frequency limits, respectively, with exact dispersion relation (5.10), using dimensionless variables ζ^+ and Ω^+ introduced in (1.25) and numerical values (5.4). The comparisons are presented

in Figure 5.6 for a low-frequency formulation with $\mu = 0.001$ and in Figure 5.7 for a high-frequency case with $\mu = 0.001$ and $\mu = 0.01$, where red dashed lines represent asymptotic approximations, blue solid curves correspond to the exact dispersion relation (5.10).

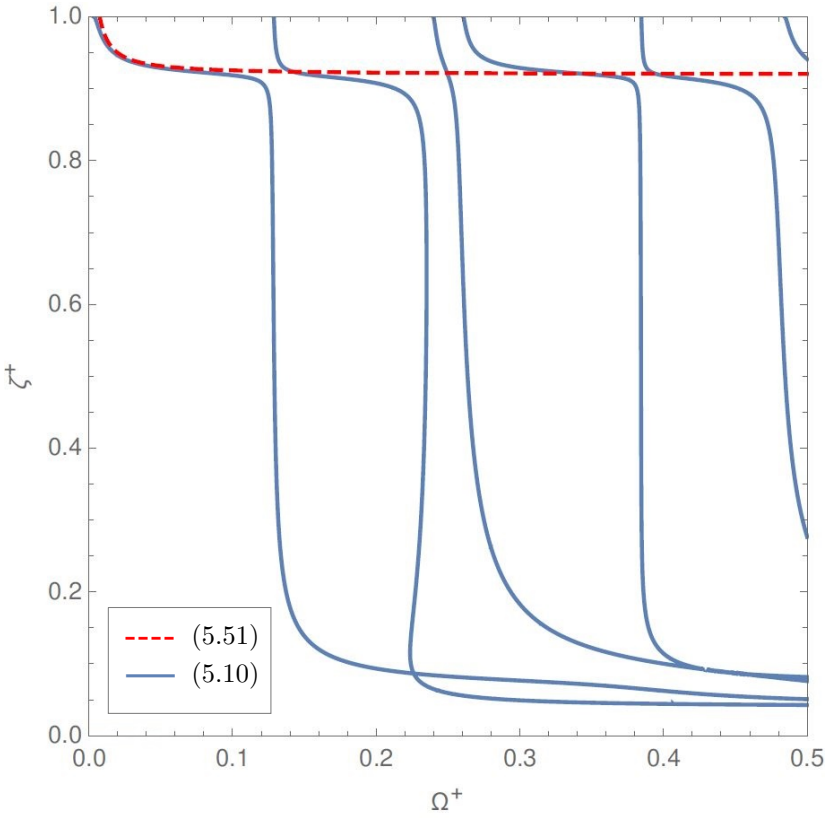

Figure 5.6: Rayleigh-type modes and low-frequency approximation for high contrast ($\mu = 0.001$)

It is observed from Figure 5.6 that, as expected, the low-frequency approximation (5.51) is close to the exact solution in the fundamental mode region only. On the contrary, Figure 5.7 shows that the high-frequency approximation (5.61) is valid over the whole range of dimensionless frequency taking into account the resonances as well.

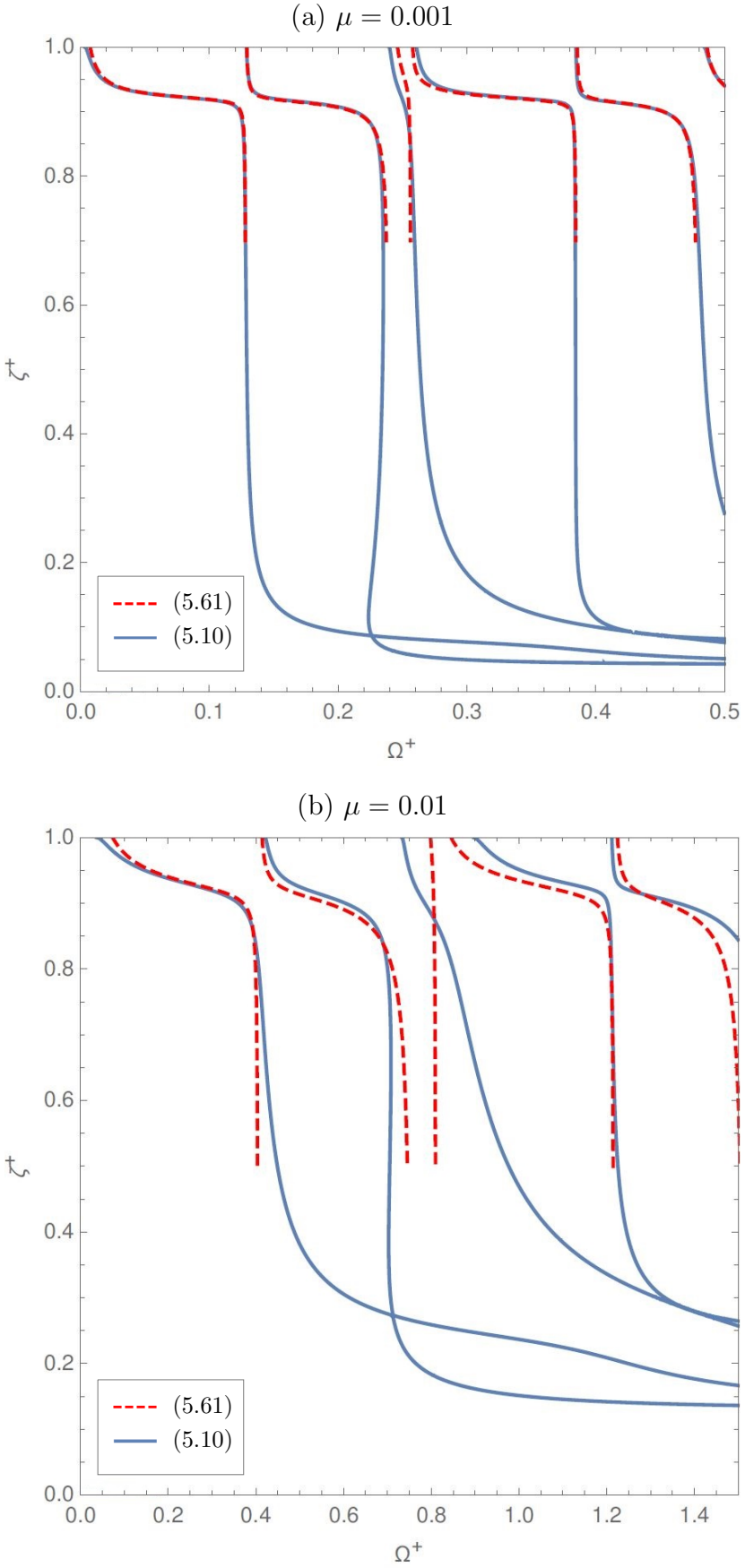

Figure 5.7: Rayleigh-type modes and high-frequency approximation

Also, for lower values of material parameter μ, i.e. for higher contrast in stiffness of the layer and substrate with the coating being softer, the asymptotic approximation is closer to the exact solution, see Figure 5.7.

Concluding remarks

A full two-parametric asymptotic analysis (in ε and μ) of the anti-plane shear deformation problem of a coated half-space is developed in Chapter 2 . It is demonstrated that in case of a relatively soft layer for a rather high contrast ($\alpha > 1$), the deformation of the substrate can be neglected, which leads to Winkler-type behaviour. In a similar situation for a relatively stiff coating ($\alpha \geq 1$), we arrive at equations of plate shear. At the same time, in the intermediate range of contrast in stiffness considered in Sections 2.3.2 and 2.3.4, the layer deformation is strongly affected by the presence of the substrate. In this case, shear deformation may be found from a simpler problem for a half-space. The latter, together with a Winkler-type behaviour term, results in two-term asymptotic formula (2.29) uniformly valid over the whole range of material parameter for a relatively soft layer. For a stiff coating, when the geometrical and material parameters are of the same order ($\alpha = 1$), it is also possible to reduce the original problem for a coated solid to a problem for a homogeneous half-space with effective boundary conditions at the surface.

The obtained solution may be useful for problems of delamination between the thin coating and the substrate, especially in tribological context, see e.g. [64, 71] and [73].

In addition, we mention related problems for the imperfect transmission conditions, see [123, 118] and [119]. Note, that such asymptotically evaluated simplified conditions

can be verified numerically with FEM analysis, see e.g. [121] and [120]. This is of crucial importance as accurate mathematical proof may not always be available. On the other hand, such conditions fail near singular points (crack tip, edges), but still may be valuable for physical applications in fracture mechanics, see [117] and [122].

In Chapter 3 the two-parametric asymptotic approach is extended to a full 3D problem with a vertical load applied at the surface of a covered solid.

For a relatively soft coating, it is established that only at a rather high contrast, when $\mu \ll \varepsilon$, and substrate deformations are negligible, the Winkler-Fuss hypothesis is valid. It does, however, unexpectedly fail at $\mu \sim \varepsilon$, when the relative thickness and stiffness of the coating are of the same order. It is also shown that the prescribed vertical surface load may always be transmitted to the interface. As a result, the sought for interfacial displacement follow from a simpler problem for a homogeneous half-space, leading to uniform two-term asymptotic formula (3.74) valid over the whole range of the contrast parameter. It is worth noting that along with local Winkler-Fuss term rw_0, this formula contains non-local term rw_h, see also [27] and [38], addressing current trends in modelling of nonlocal elastic foundations. In general case, the term rw_0 is given by a convolution using Boussinesq's solution [112]. Higher order corrections to the Winkler-Fuss approximation are also derived, including that corresponding to the Pasternak model, see e.g. [74, 129, 137].

In case of a stiff layer, it is confirmed that the Kirchhoff plate theory is also only valid for a sufficiently high contrast in the layer and substrate stiffness ($\alpha \geq 3$ or $\mu \lesssim \varepsilon^3$). Nevertheless, several approximate formulations for a homogeneous half-space are derived at $\alpha < 3$, see boundary conditions (3.135) – (3.136).

The considerations are of relevance for a range of problems for coated bodies in-

cluding modelling of contact interaction. The proposed methodology may be easily extended to anisotropic solids, shell-like coatings, as well as to the case of more sophisticated interfacial conditions. At the same time, incorporating dynamic and nonlinear phenomena in the proposed two-parametric scheme seems to be less straightforward, e.g. see [17, 51] and also [87, 90, 91] dealing with high-frequency thickness vibration.

Chapter 4 is concerned with obtaining an asymptotic correction to the leading order effective boundary conditions for a coated elastic half-space. The derived conditions are tested by comparison with the exact solutions of a plane time-harmonic and anti-plane problems. As a result, the formulation in [160] is validated at leading order, whereas its correction proposed in [22] appears to be asymptotically inconsistent. The obtained conditions are of general interest for elastodynamics, e.g. for developing refined asymptotic models for surface waves, see [81] and [82]. The latter provide a useful framework for modelling coated solids subject to high-speed moving loads, see [43] and [83].

A multiparametric treatment of a dynamic problem for a coated elastic half-space with a clamped surface was produced in Chapter 5. The non-traditional effective boundary conditions (5.31) are derived using a long-wave high-frequency asymptotic procedure. They incorporate the effect of a soft thin coating clamped along the surface, resulting in a regular operator perturbation of the equation governing the Rayleigh wave (5.37) and (5.53). It is interesting that the analogous conditions for a coating with a free surface in [36] lead to a singular perturbation.

The non-uniform asymptotic formulae for the family of Rayleigh-type waves (5.51) and (5.61), deduced from equations (5.37) and (5.53), fail in the vicinities of the thickness resonances (5.15) and zero frequency. In this case, in contrast to a coating with a

traction-free surface, the lowest wave has a cut-off frequency, which is in line with the non-existence of surface waves on a clamped homogeneous half-space.

Of course, the aforementioned formulae (5.51) and (5.61) could be readily obtained from the original equations in linear elasticity (1.16) and (1.17) subject to the established effective conditions (5.31). However, the development of the perturbed wave equation equations (5.37) and (5.53) for the Rayleigh-type waves brings a number of advantages. In particular, it allows various generalisations, including in particular taking into account external loading, 3D effects and transient phenomena, as it has been done for a homogeneous half-space, see [82].

It is also worth mentioning the useful findings in Section 5.3, including evaluation of zeros of function R, facilitating interpretation of the numerical data calculated from full dispersion relation (5.10). In this case, the similarity with more explicit results for Love-type waves, see Section 5.2, is intensively exploited.

Finally, we note the phenomenon of the lowest cut-off frequency tending to zero in case of especially high contrast ($\mu \ll 1$), which is in line with vibrations of high-contrast elastic composites, see [84].

Bibliography

[1] J. Achenbach. *Wave propagation in elastic solids*, volume 16. Elsevier, 2012.

[2] J.D. Achenbach. Explicit solutions for carrier waves supporting surface waves and plate waves. *Wave Motion*, 28(1):89–97, 1998.

[3] L. Aghalovyan. *Asymptotic theory of anisotropic plates and shells*. World Scientific, 2015.

[4] O.K. Aksentian and I.I. Vorovich. The state of stress in a thin plate. *Journal of Applied Mathematics and Mechanics*, 27(6):1621–1643, 1963.

[5] G.P. Aleksandrova. Contact problems in bending of a slab lying on an elastic foundation. *Izvestiia Akademii Nauk SSSR, Mekhanika Tverdogo Tela*, (1), 1973.

[6] V.M. Alexandrov. Contact problems on soft and rigid coatings of an elastic half-plane. *Mechanics of Solids*, 45(1):34–40, 2010.

[7] H. Altenbach, V. A. Eremeyev, and K. Naumenko. On the use of the first order shear deformation plate theory for the analysis of three-layer plates with thin soft core layer. *ZAMM-Journal of Applied Mathematics and Mechanics/Zeitschrift für Angewandte Mathematik und Mechanik*, 95(10):1004–1011, 2015.

[8] I. Argatov, A.U. Daniels, G. Mishuris, S. Ronken, and D. Wirz. Accounting for the thickness effect in dynamic spherical indentation of a viscoelastic layer: Application to non-destructive testing of articular cartilage. *European Journal of Mechanics-A/Solids*, 37:304–317, 2013.

[9] I. Argatov and G. Mishuris. *Contact mechanics of articular cartilage layers*. Springer, 2016.

[10] I. Argatov and G. Mishuris. *Indentation testing of biological materials*, volume 91. Springer, 2018.

[11] A.G. Aslanyan, A.B. Movchan, and Ö. Selsil. A universal asymptotic algorithm for elastic thin shells. *European Journal of Applied Mathematics*, 11(6):573–594, 2000.

[12] A.G. Aslanyan, A.B. Movchan, and Ö. Selsil. Estimates for the low eigenfrequencies of a multi-structure including an elastic shell. *European Journal of Applied Mathematics*, 14(3):313–342, 2003.

[13] O.A. Bauchau and J.I. Craig. Kirchhoff plate theory. In *Structural Analysis*, pages 819–914. Springer, 2009.

[14] V. Berdichevsky. *Variational principles of continuum mechanics: I. Fundamentals*. Springer Science & Business Media, 2009.

[15] V.L. Berdichevsky. An asymptotic theory of sandwich plates. *International Journal of Engineering Science*, 48(3):383–404, 2010.

[16] D. Bigoni, M. Gei, and A.B. Movchan. Dynamics of a prestressed stiff layer on an elastic half space: filtering and band gap characteristics of periodic structural models derived from long-wave asymptotics. *Journal of the Mechanics and Physics of Solids*, 56(7):2494–2520, 2008.

[17] D. Bigoni, M. Ortiz, and A. Needleman. Effect of interfacial compliance on bifurcation of a layer bonded to a substrate. *International Journal of Solids and Structures*, 34(33-34):4305–4326, 1997.

[18] M.A. Biot. Bending of an infinite beam on an elastic foundation. *Journal of Applied Mathematics and Mechanics*, 2(3):165–184, 1922.

[19] F.M. Borodich. The Hertz-type and adhesive contact problems for depth-sensing indentation. In *Advances in Applied Mechanics*, volume 47, pages 225–366. Elsevier, 2014.

[20] S. Bose. *High temperature coatings*. Butterworth-Heinemann, 2017.

[21] C. Boutin and K. Viverge. Generalized plate model for highly contrasted laminates. *European Journal of Mechanics-A/Solids*, 55:149–166, 2016.

[22] P. Bövik. A comparison between the Tiersten model and O(h) boundary conditions for elastic surface waves guided by thin layers. *Journal of Applied Mechanics*, 63(1):162–167, 1996.

[23] M. Brun, D.J. Colquitt, I.S. Jones, A.B. Movchan, and N.V. Movchan. Transformation cloaking and radial approximations for flexural waves in elastic plates. *New Journal of Physics*, 16(9):093020, 2014.

[24] Z. Cai and Y. Fu. On the imperfection sensitivity of a coated elastic half-space. *Proceedings of the Royal Society A: Mathematical, Physical and Engineering Sciences*, 455(1989):3285–3309, 1999.

[25] Z. Cai and Y. Fu. Exact and asymptotic stability analyses of a coated elastic half-space. *International Journal of Solids and Structures*, 37(22):3101–3119, 2000.

[26] P. Chadwick. Surface and interfacial waves of arbitrary form in isotropic elastic media. *Journal of Elasticity*, 6(1):73–80, 1976.

[27] N. Challamel, S.A. Meftah, and F. Bernard. Buckling of elastic beams on non-local foundation: A revisiting of Reissner model. *Mechanics Research Communications*, 37(5):472–475, 2010.

[28] C.J. Chapman. An asymptotic decoupling method for waves in layered media. *Proceedings of the Royal Society A: Mathematical, Physical and Engineering Sciences*, 469(2153):20120659, 2013.

[29] D.K. Chattopadhyay and K.V.S.N. Raju. Structural engineering of polyurethane coatings for high performance applications. *Progress in Polymer Science*, 32(3):352–418, 2007.

[30] R. Chebakov, J. Kaplunov, and G.A. Rogerson. Refined boundary conditions on the free surface of an elastic half-space taking into account non-local effects. *Proceedings of the Royal Society A: Mathematical, Physical and Engineering Sciences*, 472(2186):20150800, 2016.

[31] R. Chebakov, J. Kaplunov, and G.A. Rogerson. A non-local asymptotic theory for thin elastic plates. *Proceedings of the Royal Society A: Mathematical, Physical and Engineering Sciences*, 473(2203):20170249, 2017.

[32] M. Cherdantsev and K.D. Cherednichenko. Two-scale Γ-convergence of integral functionals and its application to homogenisation of nonlinear high-contrast periodic composites. *Archive for Rational Mechanics and Analysis*, 204(2):445–478, 2012.

[33] K.D. Cherednichenko and S. Cooper. On the existence of high-frequency boundary resonances in layered elastic media. *Proceedings of the Royal Society A: Mathematical, Physical and Engineering Sciences*, 471(2178):20140878, 2015.

[34] D.J. Colquitt, M. Brun, M. Gei, A.B. Movchan, N.V. Movchan, and I.S. Jones. Transformation elastodynamics and cloaking for flexural waves. *Journal of the Mechanics and Physics of Solids*, 72:131–143, 2014.

[35] R.V. Craster, L.M. Joseph, and J. Kaplunov. Long-wave asymptotic theories: the connection between functionally graded waveguides and periodic media. *Wave Motion*, 51(4):581–588, 2014.

[36] H.-H. Dai, J. Kaplunov, and D.A. Prikazchikov. A long-wave model for the surface elastic wave in a coated half-space. *Proceedings of the Royal Society A: Mathematical, Physical and Engineering Sciences*, 466(2122):3097–3116, 2010.

[37] M. Destrade, Y. Fu, and A. Nobili. Edge wrinkling in elastically supported pre-stressed incompressible isotropic plates. *Proceedings of the Royal Society A: Mathematical, Physical and Engineering Sciences*, 472(2193):20160410, 2016.

[38] M. Di Paola, F. Marino, and M. Zingales. A generalized model of elastic foundation based on long-range interactions: Integral and fractional model. *International Journal of Solids and Structures*, 46(17):3124–3137, 2009.

[39] S.C. Dutta and R. Roy. A critical review on idealization and modeling for interaction among soil–foundation–structure system. *Computers & Structures*, 80(20-21):1579–1594, 2002.

[40] S.A. Epshtein, F.M. Borodich, and S.J. Bull. Evaluation of elastic modulus and hardness of highly inhomogeneous materials by nanoindentation. *Applied Physics A*, 119(1):325–335, 2015.

[41] B. Erbaş, J. Kaplunov, E. Nolde, and M. Palsü. Composite wave models for elastic plates. *Proceedings of the Royal Society A: Mathematical, Physical and Engineering Sciences*, 474(2214):20180103, 2018.

[42] B. Erbaş, J. Kaplunov, and D.A. Prikazchikov. The Rayleigh wave field in mixed problems for a half-plane. *The IMA Journal of Applied Mathematics*, 78(5):1078–1086, 2013.

[43] B. Erbaş, J. Kaplunov, D.A. Prikazchikov, and O. Şahin. The near-resonant regimes of a moving load in a three-dimensional problem for a coated elastic half-space. *Mathematics and Mechanics of Solids*, 22(1):89–100, 2017.

[44] B. Erbaş, E. Yusufoğlu, and J. Kaplunov. A plane contact problem for an elastic orthotropic strip. *Journal of Engineering Mathematics*, 70(4):399–409, 2011.

[45] A. Figotin and P. Kuchment. Spectral properties of classical waves in high-contrast periodic media. *SIAM Journal on Applied Mathematics*, 58(2):683–702, 1998.

[46] M.M. Filonenko-Borodich. Some approximate theories of elastic foundation. *Uchenyie Zapiski Moskovkogo Gosudarstuennogo Universiteta Mekhanika, Moscow*, 46:3–18, 1940.

[47] A.C. Fischer-Cripps. Nanoindentation (Mechanical engineering series). *Spring-Verlag, New York, NY*, pages 74–76, 2002.

[48] F.G. Friedlander. On the total reflection of plane waves. *The Quarterly Journal of Mechanics and Applied Mathematics*, 1(1):376–384, 1948.

[49] K.O. Friedrichs and R.F. Dressler. A boundary-layer theory for elastic plates. *Communications on Pure and Applied Mathematics*, 14(1):1–33, 1961.

[50] L. Frýba. History of Winkler foundation. *Vehicle System Dynamics*, 24(sup1):7–12, 1995.

[51] Y.B. Fu and Z.X. Cai. An asymptotic analysis of the period-doubling secondary bifurcation in a film/substrate bilayer. *SIAM Journal on Applied Mathematics*, 75(6):2381–2395, 2015.

[52] Y.B. Fu and P. Ciarletta. Buckling of a coated elastic half-space when the coating and substrate have similar material properties. *Proceedings of the Royal Society A: Mathematical, Physical and Engineering Sciences*, 471(2178):20140979, 2015.

[53] Y.B. Fu and S.L.B. Hill. Propagation of steady nonlinear waves in a coated elastic half-space. *Wave Motion*, 34(1):109–129, 2001.

[54] G. Gazetas and R. Dobry. Horizontal response of piles in layered soils. *Journal of Geotechnical Engineering*, 110(1):20–40, 1984.

[55] M. Gei and R.W. Ogden. Vibration of a surface-coated elastic block subject to bending. *Mathematics and Mechanics of Solids*, 7(6):607–628, 2002.

[56] E. Godoy, M. Durán, and J.-C. Nédélec. On the existence of surface waves in an elastic half-space with impedance boundary conditions. *Wave Motion*, 49(6):585–594, 2012.

[57] A.L. Goldenveizer. The principles of reducing three-dimensional problems of elasticity to two-dimensional problems of the theory of plates and shells. In *Applied Mechanics*, pages 306–311. Springer, 1966.

[58] A.L. Goldenveizer. Asymptotic method in the theory of shells. *Theoretical and Applied Mechanics*, pages 91–104, 1980.

[59] A.L. Goldenveizer, J.D. Kaplunov, and E.V. Nolde. Asymptotic analysis and improvements of Timoshenko-Reissner-type theories of plates and shells. *Mechanics of Solids*, 25(6):126–139, 1990.

[60] A.L. Goldenveizer, J.D. Kaplunov, and E.V. Nolde. On Timoshenko-Reissner type theories of plates and shells. *International Journal of Solids and Structures*, 30(5):675–694, 1993.

[61] M.I. Gorbunov-Posadov. *Beams and Plates on Elastic Foundation [in Russian].* Gostroiizdat, Moscow, 1949.

[62] M.I. Gorbunov-Posadov. *Calculation of Constructions on Elastic Foundation.* Gostroiizdat, Moscow, 1953.

[63] M.I. Gorbunov-Posadov. *Tables for the Computation of Thin Plates on Elastic Foundations [in Russian].* Gostroiizdat, Moscow, 1959.

[64] I.G. Goryacheva and E.V. Torskaya. Modeling of fatigue wear of a two-layered elastic half-space in contact with periodic system of indenters. *Wear*, 268(11-12):1417–1422, 2010.

[65] A.E. Green. On the linear theory of thin elastic shells. *Proceedings of the Royal Society of London. Series A. Mathematical and Physical Sciences*, 266(1325):143–160, 1962.

[66] D. Gridin, R.V. Craster, and A.T.I. Adamou. Trapped modes in curved elastic plates. *Proceedings of the Royal Society A: Mathematical, Physical and Engineering Sciences*, 461(2056):1181–1197, 2005.

[67] R. Hauert. A review of modified DLC coatings for biological applications. *Diamond and Related Materials*, 12(3-7):583–589, 2003.

[68] M. Hetenyi. A general solution for the bending of beams on an elastic foundation of arbitrary continuity. *Journal of Applied Physics*, 21(1):55–58, 1950.

[69] M. Hetenyi. *Beams on Elastic Foundation.* The University of Michigan Press, Ann Arbor, 1958.

[70] R. Höller, M. Aminbaghai, L. Eberhardsteiner, J. Eberhardsteiner, R. Blab, B. Pichler, and C. Hellmich. Rigorous amendment of Vlasov's theory for thin elastic plates on elastic Winkler foundations, based on the principle of virtual power. *European Journal of Mechanics-A/Solids*, 73:449–482, 2019.

[71] K. Holmberg, H. Ronkainen, A. Laukkanen, K. Wallin, S. Hogmark, S. Jacobson, U. Wiklund, R.M. Souza, and P. Ståhle. Residual stresses in TiN, DLC and MoS2 coated surfaces with regard to their tribological fracture behaviour. *Wear*, 267(12):2142–2156, 2009.

[72] C.O. Horgan. Anti-plane shear deformations in linear and nonlinear solid mechanics. *SIAM review*, 37(1):53–81, 1995.

[73] H. Jiang, R. Browning, J.D. Whitcomb, M. Ito, M. Shimouse, T.A. Chang, and H.-J. Sue. Mechanical modeling of scratch behavior of polymeric coatings on hard and soft substrates. *Tribology Letters*, 37(2):159–167, 2010.

[74] J. Kaplunov and A. Nobili. The edge waves on a kirchhoff plate bilaterally supported by a two-parameter elastic foundation. *Journal of Vibration and Control*, 23(12):2014–2022, 2017.

[75] J. Kaplunov and A. Nobili. Multi-parametric analysis of strongly inhomogeneous periodic waveguideswith internal cutoff frequencies. *Mathematical Methods in the Applied Sciences*, 40(9):3381–3392, 2017.

[76] J. Kaplunov, E. Nolde, and D.A. Prikazchikov. A revisit to the moving load problem using an asymptotic model for the Rayleigh wave. *Wave motion*, 47(7):440–451, 2010.

[77] J. Kaplunov, D. Prikazchikov, and O. Sergushova. Multi-parametric analysis of the lowest natural frequencies of strongly inhomogeneous elastic rods. *Journal of Sound and Vibration*, 366:264–276, 2016.

[78] J. Kaplunov, D. Prikazchikov, and L. Sultanova. Justification and refinement of Winkler–Fuss hypothesis. *Zeitschrift für angewandte Mathematik und Physik*, 69(3):80, 2018.

[79] J. Kaplunov, D. Prikazchikov, and L. Sultanova. Elastic contact of a stiff thin layer and a half-space. *Zeitschrift für angewandte Mathematik und Physik*, 70(1):22, 2019.

[80] J. Kaplunov, D. Prikazchikov, and L. Sultanova. On higher order effective boundary conditions for a coated elastic half-space. In *Problems of Nonlinear Mechanics and Physics of Materials*, pages 449–462. Springer, 2019.

[81] J. Kaplunov and D.A. Prikazchikov. Explicit models for surface, interfacial and edge waves. In R. Craster and J. Kaplunov, editors, *Dynamic localization phenomena in elasticity, acoustics and electromagnetism*, number 547, pages 73–114. Springer, 2013.

[82] J. Kaplunov and D.A. Prikazchikov. Asymptotic theory for Rayleigh and Rayleigh-type waves. In *Advances in Applied Mechanics*, volume 50, pages 1–106. Elsevier, 2017.

[83] J. Kaplunov, D.A. Prikazchikov, B. Erbaş, and O. Şahin. On a 3D moving load problem for an elastic half space. *Wave motion*, 50(8):1229–1238, 2013.

[84] J. Kaplunov, D.A. Prikazchikov, and L.A. Prikazchikova. Dispersion of elastic waves in a strongly inhomogeneous three-layered plate. *International Journal of Solids and Structures*, 113:169–179, 2017.

[85] J. Kaplunov, D.A. Prikazchikov, L.A. Prikazchikova, and O. Sergushova. The lowest vibration spectra of multi-component structures with contrast material properties. *Journal of Sound and Vibration*, 2019.

[86] J. Kaplunov, A. Zakharov, and D. Prikazchikov. Explicit models for elastic and piezoelastic surface waves. *IMA Journal of Applied Mathematics*, 71(5):768–782, 2006.

[87] J.D. Kaplunov. Long-wave vibrations of a thin walled body with fixed faces. *The Quarterly Journal of Mechanics and Applied Mathematics*, 48(3):311–327, 1995.

[88] J.D. Kaplunov, L.Yu. Kossovich, and G.A. Rogerson. Direct asymptotic integration of the equations of transversely isotropic elasticity for a plate near cut-off frequencies. *Quarterly Journal of Mechanics and Applied Mathematics*, 53(2):323–341, 2000.

[89] J.D. Kaplunov, L.Yu. Kossovitch, and E.V. Nolde. *Dynamics of thin walled elastic bodies*. Academic Press, 1998.

[90] J.D. Kaplunov and D.G. Markushevich. Plane vibrations and radiation of an elastic layer lying on a liquid half-space. *Wave Motion*, 17(3):199–211, 1993.

[91] J.D. Kaplunov and E.V. Nolde. Long-wave vibrations of a nearly incompressible isotropic plate with fixed faces. *The Quarterly Journal of Mechanics and Applied Mathematics*, 55(3):345–356, 2002.

[92] J.D. Kaplunov, E.V. Nolde, and G.A. Rogerson. An asymptotically consistent model for long-wave high-frequency motion in a pre-stressed elastic plate. *Mathematics and Mechanics of Solids*, 7(6):581–606, 2002.

[93] J.D. Kaplunov, E.V. Nolde, and G.A. Rogerson. Short wave motion in a pre-stressed incompressible elastic plate. *IMA Journal of Applied Mathematics*, 67(4):383–399, 2002.

[94] J.D. Kaplunov, G.A. Rogerson, and P.E. Tovstik. Localized vibration in elastic structures with slowly varying thickness. *The Quarterly Journal of Mechanics and Applied Mathematics*, 58(4):645–664, 2005.

[95] Yu.D. Kaplunov and L.Yu. Kossovich. Asymptotic model of Rayleigh waves in the far-field zone in an elastic half-plane. In *Doklady Physics*, volume 49, pages 234–236. Springer, 2004.

[96] A.D. Kerr. Elastic and viscoelastic foundation models. *Journal of Applied Mechanics*, 31(3):491–498, 1964.

[97] L.A. Khajiyeva, D.A. Prikazchikov, and L.A. Prikazchikova. Hyperbolic-elliptic model for surface wave in a pre-stressed incompressible elastic half-space. *Mechanics Research Communications*, 92:49–53, 2018.

[98] G. Kirchhoff. Über das gleichgewicht und die bewegung einer elastischen scheibe. *Journal für die reine und angewandte Mathematik (Crelle's Journal)*, 40:51–88, 1850.

[99] A.P. Kiselev. Rayleigh wave with a transverse structure. *Proceedings of the Royal Society of London. Series A: Mathematical, Physical and Engineering Sciences*, 460(2050):3059–3064, 2004.

[100] A.P. Kiselev. General surface waves in layered anisotropic elastic structures. *Zapiski Nauchnykh Seminarov POMI*, 438:133–137, 2015.

[101] A.P. Kiselev and D.F. Parker. Omni-directional Rayleigh, Stoneley and Schölte waves with general time dependence. *Proceedings of the Royal Society A: Mathematical, Physical and Engineering Sciences*, 466(2120):2241–2258, 2010.

[102] E.V. Kovalenko and I.A. Buyanovskii. On the durability prediction for an elastic cylinder-elastic layer pair reinforced by thin coating according to the wear criterion. *Journal of Machinery Manufacture and Reliability*, 44(4):357–362, 2015.

[103] A.S. Kovalev, A.P. Mayer, C. Eckl, and G.A. Maugin. Solitary Rayleigh waves in the presence of surface nonlinearities. *Physical Review E*, 66(3):036615, 2002.

[104] V.A. Kozlov, V.G. Maz'ya, and A.B. Movchan. *Asymptotic analysis of fields in multi-structures*. Oxford University Press on Demand, 1999.

[105] A. Kudaibergenov, A. Nobili, and L. Prikazchikova. On low-frequency vibrations of a composite string with contrast properties for energy scavenging fabric devices. *Journal of Mechanics of Materials and Structures*, 11(3):231–243, 2016.

[106] V.I. Kuznetsov. *Elastic Foundations*. Gosstroiizdat, Moscow, 1952.

[107] H. Lamb. On the flexure of an elastic plate. *Proceedings of the London Mathematical Society*, 1(1):70–91, 1889.

[108] M.I. Lashhab, G.A. Rogerson, and L.A. Prikazchikova. Small amplitude waves in a pre-stressed compressible elastic layer with one fixed and one free face. *Zeitschrift für angewandte Mathematik und Physik*, 66(5):2741–2757, 2015.

[109] K.C. Le. *Vibrations of shells and rods*. Springer Science & Business Media, 2012.

[110] M. Li, Q. Liu, Z. Jia, X. Xu, Y. Cheng, Y. Zheng, T. Xi, and S. Wei. Graphene oxide/hydroxyapatite composite coatings fabricated by electrophoretic nanotechnology for biological applications. *Carbon*, 67:185–197, 2014.

[111] D.S. Liyanapathirana and H.G. Poulos. Pseudostatic approach for seismic analysis of piles in liquefying soil. *Journal of Geotechnical and Geoenvironmental Engineering*, 131(12):1480–1487, 2005.

[112] A.E.H. Love. *A treatise on the mathematical theory of elasticity*. Cambridge university press, 2013.

[113] M. Lutianov and G. Rogerson. Long wave motion in layered elastic media. *International Journal of Engineering Science*, 48(12):1856–1871, 2010.

[114] P.G. Malischewsky and F. Scherbaum. Love's formula and H/V-ratio (ellipticity) of Rayleigh waves. *Wave motion*, 40(1):57–67, 2004.

[115] R.M. Martynyak, I.A. Prokopyshyn, and I.I. Prokopyshyn. Contact of elastic bodies with nonlinear Winkler surface layers. *Journal of Mathematical Sciences*, 205(4):535–553, 2015.

[116] G.I. Mikhasev and P.E. Tovstik. *Localized vibrations and waves in thin shells. Asymptotic methods*. Fizmatlit, Moscow, 2009.

[117] G. Mishuris. Interface crack and nonideal interface concept (Mode III). *International Journal of Fracture*, 107(3):279–296, 2001.

[118] G. Mishuris. Imperfect transmission conditions for a thin weakly compressible interface. 2D problems. *Archives of Mechanics*, 56(2):103–115, 2004.

[119] G. Mishuris and A. Öchsner. Transmission conditions for a soft elasto-plastic interphase between two elastic materials. Plane strain state. *Archives of Mechanics*, 57(2-3):157–169, 2005.

[120] G. Mishuris and A. Öchsner. 2D modelling of a thin elasto-plastic interphase between two different materials: plane strain case. *Composite Structures*, 80(3):361–372, 2007.

[121] G. Mishuris, A. Ochsner, G. Kuhn, A. La Rocca, H. Power, V. La Rocca, M. Morale, C.J.S. Alves, P.R.S. Antunes, D.L. Young, and C.S. Chen. FEM-Analysis of nonclassical transmission conditions between elastic structures part 1: soft imperfect interface. *CMC-TECH SCIENCE PRESS-*, 2(4):227, 2005.

[122] G.S. Mishuris. Stress singularity at a crack tip for various intermediate zones in bimaterial structures (Mode iii). *International Journal of Solids and Structures*, 36(7):999–1015, 1999.

[123] G.S. Mishuris. Mode III interface crack lying at thin nonhomogeneous anisotropic interface. Asymptotics near the crack tip. In *IUTAM Symposium on Asymptotics, Singularities and Homogenisation in Problems of Mechanics*, pages 251–260. Springer, 2003.

[124] N.F. Morozov and P.E. Tovstik. On modes of buckling for a plate on an elastic foundation. *Mechanics of Solids*, 45(4):519–528, 2010.

[125] A.B. Movchan, N.V. Movchan, and R.C. McPhedran. Bloch–Floquet bending waves in perforated thin plates. *Proceedings of the Royal Society A: Mathematical, Physical and Engineering Sciences*, 463(2086):2505–2518, 2007.

[126] K. Naumenko and V.A. Eremeyev. A layer-wise theory for laminated glass and photovoltaic panels. *Composite Structures*, 112:283–291, 2014.

[127] A.J. Niklasson, S.K. Datta, and M.L. Dunn. On approximating guided waves in plates with thin anisotropic coatings by means of effective boundary conditions. *The Journal of the Acoustical Society of America*, 108(3):924–933, 2000.

[128] S. Nikolaou, G. Mylonakis, G. Gazetas, and T. Tazoh. Kinematic pile bending during earthquakes: analysis and field measurements. *Geotechnique*, 51(5):425–440, 2001.

[129] A. Nobili. Superposition principle for the tensionless contact of a beam resting on a Winkler or a Pasternak foundation. *Journal of Engineering Mechanics*, 139(10):1470–1478, 2012.

[130] A. Nobili and D.A. Prikazchikov. Explicit formulation for the Rayleigh wave field induced by surface stresses in an orthorhombic half-plane. *European Journal of Mechanics-A/Solids*, 70:86–94, 2018.

[131] E.V. Nolde and G.A. Rogerson. Long wave asymptotic integration of the governing equations for a pre-stressed incompressible elastic layer with fixed faces. *Wave Motion*, 36(3):287–304, 2002.

[132] J. O'Neill, O. Selsil, R.C. McPhedran, A.B. Movchan, and N.V. Movchan. Active cloaking of finite defects for flexural waves in elastic plates. *arXiv preprint arXiv:1403.0816*, 2014.

[133] J. O'Neill, Ö. Selsil, R.C. McPhedran, A.B. Movchan, and N.V. Movchan. Active cloaking of inclusions for flexural waves in thin elastic plates. *The Quarterly Journal of Mechanics and Applied Mathematics*, 68(3):263–288, 2015.

[134] N.P. Padture, M. Gell, and E.H. Jordan. Thermal barrier coatings for gas-turbine engine applications. *Science*, 296(5566):280–284, 2002.

[135] D.F. Parker. The Stroh formalism for elastic surface waves of general profile. *Proceedings of the Royal Society A: Mathematical, Physical and Engineering Sciences*, 469(2160):20130301, 2013.

[136] D.F. Parker and A.P. Kiselev. Rayleigh waves having generalised lateral dependence. *Quarterly Journal of Mechanics and Applied Mathematics*, 62(1):19–30, 2008.

[137] P.L. Pasternak. On a new method of an elastic foundation by means of two foundation constants. *Gosudarstvennoe Izdatelstvo Literaturi po Stroitelstuve i Arkhitekture*, 1954.

[138] L. Pawlowski. *The science and engineering of thermal spray coatings*. John Wiley & Sons, 2008.

[139] A.V. Pichugin and G.A. Rogerson. A two-dimensional model for extensional motion of a pre-stressed incompressible elastic layer near cut-off frequencies. *IMA Journal of Applied Mathematics*, 66(4):357–385, 2001.

[140] A.V. Pichugin and G.A. Rogerson. Anti-symmetric motion of a pre-stressed incompressible elastic layer near shear resonance. *Journal of Engineering Mathematics*, 42(2):181–202, 2002.

[141] S.B. Platts and N.V. Movchan. Low frequency band gaps and localised modes for arrays of coated inclusions. In *IUTAM Symposium on Asymptotics, Singularities and Homogenisation in Problems of Mechanics*, pages 63–71. Springer, 2003.

[142] G.Ya. Popov. Plates on a linearly elastic foundation (a survey). *Soviet Applied Mechanics*, 8(3):231–242, 1972.

[143] J. Postnova and R.V. Craster. Trapped modes in elastic plates, ocean and quantum waveguides. *Wave Motion*, 45(4):565–579, 2008.

[144] C.G. Poulton, R.C. McPhedran, N.V. Movchan, and A.B. Movchan. Convergence properties and flat bands in platonic crystal band structures using the multipole formulation. *Waves in Random and Complex Media*, 20(4):702–716, 2010.

[145] D.A. Prikazchikov. Rayleigh waves of arbitrary profile in anisotropic media. *Mechanics Research Communications*, 50:83–86, 2013.

[146] L. Prikazchikova, Y. Ece Aydın, B. Erbaş, and J. Kaplunov. Asymptotic analysis of an anti-plane dynamic problem for a three-layered strongly inhomogeneous laminate. *Mathematics and Mechanics of Solids*, page 1081286518790804, 2018.

[147] L. Rayleigh. On waves propagated along the plane surface of an elastic solid. *Proceedings of the London Mathematical Society*, 1(1):4–11, 1885.

[148] E.L. Reiss and S. Locke. On the theory of plane stress. *Quarterly of Applied Mathematics*, 19(3):195–203, 1961.

[149] E. Reissner. On the derivation of the theory of thin elastic shells. *Journal of Mathematics and Physics*, 42(1-4):263–277, 1963.

[150] G.A. Rogerson and L.A. Prikazchikova. Generalisations of long wave theories for pre-stressed compressible elastic plates. *International Journal of Non-Linear Mechanics*, 44(5):520–529, 2009.

[151] G.A. Rogerson, K.J. Sandiford, and L.A. Prikazchikova. Abnormal long wave dispersion phenomena in a slightly compressible elastic plate with non-classical boundary conditions. *International Journal of Non-Linear Mechanics*, 42(2):298–309, 2007.

[152] M. Rousseau and G.A. Maugin. Rayleigh surface waves and their canonically associated quasi-particles. *Proceedings of the Royal Society A: Mathematical, Physical and Engineering Sciences*, 467(2126):495–507, 2010.

[153] M.Yu. Ryazantseva and F.K. Antonov. Harmonic running waves in sandwich plates. *International Journal of Engineering Science*, 59:184–192, 2012.

[154] A. Selsil, A.B. Movchan, and N.V. Movchan. Asymptotic analysis of heat transfer in a system of channels connected by thin conducting walls. In *IUTAM Symposium on Asymptotics, Singularities and Homogenisation in Problems of Mechanics*, pages 455–464. Springer, 2003.

[155] A. Selsil, N.V. Movchan, A.B. Movchan, S.T. Kolaczkowski, and S. Awdry. Mathematical modelling of heat transfer in a catalytic reformer. *IMA Journal of Applied Mathematics*, 70(2):201–220, 2005.

[156] V.P. Smyshlyaev. Propagation and localization of elastic waves in highly anisotropic periodic composites via two-scale homogenization. *Mechanics of Materials*, 41(4):434–447, 2009.

[157] S.L. Sobolev. Some problems in wave propagation [in Russian]. In *Differential and integral equationsof mathematical physics (Eds. Frank P., von Mises R.)*, pages 468–617. ONTI, Moscow-Leningrad, 1937.

[158] D.J. Steigmann and R.W. Ogden. Plane deformations of elastic solids with intrinsic boundary elasticity. *Proceedings of the Royal Society of London. Series A: Mathematical, Physical and Engineering Sciences*, 453(1959):853–877, 1997.

[159] L. Sultanova. Two-parametric analysis of anti-plane shear deformation of a coated elastic half-space. *Acta Mechanica et Automatica*, 12(4), 2018.

[160] H.F. Tiersten. Elastic surface waves guided by thin films. *Journal of Applied Physics*, 40(2):770–789, 1969.

[161] P.E. Tovstik. Free high-frequency vibrations of anisotropic plates of variable thickness. *Journal of Applied Mathematics and Mechanics*, 56(3):390–395, 1992.

[162] P.E. Tovstik and T.P. Tovstik. Generalized timoshenko-reissner models for beams and plates, strongly heterogeneous in the thickness direction. *ZAMM-Journal of Applied Mathematics and Mechanics/Zeitschrift für Angewandte Mathematik und Mechanik*, 97(3):296–308, 2017.

[163] S. Veprek and M.J.G. Veprek-Heijman. Industrial applications of superhard nanocomposite coatings. *Surface and Coatings Technology*, 202(21):5063–5073, 2008.

[164] P.C. Vinh and V.T.N. Anh. Rayleigh waves in an orthotropic half-space coated by a thin orthotropic layer with sliding contact. *International Journal of Engineering Science*, 75:154–164, 2014.

[165] P.C. Vinh and V.T.N. Anh. Effective boundary condition method and approximate secular equations of Rayleigh waves in orthotropic half-spaces coated by a thin layer. *Journal of Mechanics of Materials and Structures*, 11(3):259–277, 2016.

[166] P.C. Vinh, V.T.N. Anh, and V.P. Thanh. Rayleigh waves in an isotropic elastic half-space coated by a thin isotropic elastic layer with smooth contact. *Wave Motion*, 51(3):496–504, 2014.

[167] P.C. Vinh and N.T.K. Linh. An approximate secular equation of rayleigh waves propagating in an orthotropic elastic half-space coated by a thin orthotropic elastic layer. *Wave Motion*, 49(7):681–689, 2012.

[168] P.C. Vinh and N.Q. Xuan. Rayleigh waves with impedance boundary condition: Formula for the velocity, existence and uniqueness. *European Journal of Mechanics-A/Solids*, 61:180–185, 2017.

[169] K. Viverge, C. Boutin, and F. Sallet. Model of highly contrasted plates versus experiments on laminated glass. *International Journal of Solids and Structures*, 102:238–258, 2016.

[170] J. Wang, J. Du, W. Lu, and H. Mao. Exact and approximate analysis of surface acoustic waves in an infinite elastic plate with a thin metal layer. *Ultrasonics*, 44:e941–e945, 2006.

[171] Y.H. Wang, L.G. Tham, and Y.K. Cheung. Beams and plates on elastic foundations: a review. *Progress in Structural Engineering and Materials*, 7(4):174–182, 2005.

[172] E. Winkler. Die lehre von elastizitat und festigkeit (the theory of elasticity and stiffness). *H. Domenicus. Prague*, 1867.

[173] C.-S. Yim and A.K. Chopra. Earthquake response of structures with partial uplift on Winkler foundation. *Earthquake Engineering & Structural Dynamics*, 12(2):263–281, 1984.